IMPROVEMENT OF BIOAVAILABILITY OF LM4156 USING SUPERCRITICAL AND CRYOGENIC TECHNOLOGIES

DISSERTATION

Presented in Partial Fulfillment of the Requirements for the

Degree Doctor of Philosophy in the

Doctoral School of Chemical Engineering, University of Veszprém

and the

Doctoral School of Environmental Sciences, University of Aix-Marseille III

By

Viktor MAJERIK

2006

Advisers:	Professor Géza HORVÁTH
	Professor Gérard CHARBIT
Consultants:	Professor Elisabeth BADENS
	Professor László SZOKONYA
External advisers:	Dr. Eric TEILLAUD
	Dr. Nathalie BOSC

LM4156 BIOLÓGIAI HOZZÁFÉRHETŐSÉGÉNEK NÖVELÉSE SZUPERKRITIKUS ÉS KRIOGÉN TECHNOLÓGIÁK FELHASZNÁLÁSÁVAL

Értekezés doktori (PhD) fokozat elnyerése érdekében

Írta:
Majerik Viktor

Készült a Veszprémi Egyetem Vegyészmérnöki Doktori iskolája keretében

Témavezető: *Dr. Horváth Géza és Dr. Gérard Charbit*

Elfogadásra javaslom (igen / nem)

(aláírás)**

A jelölt a doktori szigorlaton …..... % -ot ért el,

Az értekezést bírálóként elfogadásra javaslom:

Bíráló neve: …..... …..... igen /nem

…….
(aláírás)

Bíráló neve: …..... …..... igen /nem

…….
(aláírás)

***Bíráló neve: …..... …..... igen /nem

…….
(aláírás)

A jelölt az értekezés nyilvános vitáján …..... % - ot ért el

Veszprém/Keszthely, …….
a Bíráló Bizottság elnöke

A doktori (PhD) oklevél minősítése….....

……
Az EDT elnöke

Megjegyzés: a * közötti részt az egyéni felkészülők, a ** közötti részt a szervezett képzésben résztvevők használják, *** esetleges

Acknowledgments

I whish to thank my advisors, Dr. Géza Horváth and Dr. Gérard Charbit for their guidance and encouragement. They were more than simple advisors and it was good to know that I could count on them in any kind of problem.

I am grateful to Mr. and Mrs. Charbit for the warm reception I met in the Laboratoire de Procédés Propres et Environnement, for putting me up in the first weeks and lending me a helping hand.

I thank all my consultants and external advisers Dr. Elisabeth Badens, Dr. László Szokonya, Dr. Nathalie Bosc and Dr. Eric Teillaud. I appreciate the helpful and friendly discussions we used to have. Their instructions were inestimable and helped me to see things differently.

I am also grateful to all colleagues and co-workers. Thank you, Dr. Bernadett Ravasz “Detti”, Péter Gombás, Csorja Sándorné “Kati néni”, Dr. Daniel Borschneck, Dr. Renaud Denoyel, Julien Skottuba-Stepan, Carole Fargeot and Sandrine Bourrelly.

My most sincere thanks are due to my family and my fiancée Kati. Without their love and endless patience I could never have done all this work. I thank all the staff of LPPE, foremost, Adrian and Yvan for their friendship and the unforgettable days we used to have in Arbois.

Finally, but not lastly, I kindly acknowledge the financial support from Merck Santé and the fellowship from the French Government awarded by the Cultural and Cooperation Service of the French Embassy in Hungary. I also acknowledge the financial support from the foundations „Industry for Engineering Education in Veszprém” and „Peregrinatio I”.

Abstract

This thesis concerns a new orally administered active pharmaceutical ingredient: LM4156. This molecule has high biological activity and high permeability but its bioavailability is limited because of its low aqueous solubility and dissolution rate. Furthermore, conventionally crystallized LM4156 exhibits poor flow properties due to its acicular crystals. As conventional methods failed to fulfill regulatory and technological requirements, new methods involving supercritical fluids and cryogenic liquids were evaluated. In an attempt to enhance its dissolution rate and improve its flowability, LM4156 was coprecipitated with several biodegradable polymers: Eudragit E, Eudragit RL, Poloxamer 188, Poloxamer 407, PEG 8000 and PVP K17 using Supercritical Antisolvent (SAS), Solution Enhanced Dispersion by Supercritical Fluids (SEDS) and Spray-freezing (SF) technologies. Formulations were compared in terms of particle morphology, particle size, flow properties, crystallinity, polymorphic purity, residual solvent content, precipitation yield, drug content, specific surface area and dissolution kinetics. Most SAS prepared powders consisted of needle-like crystals partly covered by polymer spheres. Precipitation yield and crystallinity varied over a wide range depending on the solvent and polymer involved. Several SAS prepared formulations possessed adequate dissolution rates (2 times higher than the raw drug) and satisfied requirements on residual solvent level and polymorphic purity as well. However, powders still consisted of large particles of unfavorable properties. To overcome these difficulties SEDS was involved, but no significant difference was observed in morphology or size of particles. The newly developed SF technology was proved to be a versatile method for preparing fast-dissolving solid dispersions and solid solutions with a wide range of drug/polymer ratios. All freeze-dried formulations were composed of highly porous free-flowing spherical particles. Owing to the ultra-rapid freezing rate, SF powders were characterized by lower crystallinity and higher dissolution rate in comparison with SAS powders. Among the polymers tested, Poloxamer 407 gave the best results regardless of the method of preparation.

Key words: Supercritical fluid antisolvent, SAS, SEDS, Spray-freezing, Bioavailability, Poorly water soluble drug, Solid dispersion.

Kivonat

Az alábbi disszertáció egy új, szájon át beadható gyógyszerhatóanyaggal, az LM4156-tal foglalkozik. A kérdéses hatóanyag nagy biológiai aktivitással és jó permeábilitással rendelkezik, azonban biológiai hozzáférhetősége alacsony vízoldhatósága és kis oldódási sebessége miatt korlátozott. Továbbá a hagyományos útón előállított LM4156 tűszerű kristályai miatt rossz folyási tulajdonsággal is bír. Miután a hagyományos technikák a törvényi és technológiai előírásoknak nem feleltek meg, szuperkritikus fluidumokon és kriogén folyadékokon alapuló új módszereket vettünk górcső alá. Hogy javítsunk oldódási és folyási tulajdonságain a hatóanyagot Supercritical Antisolvent (SAS), Solution Enhanced Dispersion by Supercritical Fluids (SEDS) és Spray-freezing (SF) technikák felhasználásával a következő polimerekbe ágyaztuk: Eudragit E, Eudragit RL, Poloxamer 188, Poloxamer 407, PEG 8000 és PVP K17. A kapott szilárd termékeket az alábbi szempontok alapján hasonlítottuk össze: morfológia, szemcseméret, folyási tulajdonságok, kristályosság, polimorf módosulat, maradék oldószertartalom, hozam, hatóanyag tartalom, fajlagos felület és oldódási kinetika. Az SAS technikával kezelt legtöbb készítmény tűszerű kristályokból állt, amelyeket helyenként polimer bevonat vett körül. A kicsapás hozama és a termék kristályossága az alkalmazott oldószertől és polimertől függően tág határok közt változott. Több SAS technikával kezelt terméknél mértünk jó oldódási sebességet, elfogadható maradék oldószertartalmat és nagy polimorf tisztaságot. Ezeket azonban még mindig nagy szemcseméret és kedvezőtlen habitus jellemezte. Ezeken a tulajdonságokon javítandó, SEDS technológiát alkalmaztunk, azonban a kapott szemcsék formája és mérete alig különbözött az SAS technikával gyártottakétól. Az újonnan kifejlesztett SF technológia tökéletesen alkalmasnak bizonyult azonnal oldódó szilárd diszperziók és szilárd oldatok előállítására, amelyek hatóanyag tartalma széles határok közt változtatható. A fagyasztva szárított készítmények jó folyási tulajdonságokkal bíró porózus kerek szemcsékből álltak. Az ultra gyors fagyási folyamatnak köszönhetően az SF technikával kezelt termékek alacsonyabb kristályosságot és nagyobb oldódási sebességet mutattak, mint a hasonló SAS termékek. A vizsgált polimerek közül a Poloxamer 407 tulajdonságai voltak a legkedvezőbbek az alkalmazott technológiától függetlenül.

Kulcsszavak: Szuperkritikus fluidum másodlagos oldószer, SAS, SEDS, Spray-freezing, Biológiai hozzáférhetőség, Vízben alig oldódó hatóanyag, Szilárd diszperzió.

Résumé

Cette étude concerne un nouveau principe actif administré par voie orale le LM4156. Cette molécule a une activité biologique importante et une perméabilité adéquate mais sa biodisponibilité est limitée par de faibles solubilité et vitesse de dissolution en milieux aqueux. D'autre part, le LM4156 cristallisé par des techniques traditionnelles est caractérisé par une mauvaise coulabilité en raison de cristaux ayant un faciès aciculaire. Les techniques classiques ne convenant pas aux demandes réglementaires et technologiques, d'autres méthodes de génération de particules ont été envisagées utilisant des fluides supercritiques et des liquides cryogéniques. Afin d'améliorer sa vitesse de dissolution et sa coulabilité, le LM4156 a été co-précipité avec six polymères biodégradables: l'Eudragit E, l'Eudragit RL, le Poloxamer 188, le Poloxamer 407, le PEG 8000 et le PVP K17 en utilisant les procédés « Supercritical Antisolvent » (SAS), « Solution Enhanced Dispersion by Supercritical Fluids » (SEDS) et « Spray-freezing » (SF). Les poudres obtenues ont été comparées en terme de faciès, taille de particule, coulabilité, degré de cristallinité, nature polymorphique, taux de solvant résiduel, rendement, concentration en principe actif, surface d'aire spécifique et cinétique de dissolution. La plupart des poudres préparées par SAS sont composées de cristaux aciculaires sur lesquels le polymère a précipité sous forme sphérique. Le rendement et le degré de cristallinité ont varié dans une très large gamme selon le solvant et le polymère utilisés. Plusieurs formulations obtenues par le procédé SAS possèdent une vitesse de dissolution adéquate (2 fois plus élevée que la vitesse de dissolution de la molécule brute). Elles ont également répondu aux critères requis concernant le taux de solvant résiduel et la nature polymorphique. Néanmoins, les poudres obtenues sont caractérisées par une taille de particule trop grande et un faciès défavorable. En vue de surmonter ces difficultés, nous avons testé le procédé SEDS qui a donné des résultats comparables à ceux obtenus avec le procédé SAS. La méthode SF, développée dans le cadre de cette étude, s'est avérée très avantageuse pour la préparation de dispersions solides et de solutions solides qui se dissolvent très vite quel que soit le rapport principe actif/polymère. Elles sont composées de particules sphériques poreuses d'une bonne coulabilité. Grâce à la congélation ultrarapide, les poudres obtenues par le procédé SF ont un taux de cristallinité plus faible et une vitesse de dissolution plus élevée que les formulations obtenues par le procédé SAS. Parmi les polymères testés, le Poloxamer 407 a donné les meilleurs résultats quelle que soit la méthode de préparation utilisée.

Mots clés : « Supercritical antisolvent », SAS, SEDS, Spray-freezing, Biodisponibilité, Principe actif faiblement hydrosoluble, Dispersion solide.

Publications

Majerik, V., Charbit, G., Badens, E., Horváth, G., Szokonya, L., Bosc, N., Teillaud, E. Bioavailability enhancement of an active substance by supercritical antisolvent precipitation. *Journal of Supercritical Fluids, In press*

Majerik, V., Charbit, G., Badens, E., Horváth, G., Szokonya, L., Bosc, N., Teillaud, E. Solid dispersions of oxeglitazar in PVP K17 and Poloxamer 407 by supercritical antisolvent and co-evaporation methods. *European Journal of Pharmaceutical Sciences, In press*

Majerik, V., Horváth, G., Charbit, G., Badens, E., Szokonya, L., Bosc, N., Teillaud, E. Novel particle engineering techniques in drug delivery: review of formulations using supercritical fluids and liquefied gases. *Hungarian Journal of Industrial Chemistry*, 32 (2004) 41-56.

Majerik, V., Horváth, G., Charbit, G., Szokonya, L., Badens, E., Bosc, N., Teillaud, E. Gyógyszerhatóanyag vízoldhatósásának növelése szuperkritikus másodlagos oldószerrel (SAS) történő kicsapással. *Proceedings of The Conference on Supercritical Fluid Application in Analytical and Preparative Processes,* May 19, 2005, Budapest, pp 13.

Majerik, V., Horváth, G., Charbit, G., Szokonya, L., Badens, E., Bosc, N., Teillaud, E. Gyógyszerhatóanyag vízoldhatósásának növelése szuperkritikus másodlagos oldószerrel (SAS) történő kicsapással. *Olaj Szappan Kozmetika,* 4 (2005) 179.

Szokonya, L., Majerik, V. Crystallization in supercritical fluids. *Proceedings of The Conference on Supercritical Fluid Application in Analytical and Preparative Processes,* May 23, 2002 Budapest, pp 17.

Horváth, G., Szokonya, L., Majerik, V., Charbit, G. Micronisation of crystals using supercritical jets, *Proceedings of The 8th Conference on Colloid Chemistry,* September 18-20, 2002, Keszthely, pp 83.

Szokonya, L., Majerik, V. Kristályosítás szuperkritikus fluidumok segítségével. *Olaj Szappan Kozmetika,* 51 (2002) 40-42.

Badens, E., Teillaud, E., Charbit, G., Horváth, G., Szokonya, L., Bosc, N., Majerik, V. Solubility enhancement of a pharmaceutical ingredient using supercritical antisolvent and spray-freezing techniques. *Proceedings of The 7th International Symposium on Supercritical Fluids,* May 1-4, 2005, Orlando #154

Contents

Abbreviations

AARD	Average Absolute Relative Deviation
API	Active Pharmaceutical Ingredient
ASES	Aerosol Solvent Extraction System
BCS	Biopharmaceutics Classification System
CD	Cyclodextrin
$CHCl_3$	Chloroform
DCA	Deoxycholic Acid
DCM	Dichloromethane
DMSO	Dimethylsulfoxide
D/P	Drug/Polymer (weight ratio)
EC	Ethyl cellulose
EPAS	Evaporative Precipitation into Aqueous Solution
EtOH	Ethanol
FDA	Food and Drug Administration
GAS	Gas Antisolvent
GI	Gastrointestinal
HIP	Hydrophobic Ion-Pairing
HPC	Hydroxypropyl cellulose
HPMC	Hydroxypropyl methylcellulose
MeOH	Methanol
NDP	Number of Data Points
NMP	N-methyl-2-pyrrolidone
PCA	Precipitation with Compressed Antisolvent
PCL	Poly(ε-caprolactone)
PEG	Polyethylene glycol
PEO	Polyethylene oxide
PGSS	Particles from Gas-Saturated Solution
PLA	Poly(lactic acid)
PLGA	Poly(lactic-co-glycolic acid)
PLLA	Poly(L-lactic acid)
PMMA	Poly(methyl methacrylate)
PPO	Polypropylene oxide
PVP	Polyvinylpyrrolidone
RELGS	Rapid Expansion of Liquefied Gas Solution
RELGS-H	Rapid Expansion of Liquefied Gas Solution and Homogenization
RESAS	Rapid Expansion from Supercritical to Aqueous Solution
RESS	Rapid Expansion of Supercritical Solution
RESS-N	Rapid Expansion from Supercritical Solution with a Non-solvent
SAS	Supercritical Antisolvent
SCF	Supercritical Fluid
SDS	Sodium dodecyl sulphate
SEDS	Solution Enhanced Dispersion by Supercritical Fluids
SF	Spray freezing
SFL	Spray freezing into Liquid
*t*BuOH	*tert*-Butanol
THF	Tetrahydrofuran

1. Introduction

One out of four orally administered Active Pharmaceutical Ingredients (APIs) possesses too low aqueous solubility to be absorbed in the gastrointestinal (GI) tract (Lindenberg, 2004). Several methods were proposed to enhance the absorption of these APIs, of which the three most important – micronization, preparation of solid dispersions and cyclodextrin complexes – are discussed in chapter 1.3. However, in our case, micronization did not improved dissolution kinetics to the desired extent and cyclodextrins would have multiplied by four the total mass of pharmaceutical ingredients in the formulation. Thus, we decided to prepare solid dispersions (solutions) using various excipients described later, in chapter 1.7. In solid solutions and solid dispersions drug molecules or very fine drug crystals are dispersed in a biologically inert matrix. Dissolution rate and stability of a such formulation are directly related to the amorphous-crystalline ratio and the presence of metastable polymorphs. The methods of preparation and physical properties of crystalline solids are detailed in chapter 1.4. Most technologies developed to prepare solid dispersions i.e. spray-drying, solvent evaporation and hot melt method are known to have inherent limitations, like poor particle recovery yield, high residual solvent content or thermal degradation of the API. To overcome the problems encountered in conventional techniques, three new processes were tested: two antisolvent precipitation using supercritical CO_2 (Supercritical Antisolvent (SAS) and Solution Enhanced Dispersion by Supercritical Fluids (SEDS)) and a cryogenic process called Spray freezing (SF). Properties and applications of supercritical fluids are discussed in chapter 1.5. Chapter 1.5.3 focuses on the main particle engineering technologies giving a general description and literature review of the related techniques. Chapter 1.6 covers the history and presence of the cryogenic particle engineering. Technologies were divided into two groups according to the manner of injection. Inventions with nozzles located above the cryogenic liquid are described in chapter 1.6.1.1, while those involving injection into the cryogenic liquid are reviewed in chapter 1.6.1.2. The literature reviews were focused on drug-carrier systems where carrier was a biologically inert polymer. Results of SAS, SEDS and SF experiments are discussed in chapter 2, 3 and **Hiba! A hivatkozási forrás nem található.**, respectively. Formulations were examined for particle morphology, particle size, flow properties, crystallinity, polymorphic purity, residual solvent content, precipitation yield, drug content, specific surface area and dissolution kinetics. A

comparison was made between the different technologies and summarized in chapter **Hiba! A hivatkozási forrás nem található.** and 4.

1.1 Drug delivery and bioavailability

Throughout the past decade, formulation and delivery of APIs have played a crucial role in the development and commercialization of new pharmaceutical products. The major objective of formulation chemistry is to improve bioavailability, stability and convenience to the patient. Among the several routes of administration i.e.: oral, transdermal, parenteral, intranasal, intravenous, intramuscular, intraocular and subcutaneous; oral administration is still the most popular because it offers improved convenience (painless and simple) and patient compliance. The bioavailability of an orally administered drug depends on its solubility in aqueous media over the pH range of 1.0 – 7.5 and its permeability across membranes of the epithelial cells in the GI tract (FDA, 2002). On the basis of these factors, Amidon et al. introduced the Biopharmaceutics Classification System (BCS) that divides the active substances into four classes (Amidon, 1995).

Table 1.1. The classes of BCS and the percentage distribution of orally administered drugs.

Class	Solubility	Permeability	Distribution
I	High	High	84 %
II	Low	High	17 %
III	High	Low	39 %
IV	Low	Low	10 %

Class I consists of water-soluble drugs that are well absorbed from the gastrointestinal tract and have high bioavailability after oral administration. Drugs in Class II are water-insoluble or slowly dissolving APIs. The absorption of these drugs is dissolution-rate limited. In contrast, drugs in Class III dissolve readily but can not penetrate biomembranes of the GI tract. In the case of Class IV (low aqueous solubility, low permeability) drugs, oral administration is not recommended. Lindenberg et al. assigned 61 out of the 130 orally administered drugs listed in The WHO Model List of Essential Medicines to BCS classes (Lindenberg, 2004; WHO, 2002). The percentage distributions of the considered 61 APIs in BCS classes is shown in Table 1.1.

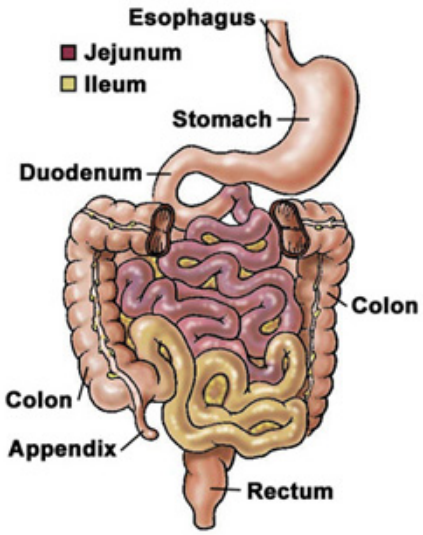

Fig. 1.1 Anatomy of the digestive tract.

Table 1.2 Transit time and pH conditions along the GI tract (Martinez 2002; Fallingborg, 1999; Russel, 1993; Song, 2002).

GI segment	Transit time	pH
Stomach	2 h	3.1 ± 1.9
Duodenum	10 min	6.6 ± 0.5
Jejunum	2 h	7.4 ± 0.4
Ileum	1 h	7.5 ± 0.4
Colon	36 – 72 h	7.0 ± 0.7

After oral administration, pharmaceutical products reach quickly the stomach, passing through the esophagus. Having short transit time, drug absorption does not normally occur in these segments. The stomach has a relatively large epithelial surface, but because of its thick mucous layer, and the comparatively short residence time, absorption is limited. The gastric transit time depends on the particle size, particle density, rate of gastric emptying and prandial state (Martinez, 2002). It was observed that heavy and/or large particles are longer retained in the stomach (Devereux, 1990; Mason, 2002). The rate of gastric emptying is affected by several factors, including age and weight of the patient, volume of liquid intake, volume of solid food intake and its fat content, intake of other drugs, pH of the stomach etc… The variability seen in the absorption of orally administered drugs is mainly due to different rates of gastric emptying. Unlike gastric transit, intestinal residence time is affected neither by particle size nor by prandial state. Additionally,

absorption of virtually all drugs is faster from the small intestine than from the stomach. The small intestine and more particularly, its first segment the duodenum has the largest surface area for drug absorption in the GI tract. In spite of the short transit time, the majority of nutrients, vitamins, and drugs are absorbed in this 20 cm long segment.

1.2 Solubility and dissolution rate

Prior to absorption, solid oral dosage forms must disintegrate and dissolve. The dissolution of an API is governed by thermodynamic and kinetic factors. The most important thermodynamic parameter is the solubility which is the saturation concentration in a given aqueous medium at equilibrium. The intrinsic solubility is an inherent property of a specific substance and cannot be increased unless temperature is changed. The measurement of intrinsic solubility may take several days or months (Briattain, 1995). Actually, in normal protocols, solubility is measured at a metastable equilibrium. The solubility obtained under these conditions is called apparent solubility and is higher than the intrinsic one. As it was discussed in the previous chapter, the time that an API passes in the digestive system is limited. Thus absorption is governed by kinetic factors rather than thermodynamic ones. The dissolution rate is the amount of active substance that leaves the surface of drug crystals and goes into the solution per unit time. According to the modified Noyes-Whitney equation (Eq. 1), the dissolution rate (dm/dt) is proportional to the surface area available for dissolution (A), the diffusion coefficient of the solute in solvent (D), and concentration difference between dissolution front – which is virtually equal to the solubility (C_S) – and the bulk concentration (C); and inversely proportional to the thickness of the diffusion layer (h) (Noyes, 1897).

$$\frac{dm}{dt} = -\frac{AD\ (C_S - C)}{h} \qquad \textit{Eq. 1}$$

1.3 Methods to increase solubility and dissolution rate of APIs

Among the factors in the Noyes-Whitney equation, only surface area and apparent solubility might be manipulated to improve significantly the dissolution rate. Theoretically, increased diffusivity, decreased boundary layer thickness and decreased bulk concentration would also result in faster dissolution but changing *in vivo* transport properties, hydrodynamics and composition of the luminal fluids is actually very difficult. Unlike

these factors, surface area can be increased easily by decreasing the particle size, optimizing the wetting characteristics or modifying the crystal habit of the API. However, the enhancement in dissolution rate attainable by increased surface area is limited. In fact, the most attractive option for increasing the release rate is improvement of the solubility using rapidly dissolving excipients or complexing agents.

1.3.1 Micronization

Micronization enhances dissolution rate by increasing the specific surface area. The point in using small particles is that no inactive pharmaceutical ingredient is needed. However, bioavailability enhancement of poorly water soluble drugs is not the primary application area of micronization technologies. They are more widely used in the pharmaceutical industry to prepare drug particles delivered by inhalation or injection. Depending on the route of administration drug products must fulfill strict requirements concerning the particle size and size distribution, for instance only nanoparticles can be injected intravenously while particles in the range of 1-5 μm and 5 - 100 μm are suitable for pulmonary and subcutaneous delivery, respectively.

Small particles are prepared either by size reduction of large crystals using mechanical means (grinding) or by precipitation of microparticles under controlled conditions. In grinding process, particle size of raw material is reduced by compression, impact or attrition. Mechanical impact mills utilize rotating hammers, pins or beater bars to accelerate and impact particles against another hard surface or other particles. Fluid energy (air jet) mills utilize high velocity gas jets to accelerate particles against a hard surface or against other particles. Grinding is a simple and inexpensive method for the formation of small particles. However, common disadvantages include the evolution of heat upon structural failure, structural changes, difficult to handle electrostatically charged powders, irregular particle shapes, broad size distributions and low efficiency (Ganderton, 1968).

For avoiding these inconveniences one can directly precipitate particles of desired size in a single-step process. This approach involves dissolution of the pharmaceutical ingredient(s) and precipitation of the solute(s) at high supersaturation. When crystallization occurs at high level of supersaturation nucleation dominates over crystal growth and very fine particles are formed. However, in the case of highly crystalline substances, large crystals are obtained even at high supersaturation. Some of the technologies producing micro-sized particles will be discussed later (Spray-drying, liquid antisolvent, SAS, SEDS, GAS, RESS, SFL).

In liquid antisolvent and RESS technologies, crystal growth can be impeded by forming a protective layer of stabilizing agents on the crystal surface (Rasenack, 2002; Rasenack, 2003a; Rasenack, 2003b; Steckel, 2003a; Steckel, 2003b; Rasenack, 2004; Frederiksen, 1994; Pace, 1999; Frederiksen, 1997; Henriksen, 1997; Bausch, 1999; Young, 2000).

The liquid antisolvent (solvent change or in-situ-micronization) method consists of three steps: (1) dissolving the drug in an appropriate solvent as well as dissolving the stabilizing agent in another solvent which is miscible with the first one and is non-solvent for the drug (2) pouring the solution of the stabilizer into the drug solution to induce precipitation, (3) spray-drying of the resulting suspension. In the case of poorly water-soluble drugs, the active substance is dissolved in a water-miscible organic solvent and precipitated upon the addition of the aqueous solution containing the polymer (Rasenack, 2004; Rasenack, 2003b; Steckel, 2003b). Alternatively, both drug and polymer are dissolved in water and the organic solvent plays the role of antisolvent (Rasenack, 2004; Steckel, 2003a). Owing to the instantaneous mixing and the presence of stabilizing agent, powders have small mean particle sizes (~1 μm), uniform size distributions, high specific surface areas, decreased contact angles, good flow and aerosolization properties.

Rasenack et al. (2003b) prepared microcrystals of a poorly water-soluble orally administered API. Authors compared 22 hydrophilic excipients including cellulose ethers, chitosan, gelatin, PVA, PVP K30, etc. Processed powders exhibited enhanced dissolution rate, high degree of crystallinity and high polymorphic purity. Cellulose ethers containing methoxyl or hydroxypropyl groups were proved to form stable and homogeneous dispersions of very fine microcrystals due to their high affinity to the drug surface. Steckel et al. (2003) compared the physical properties and in vitro inhalation behavior of jet-milled, in-situ-micronized and commercial disodium cromoglycate. Jet-milled powders consisted of electrostatically charged, agglomerated particles of large aerodynamic particle size. In contrast, the in-situ-micronized drug showed beneficial dispersion and de-agglomeration properties. The mean particle size of the drug was around 3,5 μm and consequently it was in the respirable range. Vidgrén et al. (1987) studied the same API, processed by mechanical micronization and spray-drying. Spray-dried powders had smaller particle size (1 – 5 μm), higher amorphous drug content and better dissolution kinetics than mechanically micronized ones.

In-situ-micronization in the presence of stabilizing agents offers a versatile method for the production of fast dissolving microparticles for oral and pulmonary delivery. Compared with solid dispersion-, or cyclodextrin-based delivery, the amount of drug in the formulation is high (> 90%). The manufacturing of the microcrystals can be performed continuously (static mixer) and discontinuously as well; and only commonly used, commercially available equipments are needed. However, in vivo dissolution mechanisms of surface-modified microparticles are little known being a relatively new area of particle engineering.

Table 1.3. Particle size ranges of different miconization techniques (Miranda, 1998; Majerik, 2004)

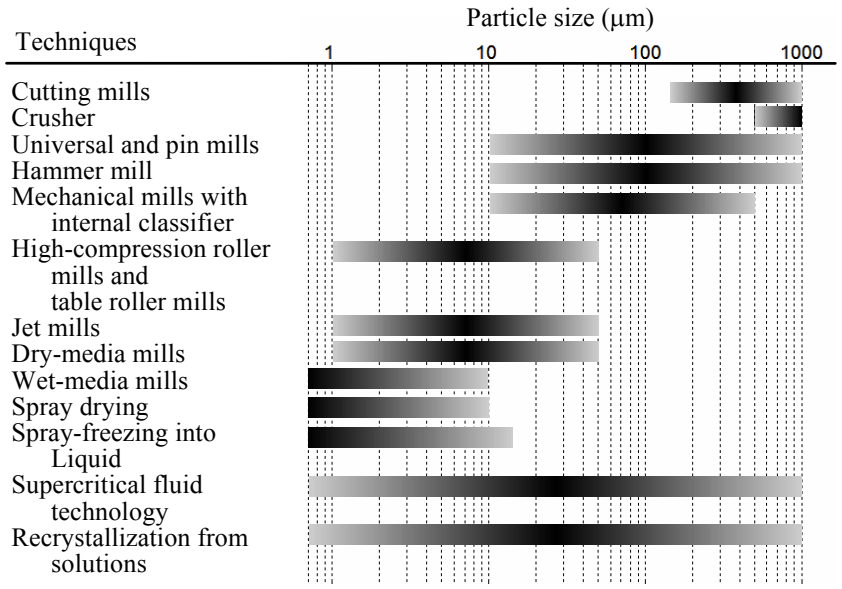

1.3.2 Solid dispersions

In solid dispersions, drug molecules or very fine drug crystals are dispersed in a biologically inert matrix. When the bonding strength between the two components is stronger than the bonding strength between the molecules of the same component, the active and inactive ingredients are miscible in all proportion leading to a continuous solid solution. However, molecular structure and physical properties of APIs and excipients are usually very different, which allows them to form homogenous solid solution only in a limited concentration range. A typical phase diagram of a discontinuous solid solution is shown in Fig. 1.2. When two substances are not miscible in solid state they usually form eutectic mixtures (Fig. 1.3). These systems are similar to a physical mixture of very fine crystals of the two components.

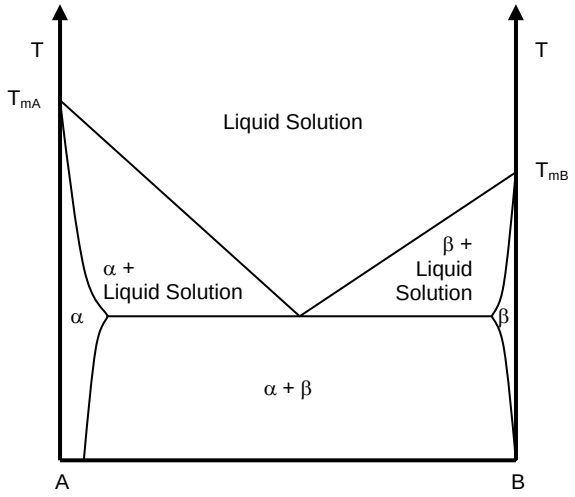

Fig. 1.2. Phase diagram of a discontinuous solid solution (α: solid solution of B in A; β: solid solution of A in B).

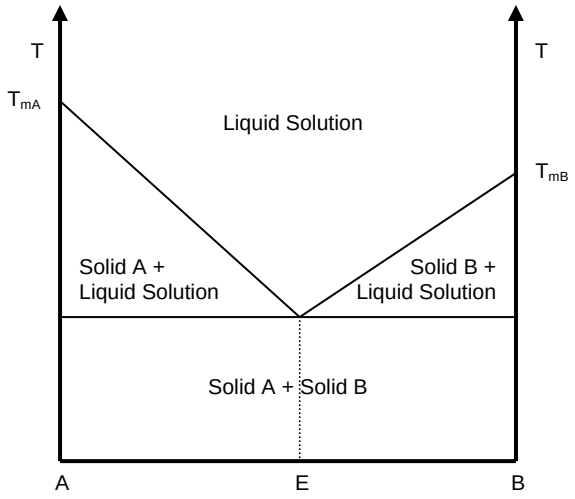

Fig. 1.3. Phase diagram of a binary eutectic mixture

In crystalline solid solutions, the drug molecules can either substitute for excipient molecules in the crystal lattice or fit into the interstices between the excipient molecules (Fig. 1.4). Substitution is only possible when the sizes of drug and excipient molecules differ by less than 15 % or so, which is rarely the case in drug-carrier systems. In interstitial solid solutions, the dissolved molecules occupy the interstitial spaces in the crystal lattice (Fig. 1.4). In this case the drug molecules should have a diameter that is no greater than 59 % and a volume smaller than 20 % of the corresponding parameters of the excipient.

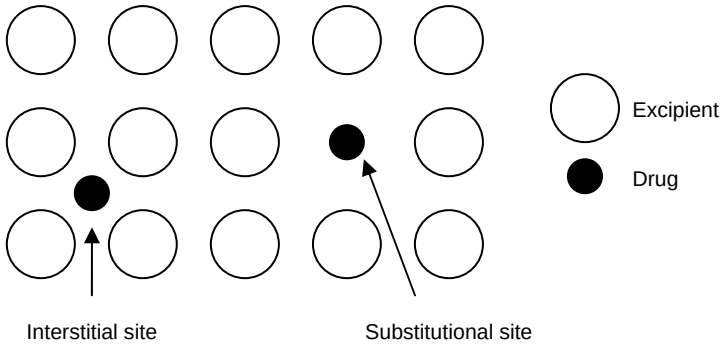

Fig. 1.4. Crystalline solid solution.

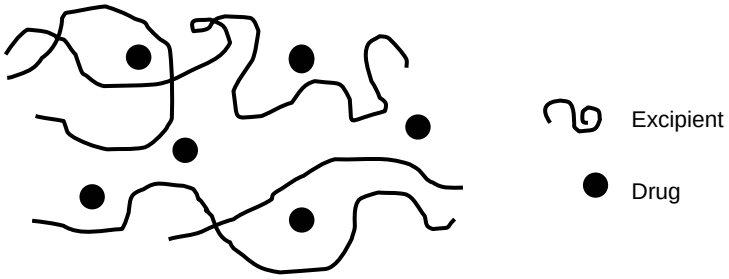

Fig. 1.5. Amorphous solid solution.

In an amorphous solid solution, the solute molecules are dispersed molecularly but irregularly within the amorphous excipient (Fig. 1.5). The determination of the type of solid dispersion requires several analytical methods. The most commonly used are Differential Scanning Calorimetry (DSC), X-ray Diffraction (XRD), Infra Red Spectroscopy (IR, FTIR) and Scanning Electron Microscopy (SEM). XRD provides information about the degree of crystallinity and the polymorphic form but a solid solution cannot be distinguished from a mixture of amorphous pharmaceutical ingredients (Ye, 2000). DSC can be used to determine crystallinity, polymorphism and glass transition temperature. One can find out whether the phase is monotectic or eutectic. However, melting endotherms of crystalline substances are not detectable if the lower melting polymer dissolves the higher melting crystalline ingredients. Weak interactions like H-bonds can be identified by using IR spectroscopy. The broadenings and shifts of IR bands imply drug - polymer interactions inside the solid dispersion (Sethia, 2004). SEM is usually used to study the morphology and microstructure of particles. Local elementary composition can be determined by energy dispersive X-ray (EDX) analyzer which is a common accessory of SEM apparatuses (Taki, 2001). One can obtain further information

about solid dispersions using solid state Nuclear Magnetic Resonance (NMR) and Transmission Electron Microscopy (TEM) (Vaughn, 2005).

Although, several potential and realized advantages of solid dispersions have been described in the literature, the most important one is still the improvement in dissolution rate. In spite of the remarkable enhancement achieved with solid dispersions, the governing mechanism of their dissolution is poorly understood. Craig pointed out that two mechanisms may be of relevance, involving either carrier or drug controlled release (Craig, 2002). In a carrier-controlled system the dissolution rate of the solid dispersion is virtually equal to that of pure excipient. Beneath Corrigan et al., who measured not only the dissolution rate of the embedded drug but also that of excipient, several authors have observed similar dissolution characteristics (Corrigan, 1985 and 1986; Dubois, 1985; Craig, 1992). However, at high drug loading it is the dissolution rate of the API that dominates. To predict the D/P ratio where carrier-controlled release is changing to drug-controlled release Corrigan recommended the model of Higuchi (Corrigan, 1985; Higuchi, 1965, 1967). This model applies the Noyes-Whitney equation for a two-component system where both components dissolve at rates proportional to their solubility and diffusion coefficient. This approach implies that the interfacial layer between the dissolving front and the solvent will be rich in the rapidly dissolving component and the slower dissolving component has to diffuse through this surface layer. Applying this model to drug-carrier systems, the dissolution of a solid dispersion is carrier-controlled if,

$$D / P < \frac{D_D C_{SD}}{D_P C_{SP}} \qquad \textit{Eq. 2}$$

where *D/P* is the drug/polymer ratio, *D* is the diffusion coefficient, *C* is the solubility and the indexes *D*, *P* and *S* refer to the drug, the polymer and the equilibrium solubility, respectively. In this case the dissolution rate of the carrier is

$$\frac{dm_P}{dt} = -\frac{AD_P\left(C_{SP} - C_P\right)}{h} \qquad \textit{Eq. 3}$$

While the dissolution rate of the drug is

$$\frac{dm_D}{dt} = D / P \frac{dm_P}{dt} \qquad \textit{Eq. 4}$$

In other words, the release rate of the incorporated drug is dominated by the dissolution behavior of the carrier. Sjökvist-Saers et al. (1992) studied the solubility,

melting and dissolution behavior of methyl, ethyl, propyl and butyl p-aminobenzoates alone or dispersed in PEG 6000 by the fusion method. The initial dissolution rates of both pure drugs and solid dispersions were directly proportional to the solubility of pure APIs. Furthermore, the initial dissolution rate of formulations with a drug loading higher than 20 % or so were lower compared to that with 10 % drug and were virtually independent of composition suggesting that the limit of carrier- and drug-controlled release is between 10 and 20 % drug content. The authors proposed a model whereby at low concentrations the drug is released into the medium as individual particles and dissolution occures over a large surface area; while at higher drug levels, the drug forms a continuous diffusion layer over the dissolving surface. However this model does not provide any explanation for drug-controlled dissolution behavior at low drug loadings. In 2002, Craig has completed this theory by proposing two scenarios for formulations with low drug levels. The process associated with carrier-controlled dissolution is shown in Fig. 1.6a. The model works on the premise that the dissolution rate of drug in polymer-rich diffusion layer is faster than the migration of the dissolution front. This allows embedded drug particles to dissolve and form molecular dispersion prior to release even if it was not the case in solid state. As the polymer-rich diffusion layer has a high viscosity, the diffusion of drug is very slow and it can reach the bulk solution only when the surface layer is completely dissolved. Thus, the rate-limiting step is the dissolution of the carrier matrix. If the migration of dissolution front is faster compared to the dissolution rate of drug in the surface layer the drug is released as solid particles (Fig. 1.6b). Even though the dissolution rates of these systems are drug-controlled, excipients have some beneficial effect on dissolution kinetics, like improved stability, increased surface area and better wettability.

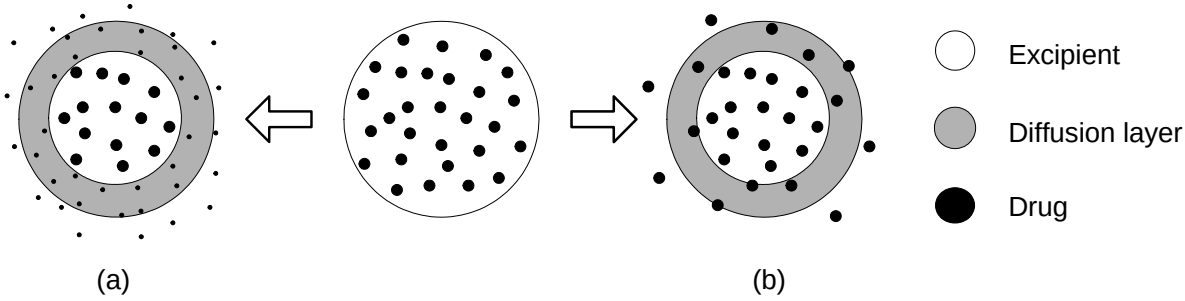

Fig. 1.6. Possible dissolution mechanisms at low drug loadings (Craig, 2002).

However, the mechanism of dissolution is not the only point left to clarify. Amorphous state was considered for long time as unsuitable for pharmaceutical application due to the inherent stability problems (Debenedetti, 2002). Amorphous formulations of drug substrates having low glass transition temperature (T_g) were proved to undergo recrystallization during storage to get in lower free energy state. The nature of these processes (structural relaxation) and their intrinsic kinetics are not well understood. Spontaneous crystallization of an active substance may decrease its dissolution rate and occasionally result in metastable polymorphs. The use of polymers with a high glass transition temperature for the formulation of solid dispersions is often sufficient to prevent crystallization. These amorphous polymer matrices reduce considerably the molecular mobility of the incorporated APIs which are in most cases linked by weak interactions such as H-bonds to the polymers (Khougaz, 2000; Matsumoto, 1999). However, the basis of this stabilization on a molecular level is not yet clearly understood. In addition, solid dispersions are often sensitive to water sorption, mechanical and thermal stresses. Thus, stability assessment (shelf life study) of solid dispersions is a crucial point of the development of such systems.

Basically, solid dispersions can be prepared by melting and solvent methods. In the melting method (hot melt method), a physical mixture of drug and carrier is melted and solidified by rapid cooling. Melting method is a simple and economic technology that does not requires any organic solvent. However, it has two important limitations. First, pharmaceutical ingredients must be miscible in the molten form. When there are miscibility gaps in the phase diagram, product will not be molecularly dispersed. The other limitation is the thermostability of the drug and the carrier. Heat-sensitive APIs (peptides, DNA) as well as polymers may undergo thermal degradation at high temperatures (Dubois, 1985). As polymers in high pressure or supercritical CO_2 melt at lower temperatures the degree of thermal degradation can be limited by using PGSS technology.

In the solvent method, solid dispersions are obtained by removing solvent from a solution containing both pharmaceutical ingredients. Solvent can be removed by evaporation (solvent evaporation, spray-drying, EPAS), lyophilization (freeze-drying, SFL) or extraction using supercritical antisolvents (SAS, SEDS, GAS). Tachibani et al. (1965) were the first to use solvent evaporation under reduced pressure to produce a solid solution. Previously solid solutions were prepared exclusively by the melting method. With the discovery of the solvent method, many of the problems associated with the melting method

were solved. Firstly, it is possible to form solid dispersions of thermolabile APIs and polymers with high melting points (e.g.: PVP) since the working temperatures usually range from 23 to 65 °C in solvent evaporation and from 35 to 60 °C in supercritical antisolvent methods (Leuner, 2000). Evidently, freeze-dried formulations do not undergo any thermal degradation as they are exposed to temperatures higher than ambient only during the secondary drying but 40 °C is rarely exceeded. As most of these technologies involve atomization of the feed solution, micronized dry powder can be obtained in a single-step process. However, the rate of solvent removal directly affects the physicochemical properties of the solid dispersion and may be difficult to control. Sometimes, small variations in the manufacturing conditions lead to quite large changes in product performance. Furthermore, these methods require a solvent in which both active substance and carrier are sufficiently soluble. As excipients are hydrophilic while Class II APIs are generally hydrophobic substances, the solubility of either or both may be limited in one common solvent. In the EPAS process, the drug is dissolved in a low boiling organic solvent; this solution is heated under pressure above the solvent's boiling point and sprayed into a heated aqueous solution (Sarkari, 2002). The rapid evaporation of the organic solvent leads to high supersaturation. One or more stabilising surfactants can be added to the organic and/or the aqueous solution in order to stabilize the particles by preventing crystallization and agglomeration. Vaughn et al. (2005) compared the physical properties of EPAS and SFL prepared danazol/PVP K15 powders. Although, the authors have increased dissolution rates by using both methods SFL exhibited better dissolution kinetics and more homogenous structure. Bitz et al. (1996) prepared pure and drug-loaded PLA and PLGA microparticles using spray-drying, (w/o)w solvent evaporation and ASES method in order to study the influence of preparation method on residual solvent content and other physical properties. The smallest mean particle size was achieved using spray-drying (2.4 – 3.6 μm) followed by ASES process (5.2 – 5.4 μm). Solvent evaporation from (w/o)w emulsion resulted in particles of slightly higher diameters (12.5 – 14.2 μm). Spray-dried batches showed high encapsulation efficiencies (87.0 – 95.6 %) and low residual DCM and MeOH contents. However, rather poor yields were achieved when using spray-drying (33 – 55 %) which is in agreement with other studies (Conte, 1994; Raffin Pohlmann, 2002). In spray-drying technology, product recovery is a challenging task as submicron particles are difficult to separate from exhaust gas and dry powder usually adheres on the apparatus elements.

1.3.3 Complexation (Cyclodextrins)

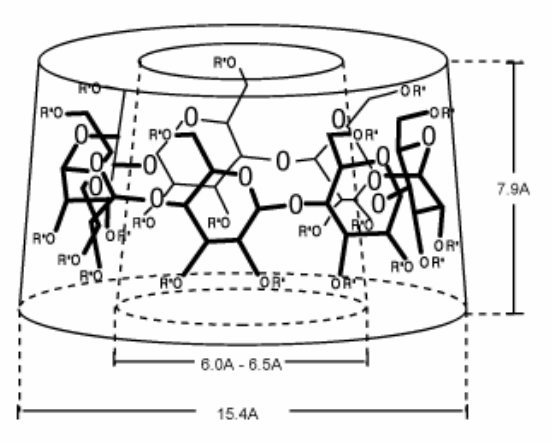

Fig. 1.7. 3-D sketch of β-CD derivatives.

Cyclodextrins (CDs) are cyclic oligosaccharides, consisting of glucopyranose (Glc) units linked through β (1-4) glycosidic bonds (Fig. 1.7). The most common naturally occurring CDs are α,β, and γ CDs containing 6,7 and 8 glucopyranose units, respectively. Due to its higher stability glucose units are in chair conformation with all the hydroxy and methoxy groups in equatorial position. Hence, the outside of surface of the ring is hydrophilic, while the internal cavity is slightly lipophilic. This amphiphilic nature together with its toroidal shape enables CDs to form inclusion complexes with guest molecules of appropriate size (Foster, 2002, Charoenchaitrakool, 2002). The solubility of these complexes depends virtually only on the solubility of pure CD excipient. During the past decade a huge number of chemically- and enzyme-modified CD derivatives were synthesized to find more and more hydrophilic CDs (Szente, 1999). The aqueous solubility of some methylated,- hydroxypropylated,- sulphated,- sulfobutylated, and branched (glucosyl- and maltosyl-β-CD) β-CDs derivatives exceeds 600 g/l. In addition, CDs reduce local irritation and enhance the stability and bioavailability of incorporated drugs. Some of these excipients have further attractive properties like anti-virial and anti-inflammatory effects (sulphated β-CDs). In oral administration only the free drug molecule, which is in equilibrium with the complexed form is capable of crossing the GI membrane (Uekama, 1999). While in pulmonary route, both free drug molecule and inclusion complex are absorbed (Nakate, 2003). Even though CD-derivatives seem to be ideal carriers they have some limitations. The main drawback of CD-based drug delivery is the 1:1 stoichiometric ratio that results in low drug-carrier weight ratio. To solubilize one mole active substance at least one mole CD is necessary, but the quantity of required CD increases with the molecular weight of the active substance (Nakate, 2003).

In 2002, Perrut et al. patented two processes using supercritical fluid or liquefied gas with the aim of preparing inclusion complexes of APIs and cyclodextrin-type host molecules (Perrut, 2002a, 2002b). In one of these methods, SCF antisolvent is mixed with a solution containing the drug and the CD in a premixing chamber (0.5 cm^3) and the resulting mixture is dispersed in a precipitation vessel through a narrow nozzle (60 μm i.d.) (Perrut, 2002a). The other process involves a pressurized vessel containing the API-CD physical mixture (Perrut, 2002b). The vessel is filled with SCF or liquefied gas and stirred for a while (8-30 min) so that the drug molecules diffuse through the SCF phase in the cavities of CD molecules. Freiss and Lochard have improved this method by wetting the API-CD physical mixture prior to pressurization (Freiss, 2003a, 2003b, Lochard, 2003, 2004, Rodier, 2005). Inventors prepared γ-cyclodextrin/eflucimibe inclusion complexes in a three step process comprising 1, a supercritical antisolvent precipitation (SAS), 2, a "maturation" or static step (6 h) and 3, a solvent stripping step (2 h). Although, eflucimibe exhibited very low solubility (100 mg/L from physical mixture after 20 h) dissolution curves reached 500 mg/L after the static step and 700 mg/L after static step and solvent stripping.

1.4 Crystallization

1.4.1 Thermodinamic background

A crystal is defined as a solid composed of atoms or molecules arranged in an orderly, repetitive array. Crystallization is an important process in pharmaceutical industry because a large number of pharmaceutical products are marketed in crystalline form. Crystallization may be carried out from vapor, melt or solution. Most industrial applications of the operation are solution-based crystallization. There are two steps involved in crystallization process from solution: (1) nucleation, i.e. formation of new solid phase and (2) growth, i.e. increase in the size of the nucleus. The rate of nucleation plays an important role in controlling the final particle size distribution; this step is the most complex and still the most poorly understood. Nucleation process is composed of primary homogenous, primary heterogeneous and secondary nucleation (Dirksen, 1991). Primary nucleation is prevailing in supersaturated solutions free from solute particles. Homogenous primary nucleation occurs in the absence while the heterogeneous one occurs in the presence of a solid interface of a foreign seed. In practice, primary heterogeneous nucleation is more important, because nucleation on a foreign surface takes place at lower critical supersaturation. However, once the heteronuclei are used up, heterogeneous

nucleation stops, thus the maximum possible heterogeneous nucleation rate is limited (Perry, 1984). Secondary nucleation refers to several mechanisms of nuclei production which have all in common mechanical aspects induced by the stirring of the medium and the interaction between the crystals already present and their environment: fluid, stirrer, reactor wall and other crystals. Secondary nucleation is predominant in continuous industrial crystallizers operated at low supersaturation levels. On the contrary, at high level of supersaturation, primary nucleation is the main source of nuclei.

Both nucleation and crystal growth have supersaturation as common driving force. The level of supersaturation is characterized by the saturation ratio (S) which means the ratio of the actual concentration to the equilibrium concentration of the solute.

$$S = \frac{C}{C_S} \qquad \textit{Eq. 5}$$

The phase change associated with crystallization and precipitation processes can be explained by thermodynamic principles. When a substance is transformed from one phase to another, the change in the molar Gibbs free energy (ΔG) of the transformation, at constant pressure and temperature, is given by

$$\Delta G = \left(\mu_1 - \mu_2\right) \qquad \textit{Eq. 6}$$

where μ_1 and μ_2 are the chemical potentials of phase 1 and phase 2, respectively. In crystallization process, Gibbs free energy can also be expressed in terms of supersaturation.

$$\Delta G = -RT \ln S \qquad \textit{Eq. 7}$$

When $C>C_S$, $\Delta G<0$ crystals are growing in the supersaturated solution. Alternatively, when $C<C_S$, $\Delta G>0$ crystals are dissolving. In equilibrium $C = C_S$, $\Delta G = 0$ and the solution is saturated.

Classical theories of primary homogenous nucleation assume that solute molecules in a supersaturated solution combine to produce embryos. In a supersaturated solution embryos larger than the critical size become stable nuclei which grow to form macroscopic particles. The critical nuclear size is defined as follows

$$r^* = \frac{2\beta_a \gamma v}{3\beta_v k_B T \ln S} \qquad \textit{Eq. 8}$$

where β_a and β_v are the surface and volume conversion factors, respectively (β_a = surface area/r^2 and β_v = volume/r^3); k_B is the Boltzmann constant, ν is the molecular volume of the precipitated embryo and γ is the surface free energy per unit area. For a given value of S all particles with $r > r^*$ will grow and all particles with $r < r^*$ will dissolve.

Crystal growth is a layer-by-layer process that occurs only at the face of the crystal, so that material must be transported to that face from the bulk of the solution. Crystal growth consists of the two steps: diffusion of molecules to the growing crystal face and integration of molecules into the crystal lattice. In fact, different faces have different rates of growth. The ratio of these growth rates as well as the geometry of the unit cell determine the final crystal habit. The shape of a crystal can be either thermodynamically or kinetically controlled. The thermodynamically controlled one is only important for crystals grown at very low saturation ratios. In most cases, kinetic factors are governing crystal growth i.e. fast-growing faces disappear and slow faces dominate the final shape (overlapping principle). There are several methods that aim to modify the shape: combination of two or more forms, crystal twinning, crystallization under controlled conditions (i.e.: temperature) or in presence of additives and trace impurities.

In solution based crystallization, drug is dissolved in solution, and supersaturation is induced by mechanical means which finally leads to precipitation. There are several ways to induce supersaturation in a solution including heating, cooling, evaporation and addition of a third component (non-solvent, precipitant or reactant) (Table 1.4). The possible paths of cooling and antisolvent crystallization processes are shown in Fig. 1.8 and Fig. 1.9. Both diagrams are divided into three domains. In the stable region concentration of solute is below the solubility ($C<C_S$, $\Delta G>0$); neither nucleation nor crystal growth occurs in this zone. In the metastable region, the system is not in equilibrium; still the driving force is too low to induce nucleation ($C>C_S$, $\Delta G<0$, $r<r^*$). However, if seed crystals are added to the solution they provide surface area for crystal growth and nucleation (Fig. 1.8a). Seeding is widely used for preparing relatively large but easy-to-handle crystals because it allows controlling the size and number of crystals produced, as well as the polymorphic form. In the labile zone ($C>C_S$, $\Delta G<0$, $r>r^*$), spontaneous homogeneous nucleation and crystal growth occur simultaneously (Fig. 1.8b). High nucleation rates lead to very fine particles which are often difficult to separate from mother liquor and show high tendency to aggregate.

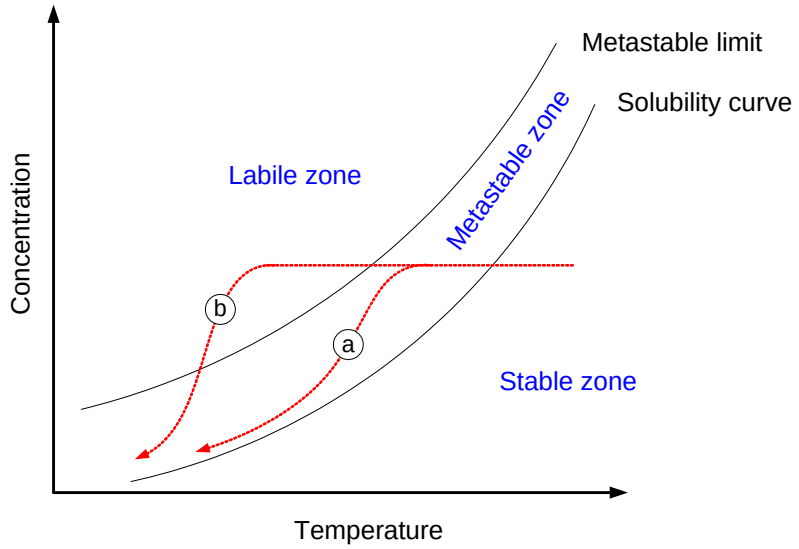

Fig. 1.8. The paths of (a) seeded and (b) unseeded cooling crystallization.

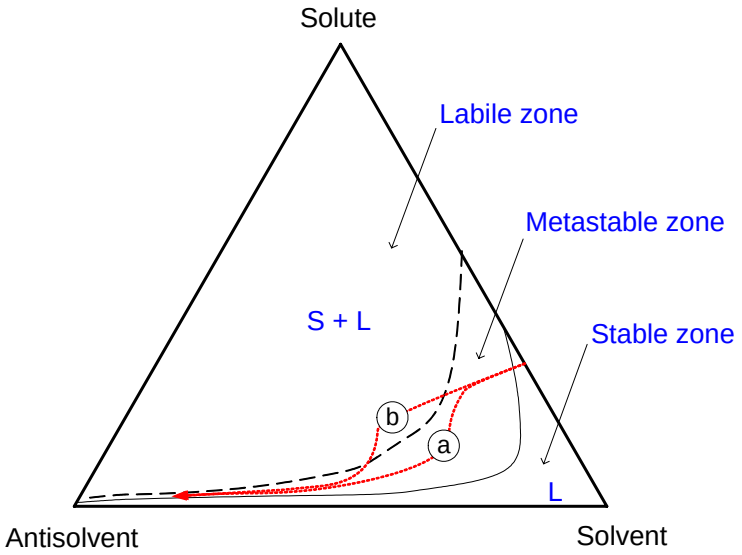

Fig. 1.9. The paths of (a) seeded and (b) unseeded antisolvent crystallization.

Table 1.4. Operating principles of different crystallizers.

Operating principles	Mechanisms
Cooling	↘ Temperature ⇨ ↘ Solubility [a]
Heating	↗ Temperature ⇨ Solvent evaporation ⇨ ↗ Concentration ⮑ ⇨ ↘ Solubility [b]
Vacuum	↘ Pressure ⇨ Solvent evaporation ⇨ ↗ Concentration ⮑ ↘ Temperature ⇨ ↘ Solubility
Antisolvent	+ Antisolvent ⇨ ↘ Solubility
Precipitant	+ Precipitant ⇨ ↘ Solubility
Chemical reaction	+ Reactant ⇨ Chemical reaction ⇨ Insoluble product

[a] the solubility is proportional to the temperature; [b] the solubility is inversely proportional to the temperature;

1.4.2 Polymorphism

Some materials may exist in more than one crystal structure, this is called polymorphism. Nowadays, more than 50 % of the APIs are known to exist in several crystal forms as polymorphs or pseudopolymorphs (hydrates or solvates) or both. Although, polymorphs are identical in the liquid and vapour states, owing to the same chemical composition, they may exhibit different physical and chemical properties such as melting point, density, solubility, crystal morphology and habit, physical and chemical stability, dissolution kinetics and spectroscopic behavior. Two polymorphs can form an enantiotropic or a monotropic system and phase transitions can be observed, as described below.

In **enantiotropic systems** each form has a temperature range over which it is stable with respect to the other form. A schematic Gibbs free energy diagram of an enantiotropic system is shown in Fig. 1.10. The free energy curves of the two enantiotropic forms (A, B) intersect below the melting points (T_{mA} and T_{mB}) when plotted against temperature. The x-coordinate of the point of intersection is (T_{AB}) is called transition point. The form showing the smaller free energy at a given temperature is the most stable form. For a temperature below T_{AB}, form A is stable and form B is metastable while the contrary is true above T_{AB}. The solubility versus temperature curves also intersect in the transition point. The stable form exhibits lower solubility.

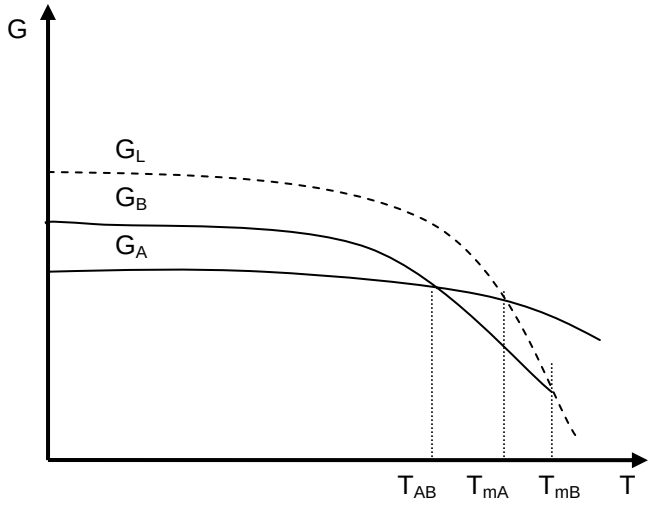

Fig. 1.10. Free energy versus temperature diagram for an enantiotropic system.

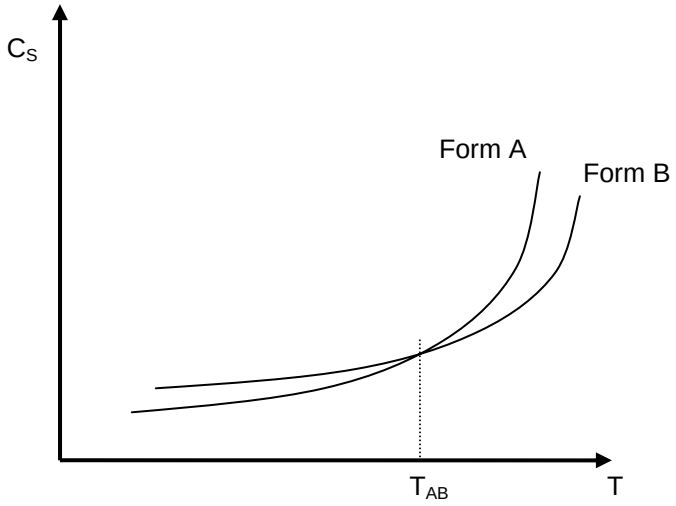

Fig. 1.11. Solubility versus temperature curves for an enantiotropic system.

In a **monotropic system** one form is metastable with respect to the other form at all temperatures. There is no observable transition point, although thermodynamics imply a theoretical transition point above the melting point. The free energy curves of such systems do not intersect below the melting points (Fig. 1.12), neither do their solubility curves (Fig. 1.13).

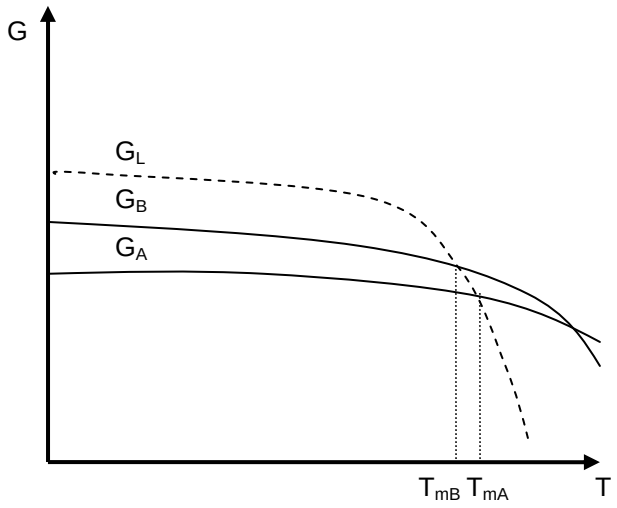

Fig. 1.12. Free energy versus temperature diagram for a monotropic system.

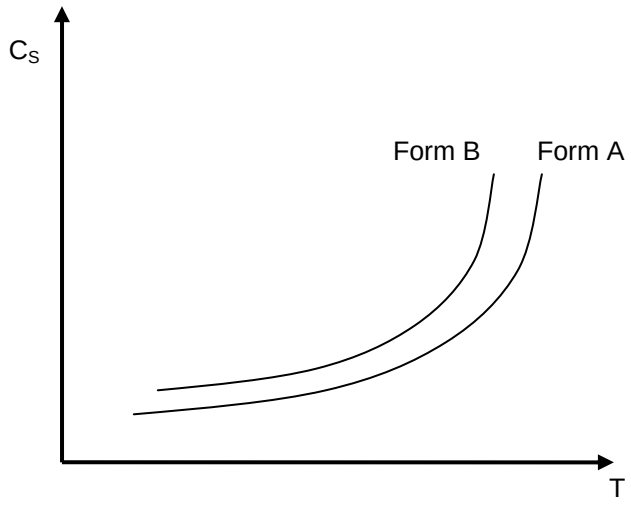

Fig. 1.13. Solubility versus temperature curves for a monotropic system.

The term **pseudopolymorphism** characterizes substances incorporating solvent in their crystal lattice. These substances are also called solvates or hydrates, if water molecules are part of the crystal structure. Like polymorphs, different pseudopolymorphs of one substance can have different physical properties. However, due to the incorporation of solvent, pseudopolymorphs are chemically not identical, and therefore not only the physical properties may be different, but also the chemical ones.

1.5 Supercritical fluid technology

1.5.1 Physico-chemical characteristics of supercritical fluids

The supercritical fluid phenomenon was first observed by Cagniard de la Tour in 1822. A cannon was field with a substance in both liquid and vapor phase, closed and heated. Above a certain temperature splashing of liquid phase has ceased in the shaken cell indicating that the substance formed one single phase. Moving upwards along the gas-liquid coexistence curve the density of liquid phase gradually decreases owing to the thermal expansion while density of the gas phase increases owing to its high compressibility and increased pressure (Fig. 1.14). The densities of the two phases converge and become equal in the critical point. Beyond the critical point the substance exists as a single phase, called supercritical fluid. The critical point is defined by the critical pressure (P_c) and the critical temperature (T_c), their values are specific to each compound.

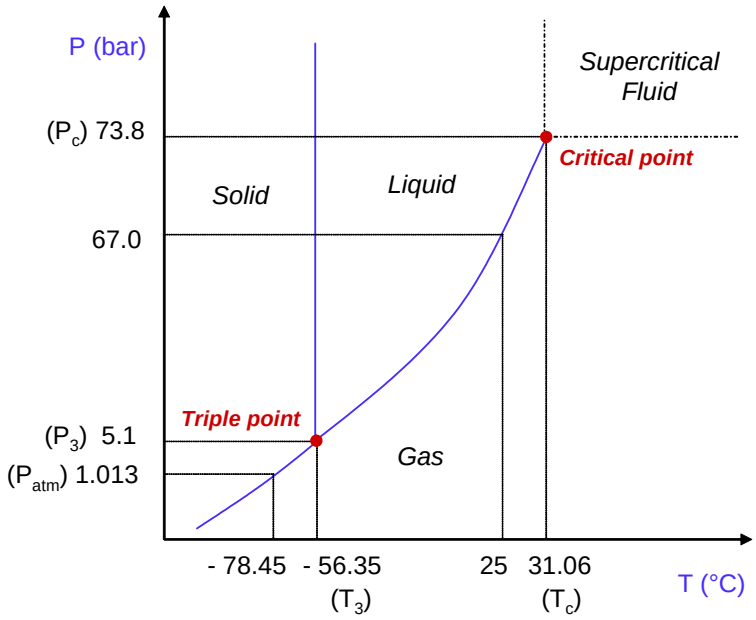

Fig. 1.14. Phase diagram of CO_2.

Critical pressures, critical temperatures and acentric factors of CO_2 and solvents used in this work are listed in Table 1.5.

Table 1.5. Critical properties and acentric factors (Aspen Properties®).

Components	P_c (bar)	T_c (K)	ω
Carbon dioxide	73.83	304.2	0.2236
Ethanol	61.37	514.0	0.6436
Methanol	80.84	512.5	0.5658
Tetrahydrofuran	51.90	540.2	0.2254
Dichloromethane	60.80	510.0	0.1986
Chloroform	54.72	536.4	0.2219
N-methyl-2-pyrrolidone	45.20	721.6	0.3732
Dimethylsulfoxide	56.50	729.0	0.2805
tert-Buthanol	39.72	506.2	0.6152

There are drastic changes in some important properties like density, viscosity, thermal conductivity, surface tension and constant-pressure heat capacity of a pure substance near the critical point (Fig. 1.15). Similar behavior can be observed for liquid mixtures as they approach the critical loci, as well.

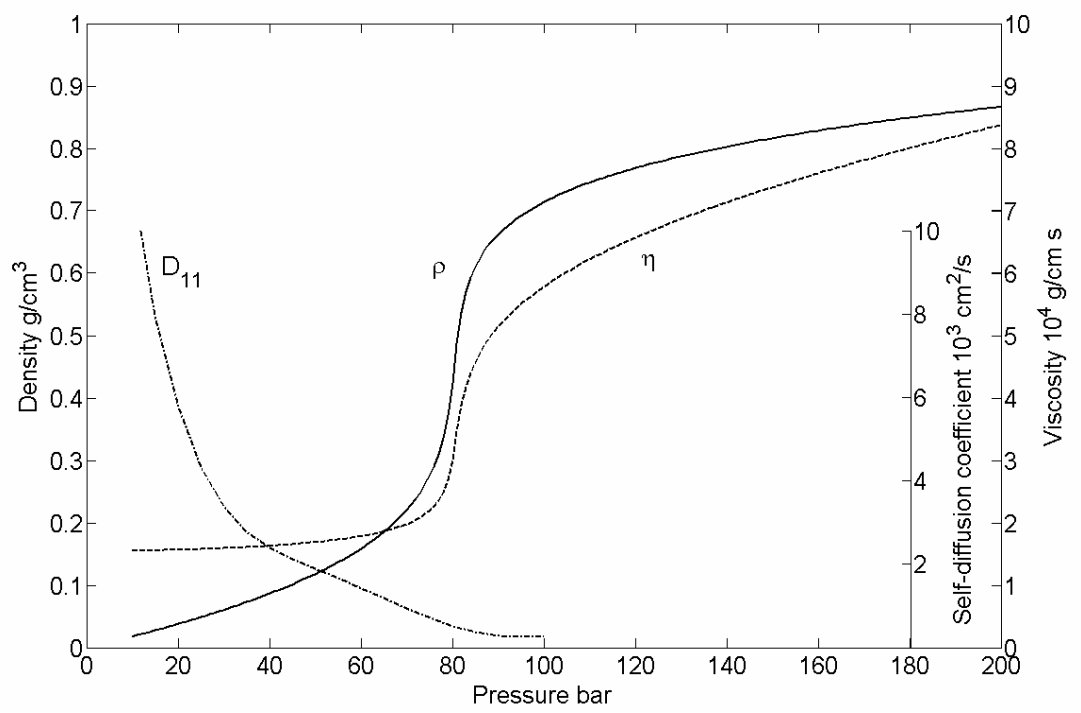

Fig. 1.15. Density (ρ), viscosity (η) and self-diffusion coefficient (D_{11}) of CO_2 at 35 °C (Huang, 1985; Fenghour, 1998; O'Hern, 1955,).

In the critical region, fluids are highly compressible; their densities vary between liquid-like and gas-like values as a function of pressure and temperature. Most of the processes using SCFs exploit their enhanced transport properties due to their gas-like viscosity, liquid-like solvent power and intermediate diffusivity as well as the possibility to tune these properties by controlling the pressure and temperature (Table 1.6).

Table 1.6. Diffusion coefficient, density and viscosity of gases, liquids and SCFs.

	D_{12} [cm^2/s]	ρ [g/cm^3]	η [g/cm s]
Gas	10^{-1}	10^{-3}	10^{-4}
SCF	10^{-3}	0.2 – 1	10^{-4}-10^{-3}
Liquid	10^{-6}	1	10^{-2}

In addition, SCFs exhibit almost zero surface tension, which allows easy penetration into microporous materials. As a result of advantageous combination of physicochemical properties, the extraction process can often be carried out more efficiently with supercritical than with organic liquid solvent. The transition from supercritical to "subcritical" region by decreasing either the pressure or the temperature is continuous. In

fact, the subcritical liquid region has many of the characteristics of the supercritical fluids and is usually exploited in a similar way.

The relationship between pressure, temperature and density is described by the equations of state (EOSs). The goals of using EOSs are both the correlation of existing data and the prediction of data in regions where experimental results are not available. However, existing theoretical models result in poor accuracy because of the highly non-ideal behavior of SCFs. Thus, the great majority of EOSs are empirical or semi-empirical. These models contain several parameters that are fitted to experimental results, and depending on the model and the number of parameters very high accuracy can be obtained over a wide range of temperatures and pressures. The most widely used empirical equation for pure CO_2 was published by Bender (Bender, 1971). His model aimed to predict the density of $scCO_2$ with high accuracy by using a polynomial equation with 20 coefficients (Eq. 9).

$$P = \rho T\left\{R + \rho\left(a_1 + \frac{a_2}{T} + \frac{a_3}{T^2} + \frac{a_4}{T^3} + \frac{a_5}{T^4}\right) + \rho^2\left(a_6 + \frac{a_7}{T} + \frac{a_8}{T^2}\right) + \rho^3\left(a_9 + \frac{a_{10}}{T}\right) + \rho^4\left(a_{11} + \frac{a_{12}}{T}\right) + \rho^5\left(\frac{a_{13}}{T}\right) + \rho^2\left(\frac{a_{14}}{T^3} + \frac{a_{15}}{T^4} + \frac{a_{16}}{T^5} + \rho^2\left(\frac{a_{17}}{T^3} + \frac{a_{18}}{T^4} + \frac{a_{19}}{T^5}\right)\right)e^{\left(-a_{20}\rho^2\right)}\right\} \quad \textit{Eq. 9}$$

Huang et al. (1985) have published another EOS for CO_2 which was a combination of an analytical part, similar to the form used by Bender, and a non-analytical part, in the form of Wagner's function (Eq. 10 - Eq. 12). All the 27 coefficients of the equation were determined by fitting the model to P-V-T, vapor pressure and thermal data. The model was found to be suitable to calculate the density in the temperature range of 216 – 423 K up to 3100 bar with an accuracy between 0.1 and 1 %.

$$\begin{aligned} Z = \frac{P}{\rho RT} &= 1 + b_2\rho_r + b_3\rho_r^2 + b_4\rho_r^3 + b_5\rho_r^4 + b_6\rho_r^5 \\ &+ b_7\rho_r^2\exp\left(-c_{21}\rho_r^2\right) + b_8\rho_r^4\exp\left(-c_{21}\rho_r^2\right) \\ &+ c_{22}\rho_r\exp\left[-c_{27}(\Delta T)^2\right] \\ &+ c_{23}\,\Delta\rho/\rho_r\exp\left[-c_{25}(\Delta\rho)^2 - c_{27}(\Delta T)^2\right] \\ &+ c_{24}\,\Delta\rho/\rho_r\exp\left[-c_{26}(\Delta\rho)^2 - c_{27}(\Delta T)^2\right] \end{aligned} \quad \textit{Eq. 10}$$

$$\Delta T = 1 - T_r \qquad \textit{Eq. 11}$$

$$\Delta \rho = 1 - 1/\rho_r \qquad \textit{Eq. 12}$$

Although these empirical equations provide near approximation to experimental results, they are limited to one or some substances. However, in SCF application, a single-component system is very rare. In most cases, phase equilibriums of multi-component systems like SCF – solute and SCF – solute – solvent are considered. These calculations require more general models.

The most widely used EOSs for mixtures are the semi-empirical cubic EOSs. These models require little input information (critical pressure (T_c), critical temperature (P_c) and acentric factor (ω) of the pure components and the binary interaction parameters (k_{ij}, l_{ij})) and the same EOS can be used for both pure fluids and mixtures. The general form of cubic EOSs is (Holderbaum, 1991):

$$P = \frac{RT}{\upsilon - b} - \frac{a}{(\upsilon + \lambda_1 b)(\upsilon + \lambda_2 b)} \qquad \textit{Eq. 13}$$

where the mixing parameters *a* and *b* are calculated assuming that in the critical point the first and the second derivatives of pressure with respect to volume is equal to zero. *b* is related to the size of hard sphere, it is equal to the molar volume at infinite pressure; *a* represents the intermolecular attraction force. The parameters of the most widely used EOSs are listed in Table 1.7.

Table 1.7. Parameters of cubic EOSs.

Equation	λ_1	λ_2	a	b	Reference
Van der Waals	0	0	$\frac{27}{64}\frac{R^2T_c^2}{P_c}$	$\frac{RT_c}{8P_c}$	Van der Waals, 1873
Redlich-Kwong	1	0	$0.42748\ \frac{R^2T_c^{2,5}}{P_cT^{0,5}}$	$0.08664\frac{RT_c}{P_c}$	Redlich, 1949
Soave	1	0	$0.42748\frac{R^2T_c^2}{P_c}\alpha(T_r)$	$0.08664\frac{RT_c}{P_c}$	Soave, 1972
Peng-Robinson	$1+\sqrt{2}$	$1-\sqrt{2}$	$0.45724\frac{R^2T_c^2}{P_c}\alpha(T_r)$	$0.0778\frac{RT_c}{P_c}$	Peng, 1976

The temperature dependence of the *a* parameter in Soave and Peng-Robinson equations is:

$$\alpha(T_r) = \left[1 + \kappa(1 - \sqrt{T_r})\right]^2 \qquad \textit{Eq. 14}$$

where κ for the Soave equation is:

$$\kappa = 0.48 + 1.574\omega - 0.176\omega^2 \qquad \textit{Eq. 15}$$

for the Peng-Robinson equation:

$$\kappa = 0.37464 + 1.54226\omega - 0.26992\omega^2 \qquad \textit{Eq. 16}$$

The acentric factor of the pure components are derived from the vapor pressure data and the basic definition of the acentric factor is:

$$\varpi_i = -\log\left(\frac{P_i^{sat}}{P_{c,i}}\right)_{T_{r,i}=0,7} - 1 \qquad \textit{Eq. 17}$$

To apply the EOS for mixtures, *a* and *b* parameters have to be calculated using mixing rules. The traditional van der Waals "one-fluid" mixing model is:

$$a = \sum_i \sum_j x_i x_j a_{ij} \qquad \textit{Eq. 18}$$

$$b = \sum_i \sum_j x_i x_j b_{ij} \qquad \textit{Eq. 19}$$

The unlike interaction parameters a_{ij} and b_{ij} are related to the corresponding pure-component parameters by the following combining rules (vdW II):

$$a_{ij} = \sqrt{a_i a_j}\left(1 - k_{ij}\right) \qquad \textit{Eq. 20}$$

$$b_{ij} = \frac{b_i + b_j}{2}\left(1 - l_{ij}\right) \qquad \textit{Eq. 21}$$

The fugacity coefficient (φ) of component *i* in the mixture is:

$$\ln\varphi_i = \left(\frac{\partial n_T \ln\varphi}{\partial n_i}\right)_{T,P,n_{j\neq i}} \qquad \textit{Eq. 22}$$

$$\ln \varphi_i^F = \frac{\bar{b}_i}{b}(z-1) - \ln\frac{P(\upsilon - b)}{RT} - \frac{a}{(\lambda_1 - \lambda_2)bRT}\ln\left(\frac{\upsilon + \lambda_1 b}{\upsilon + \lambda_2 b}\right)\left(\frac{\bar{a}_i}{a} - \frac{\bar{b}_i}{b} + 1\right) \quad \textit{Eq. 23}$$

where z is the compressibility factor of the mixture:

$$z = \frac{P\upsilon}{RT} \quad \textit{Eq. 24}$$

Furthermore $\bar{a}_i$ and $\bar{b}_i$ are partial derivatives of a and b with respect to the number of moles of component i.

$$\bar{a}_i = \left(\frac{\partial(n_T a)}{\partial n_i}\right)_{T,P,n_{j\neq i}} \quad \textit{Eq. 25}$$

$$\bar{b}_i = \left(\frac{\partial(n_T b)}{\partial n_i}\right)_{T,P,n_{j\neq i}} \quad \textit{Eq. 26}$$

Substituting Eq. 18 and Eq. 19 in Eq. 25 and Eq. 26 the following equations are obtained:

$$\bar{a}_i = 2\left(\sum_j x_j a_{ij}\right) - a \quad \textit{Eq. 27}$$

$$\bar{b}_i = 2\left(\sum_j x_j b_{ij}\right) - b \quad \textit{Eq. 28}$$

Cubic EOSs were originally developed for single and multi-component phase equilibrium calculations. Van Konynenburk et al. (1980) classified the binary systems according to the P-T projections of mixture critical curves and the three phase equilibrium lines using the van der Waals EOS. Most systems can be related to one of the nine different types described by the authors. Fig. 1.16 shows the phase diagrams of the simplest, type I binary system at constant temperature and pressure. In Fig. 1.16a, T_1 and T_2 fall between the critical temperatures of the pure components. The closed loop is a two-phase area which represents the compositions of coexisting phases at a constant temperature. The critical pressure is always the upper limit of the loop (Fig. 1.16a). Unlike critical pressure, the critical temperature does not limit the two-phase region in a binary system at constant pressure (Fig. 1.16b). On the contrary, the two-phase region may well extend beyond the critical temperature.

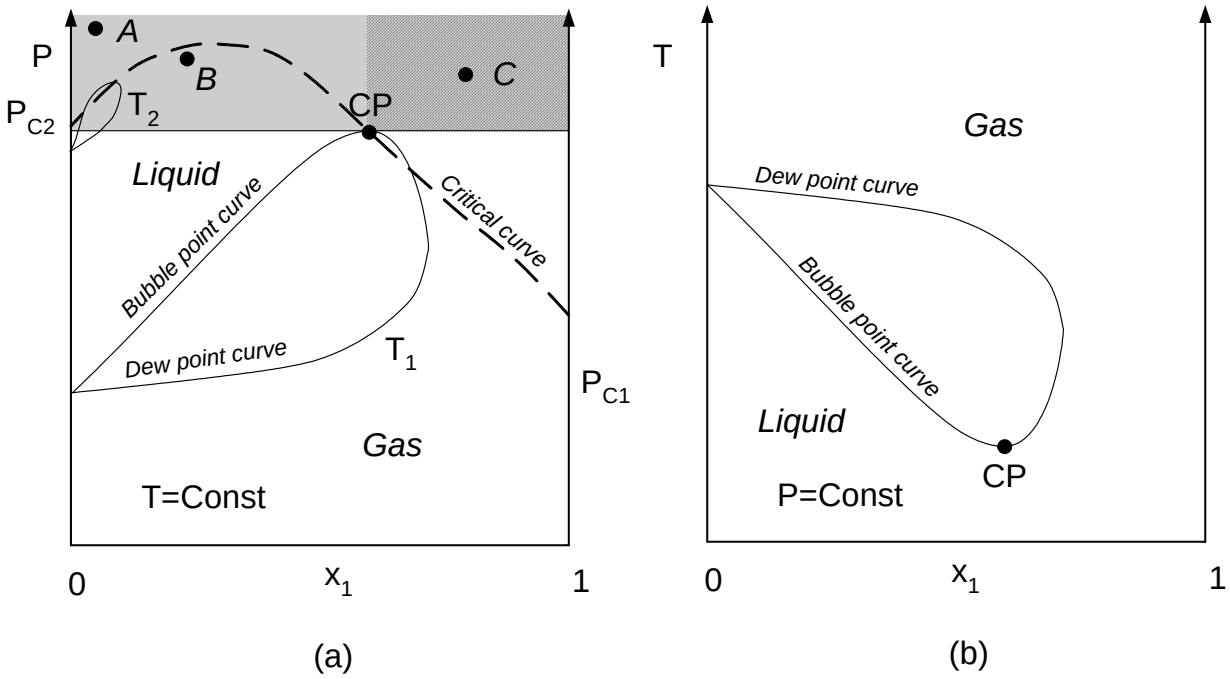

Fig. 1.16. P-x and T-x binary phase diagrams.

According to Brunner (1994) a binary mixture at constant temperature is supercritical for all pressures higher than the critical pressure of the mixture (grey area in Fig. 1.16a). This means that *A, B* and *C* points are all in the supercritical region, even though, the point *B* is below the critical curve. Mukhopadhyay (2004) considered a binary mixture as supercritical fluid only when the mol fraction of the volatile component is above the critical value (hatched area in Fig. 1.16a). Thus, at temperature T_1 only the mixture represented by the point *C* is supercritical. This approach leaves out of consideration that in most cases, the critical curve has a maximum with respect to temperature. It seems to be contradicting, that at temperature T_2, point *A* is not supercritical because its molar ratio is below the critical composition but the system indicated by point *B* is supercritical even if it is situated below the critical curve in the binary phase diagram. Although, one-phase regions (e.g.: point *B* at T_1 temperature) are often referred to as supercritical it seems to be thermodynamically correct to define a binary (or any multi-component) mixture as supercritical fluid if the pressure exceeds the critical pressure at constant temperature and composition. Thus temperature, pressure and composition have to be considered to find out whether a mixture is supercritical or not. A typical pressure-temperature-composition (*P-T-x*) diagram of type I system and its different projections are shown in Fig. 1.17 - Fig. 1.19. Component 1 is a gas at atmospheric pressure and component 2 is a medium volatile compound. In Fig. 1.18, 7 isotherms (*P-x* projections) and 3 isobars (*T-x* projections) at P_1, P_2, and P_3 pressures ($P_1 < P_{c1} < P_{c2}$, $P_{c1} < P_2 < P_{c2}$ and $P_{c1} < P_{c2} < P_3$) are presented. Broken

line represents the critical curve that passes through the critical points. The critical curve of a binary mixture depends on the ratio of the critical pressure and the critical temperature of the pure components (Fig. 1.18a). In the case of chemically similar components the critical curve is nearly a straight line. While binary mixtures of components of very different molecular size, may have very high critical pressures, much higher than pure components. The critical curve in Fig. 1.18a and Fig. 1.19 exhibits high slope near the critical point of gas component (PC_1), suggesting that the critical pressure increases considerably with the molar ratio of component 2 in this region. However, most supercritical technology (extraction, particle formation) has its working domain in this region. As these processes do not require high working pressure – higher than the actual critical pressure – the notion "single phase region" is more correct than "supercritical phase".

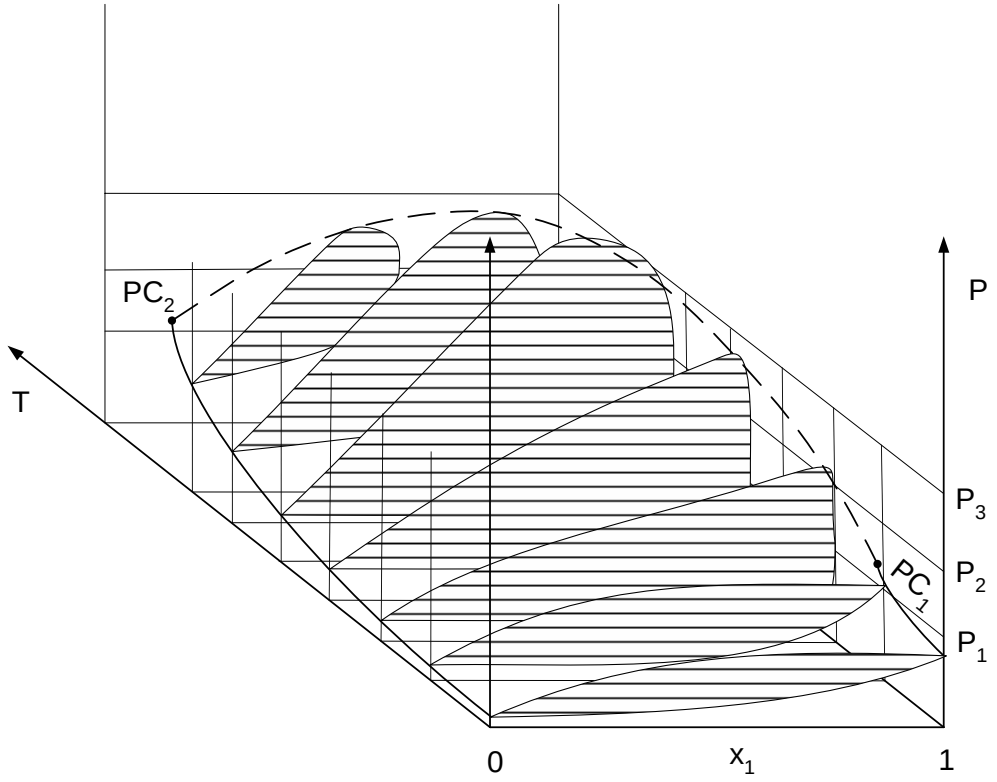

Fig. 1.17. Schematic 3D plot of the phase behavior of binary type I mixture.

In the SAS and SEDS technologies, precipitation must be carried out at a pressure above the bubble point pressure to obtain homogenous particle morphology throughout the vessel. However, the addition of a high-boiling component (model compound, excipient, etc.) may increase the bubble point pressure curve and shift the working point into the two-phase region where precipitation leads to large particle size, broad size distribution and low yield.

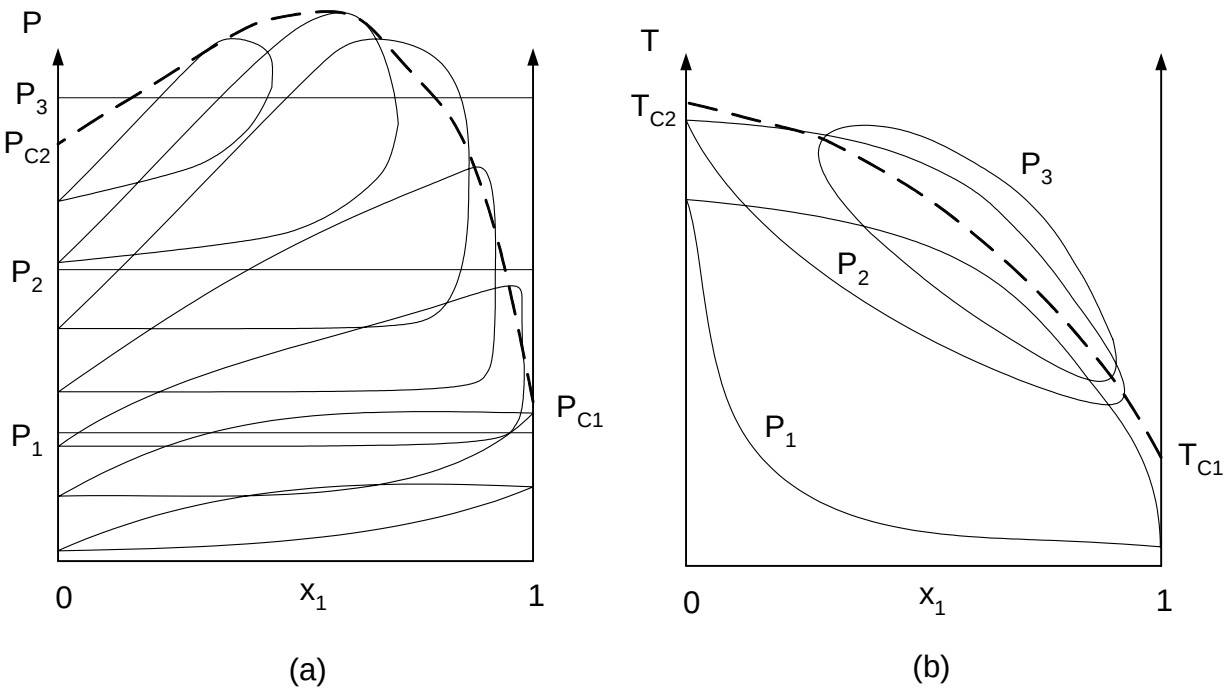

Fig. 1.18. P-x (a) and T-x (b) projections of the 3D plot.

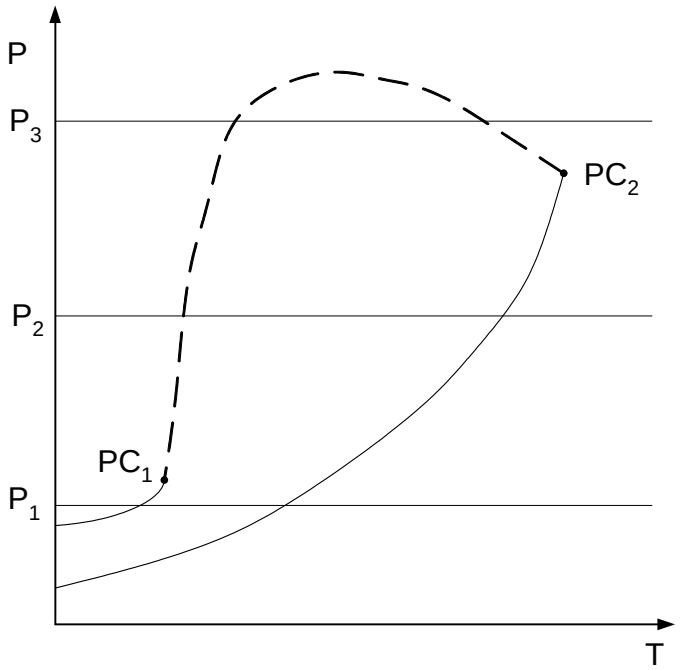

Fig. 1.19. P-T projection (critical curve).

1.5.2 Application

In spite of the early discovery of SCFs, their industrial application starts only in the late ’70s. The first industrial scale plant for the decaffeination of coffee beans was built 1976 by the HAG Corporation. In the 1980’s many industrial applications were studied, including chemical reactions, purification of surfactants and pharmaceuticals, polymerization and fractionation of polymers. In the same period, interest in using supercritical fluids for precipitation and crystallization process was developing for pharmaceutical materials and this activity has steadily increased over recent years. In our days, SCFs are used in almost all areas and many new applications are actually being developed:

Food industry: decaffeination of coffee beans and tee; extraction of plant seeds (black currant, grape, borage, saw palmetto) hops, tobacco; extraction of cholesterol from eggs; extraction of spice and aromas.

Textile industry: dyeing, scouring, bleaching and dry cleaning.

Cosmetic industry: extraction of essential oils (flavors and flagrances).

Oil industry: recovery of organics from oil shale; petroleum recovery; crude de-asphalting and de-waxing; coal processing (reactive extraction and liquefaction); selective extraction of fragrances.

Fine chemistry: chemical reactions, such as oxygenation, hydroformulation, alkylation and enzyme-catalyzed reactions; polymerization and fractionation of polymers.

Pharmaceutical industry: micronization of pharmaceutical ingredients for injectable, oral and pulmonary drug delivery systems, preparation of immediate-release and controlled release systems; bioavailability enhancement; separation and purification, fermentation broth extraction, sterilization.

Medicine: sterilization of tissue implants and orthopaedic devices.

Analytical chemistry: SCF chromatography, purification.

Waste treatment: waste water treatment (wet oxidation); soil remediation (extraction of VOCs and PAHs), extraction of scrap tires.

Microelectronics: manufacturing of semiconductors (precipitation and cleaning).

1.5.3 Particle engineering

Particle formation is one of the most researched areas of SCF application (Charbit, 2004; Jung, 2001). SCF technologies may reduce particle size and residual solvent content in one step and allow a certain control of particle size, particle size distribution, habit, morphology and polymorphic nature (Beach, 1999; Badens, 2004: Fargeot, 2003). These methods use SCFs either as solvent (RESS, RESS-N, RESAS, RELGS, RELGS-H) or antisolvent (GAS, SAS, ASES, SEDS) and/or dispersing fluid (SEDS, PGSS, PLUSS). Unlike liquid solvents, SCFs are easy to separate from solid products (and organic solvents, if used) because most of them are gases at ambient temperature and pressure. Furthermore, SCF extraction is more efficient to reduce residual solvents in heat-sensitive materials, compared to spray freezing, freeze-drying and vacuum-drying. Gases with low critical temperature are suitable to treat explosives, peptides, plasmid DNA, steroids etc. which would undergo thermal degradation when processed by conventional methods. Additionally, SCF particle formation processes have several attractive features in terms of Good Manufacturing Practice (GMP) requirements including light-, oxygen- and moisture-free environment as well as totally enclosed equipment which is free from moving parts (York, 1999). Fig. 1.20 is a schematic presentation of the different technologies discussed in the following chapters.

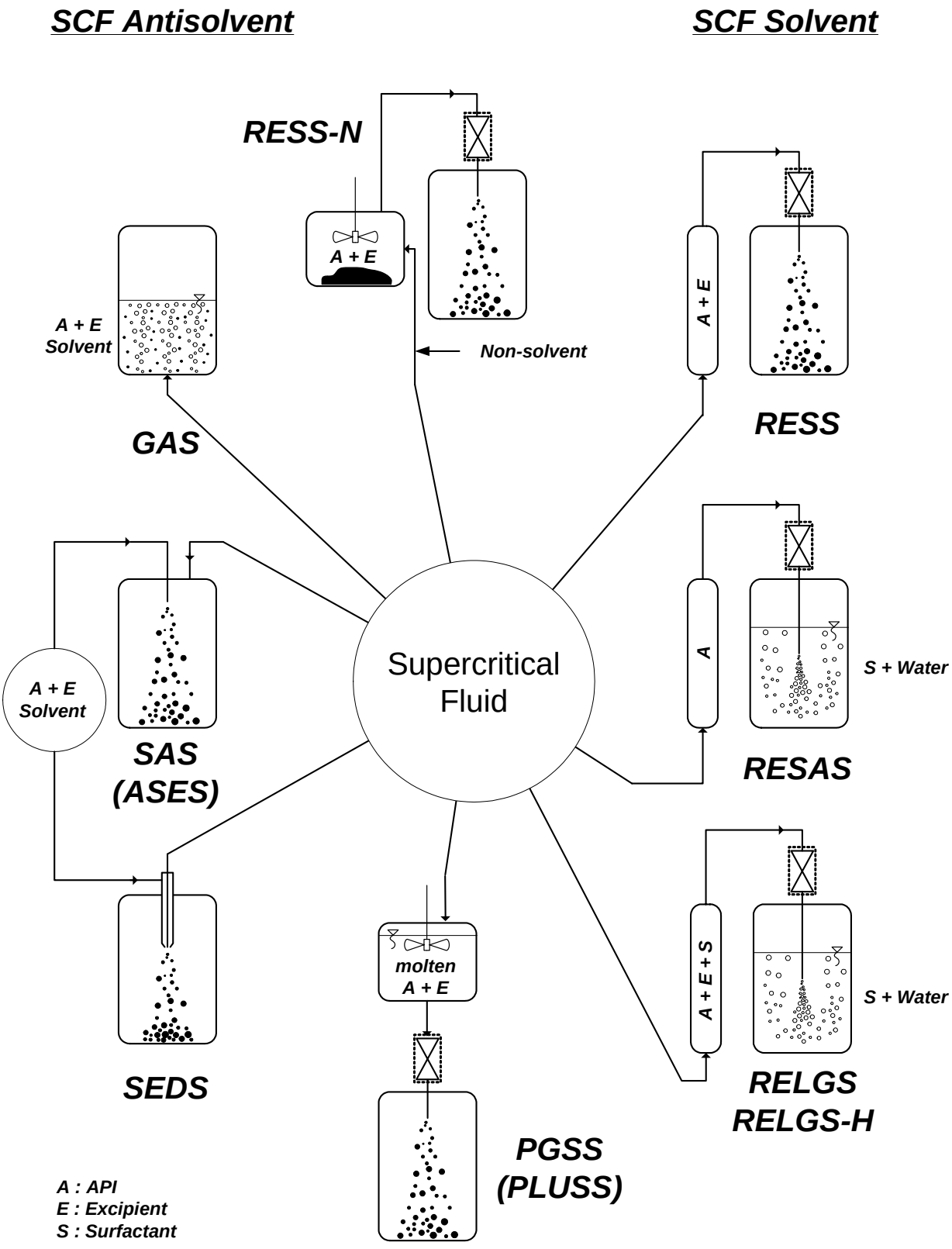

Fig. 1.20. Particle formation technologies using supercritical fluids.

1.5.3.1 Rapid Expansion of Supercritical Solution (RESS)

In the RESS technology, the material(s) of interest are dissolved in SCF and the resulting solution is expanded through a restriction or an orifice (10-50 μm, i.d.). Resulting pressure drop decreases dramatically the solvent power and leads to extremely rapid nucleation ($t<10^{-5}$ s). This process is attractive due to the absence of organic solvent and the uniform condition of particle formation. RESS seems to be the ideal method to prepare very small (0.5-20 μm) and monodisperse particles but its application is limited to ingredients soluble enough in SCFs (apolar compounds). Particle collection in the gaseous stream is also a challenging task. Lovastatin, naproxen and pyrene were successfully coprecipitated with L-PLA using RESS (Debenedetti, 1993; Debenedetti, 1994, Kim, 1996; Ye, 2000).

To overcome the difficulties associated with SCF-insoluble polar compounds, Mishima et al. (1996) have invented a new method called *Rapid Expansion from Supercritical Solution with a Non-solvent* (*RESS-N*), wherein a polymer dissolved in a SCF containing a cosolvent is sprayed through a nozzle to atmospheric pressure. The cosolvent increases significantly the solubility of the API of interest in $scCO_2$, but the API itself is virtually insoluble in the cosolvent (Mishima, 1997; Mishima, 2000a, 2000b).

In 1994, Frederiksen et al. patented a method suitable to prepare liposomes containing at least one phospholipid, an excipient and a water soluble API (Frederiksen, 1994, 1997). Phospholipids and excipients were dissolved in an appropriate polar solvent and homogenized in $scCO_2$, this solution was afterwards expanded to atmospheric pressure and simultaneously dispersed in the aqueous solution of the API. Residual organic solvent can be removed by evaporation, dialysis or gel filtration.

In order to obtain sub-micron particles (100-300 nm) of water-insoluble APIs Henriksen et al. (1997) submerged the nozzle in aqueous solution containing one or more surfactants. Young et al. (2000) detailed the precipitation of cyclosporine sprayed in a solution of Tween-80 polymer using the RESAS technology. The mean particle size was between 400 and 700 nm and the solubility of cyclosporine increased significantly.

Pace et al. (1999) have improved RESAS by dissolving a surface modifier together with the API in SCF and expanding it in an aqueous solution containing surface modifiers and additives. These techniques were patented by the name of Rapid Expansion of

Liquefied Gas Solution (RELGS) and Rapid Expansion of Liquefied Gas Solution and Homogenization (RELGS-H).

1.5.3.2 Supercritical Antisolvent (SAS)

When a gas or a SCF is absorbed in a solution, this latter gradually expands and looses its solvent strength. This drop in solvent strength leads to the precipitation of dissolved ingredients poorly soluble in SCF and SCF + solvent mixture. Although, supercritical antisolvent techniques (SAS, SEDS, GAS) differ in the manner in which the solution is contacted with the SCF, they all have in common the above phenomena.

SAS (ASES, PCA) involves a capillary nozzle through which the solution, containing one or more dissolved substance, is dispersed in a continuous co-current SCF flow. Under adequate working conditions, liquid solvent and SCF are completely miscible. In other words, the surface tension of the solvent tends to zero in SCF atmosphere and no well defined droplets are formed. Supersaturation is induced by the mutual diffusion of the SCF antisolvent into the solution and the solvent into the bulk phase. Since the continuous-phase densities of liquid-SCF jets are comparable to those of liquid-liquid systems and their continuous-phase viscosities are close to those of liquid-gas systems, the mixing between the core jet flow and bulk SCF flow is very intensive (Carretier, 2003). Due to the intensive mixing and the absence of phase boundary improved mass transfer and high supersaturation can be achieved (Werling, 2000).

Several APIs and model compounds were coprecipitated with biodegradable polymers using SAS technology (Table 1.8).

Table 1.8. Summary of active compound-carrier systems precipitated by SAS, ASES, PCA and related methods.

Active substance	Excipient	Observation	References
Clonidin-HCL	D-PLA	Agglomerates, 10-100 μm	Fischer, 1991
Hyoscine butyl-bromide	L-PLA	Particle size: 1 - 10 μm	Bleich, 1993
Hyoscine butyl-bromide	L-PLA	Agglomerates, < 20 μm	Bleich, 1994
Chlororphenilamine maleate, Indomethacin	EC, PCL PMMA L-PLA, PLGA	Agglomerated fibers and particles	Bodmeier, 1995
Hyoscine butylbromide, Indomethacin, Piroxicam, Thymopentin	L-PLA	Microcapsules	Bleich, 1996
Tetracosactide	L-PLA	Oval particles, 10.1 μm	Bitz, 1996
Thymopentine	PLGA, Lecithin	Microcapsules	Ruchatz, 1996
Naproxen	L-PLA	Mean particle size: 5 μm	Chou, 1997
Steroids[a]	PC[b]	Mean particle size: 2 - 9 μm	Steckel, 1997
Gentamycin, Naltrexone, Rifampin	AOT[c] L-PLA	Spherical particles, 0.2 - 1 μm	Manning, 1998 Falk, 1997
Tetracosactide	L-PLA	Microcapsules, 5.9 μm	Witschi, 1998a, b
p-HBA	L-PLA, PLGA	Fibrous network Microcapsules	Sze Tu, 1998
α-Chymotrypsin	AOT, L-PLA	Spherical particles, 2 - 3 μm	Manning, 1998
Insulin	SDS	Spherical and irregular particles, 1 - 5 μm	
Ribonuclease	PEG SDS	Fiber-like and spherical particles, 0,5 - 1 μm	
Cytochrome C	SDS	Spherical particles, 5 μm	
Pentamidine	SDS	Spherical particles, 0.1 – 1 μm	
Streptomicin	AOT	Spherical particles, 0.4 – 1 μm	
Albumin, Estriol	PLGA	Agglomerated spherical particles, 10 – 130 μm	Engwicht, 1999
Chimotrypsin-AOT, Insulin-lauric acid conjugate, Insulin, Lysozyme	L-PLA	Mean particle size: 1 – 5 μm	Elvassore, 2000
Diuron	L-PLA	Microspheres, 1 - 5 μm	Taki, 2001
Insulin	PEG, L-PLA	Drug-loaded spheres, 0.4 – 0,6 μm	Elvassore, 2001a
Insulin	L-PLA	Drug-loaded spheres, 0.5 – 2 μm	Elvassore, 2001b
p-HBA Lysosyme	L-PLA	Agglomerates	Sze Tu, 2002
Budesonide	L-PLA	Spherical particles, 1 – 2 μm	Martin, 2002
rhDNase[d] Lysosyme	Lactose	Agglomerates	Bustami, 2003
Copper indomethacin	PVP	Solid dispersion, 0.05 – 4 μm	Meure, 2004
Insulin	PEG, L-PLA	Agglomerates, 360-720 nm	Caliceti, 2004
Felodipine	HPMC, Poloxamer 188 and 407, PEG 60		Won, 2005

[a] beclomethasone-17,21-dipropionate, betamethasone-17-valerate, budesonide, dexamethasone-21-acetate, flunisolide, fluticasone-17-propionate, prednisolone and triamcinolone acetonide; [b]Phosphatidylcholine; [c]bis-(2-ethylhexyl) sodium sulfosuccinate; [d]Recombinant human deoxyribonuclease;

1.5.3.3 Solution Enhanced Dispersion by Supercritical Fluids (SEDS)

SEDS was described in sequential patents (Hanna, 1995, 1996, 1999a, 1999b, York, 2001) associated with the name of the University of Bradford and Bradford Particle Design PLC. This process involves a coaxial nozzle to co-introduce the SCF and the solution in the precipitation vessel. The solution is feed in the outer passage and dispersed by the high velocity SCF which is preferably introduced in the inner passage. Owing to the premixing chamber, located at the tip of the inner capillary, solution and antisolvent get molecularly dispersed before the formation of solution jet. The high dispersion leads to almost instantaneous precipitation of micron and sub-micron size uniform particles. The main advantage of SEDS over the other SCF-based techniques is the direct control over the mean size and size-distribution of the product by controlling the pressure, temperature, and flow rates.

In the first patent Hanna et al. (1995) described the coprecipitation of salmeterol xinafoate and HPC using both two- and three-passage nozzles. In both cases peaks of salmeterol xinafoate were weaker in X-ray Diffraction patterns due to the amorphous fraction of the incorporated drug. Since water is hardly miscible with $scCO_2$, hydrophilic compounds like sugars can not be processed directly. For this reason Hanna et al. (1996) have completed their previous patent by describing a process in which sugars are precipitated from aqueous solution by mixing it with a second vehicle (ethanol or methanol) which is readily miscible with both $scCO_2$ and water.

As amorphous drugs are generally considered to be meta-stable, their stability over the storage period at ambient temperature is a crucial point. To demonstrate the feasibility of SEDS, York et al. (2001) have devoted a whole patent to describe the coprecipitation of drug-carrier systems. Drugs were chosen to cover a broad range of polarities including the highly apolar ketoprofen and in ascending order of polarity, indomethacin, carbamazepine, paracetamol, theophylline and ascorbic acid. The coformulation of these drugs with both hydrophilic HPMC, PVP K17 and hydrophobic EC polymers revealed that the more they are alike in polar and hydrogen bonding characteristics the higher the concentration of amorphous phase. In spite of the high amorphous content, the drug-carrier systems proved to be stable for at least three months.

Table 1.9. Summary of active compound-carrier systems precipitated by SEDS.

Active substance	Excipient	Observation	References
Salmeterol Xinafoate	HPC	Cristalline drug enbedded in polymer matrix	Hanna, 1995
Hydrocortisone, Lysozyme, Urease	PLGA	Microcapsules, 9 - 13 μm	Ghaderi, 2000
Ascorbic acid, Carbamazepine, Indomethacin, Ketoprofen, Paracetamol, Theophyline, Model drug[a, b]	EC HPC HPMC PVP K17 Poloxamer 237	Agglomerates, 0.1 – 100 μm	York, 2001
Plasmid-DNA	Mannitol	DNA-loaded particles	Tservistas, 2001
Chlorpheniramine maleate	Eudragit RL	Drug crystals incorporated in swelled polymer	Squillante, 2002
Model drug[c]	Mannitol Eudragit E	Mixture of drug particles and polymer fibers, 1 - 20 μm Solid solution	Juppo, 2003

[a] ((Z)-3-[1-(4-chlorophenyl)-1-(4-methansulfonyl)methylene]-dihydrofuran-2-one); [b] ((Z)-3-[1-(4-bromophenyl)-1-(4-methansulfonyl)methylene]-dihydrofuran-2-one); [c] 2,6-dimethyl-8-(2-ethyl-6-methylbenzylamino)-3-hydroxymethylimidazo-[1,2-a]pyridine mesylate;

1.5.3.4 Gas Antisolvent (GAS)

GAS process claims a precipitator, which is partially filled with the fedd solution. The vessel is closed and pressurized by introducing the SCF antisolvent. The SCF is preferably introduced at the bottom to achieve a better mixing. When precipitation is thought to be complete, solution is drained and remaining particles are washed in pure SCF. Unlike the other antisolvent processes previously discussed, in that case the liquid phase is the continuous one and the antisolvent constitutes the dispersed phase. As the liquid phase expands in batch and not in continuous mode, larger precipitation vessel is required compared to SAS and SEDS. Working in transitory state, particle size and size distribution are also difficult to control in GAS process. In most cases, mother liquor cannot be completely removed, and additional drying processes are required. In spite of these drawbacks, several APIs and explosives were successfully processed in this manner (Gallagher, 1989; Krukonis 1994; Pallado, 1996; Bertucco 1996, 1997; Moneghini, 2001; Corrigan, 2002; Kikic, 2002; Sethia 2002, 2004).

1.5.3.5 Particles from Gas-Saturated Solution (PGSS)

PGSS consists in dissolving a compressed gas or a SCF in a melt substance or in a solution or suspension of a solid substance followed by a rapid expansion to lower (atmospheric) pressure (Weidner, 1995; Senccar-Bozzics, 1997; Kerc, 1999). Since the solubilities of compressed gases in liquids and polymers are usually much higher then those of such liquids and solids in the compressed gas, this method is proved to be more advantageous over RESS. The patents granted in this field are related mostly to paints, polymers and powder coating products. Pure pharmaceutical products are generally precipitated from aqueous solution, to avoid their thermal degradation. Coprecipitation of drugs and carriers can be achieved from melt phase due to the lower melting temperature of polymers in high pressure CO_2 atmosphere.

In 1998, Shine et al. patented a method called Polymer Liquefaction Using Supercritical Solvating (PLUSS) whereby PGSS method is applicable below the melting point of the processed material (Shine, 1998). As polymers in high pressure CO_2 atmosphere swell and melt at lower temperature, active substrates can be dispersed and encapsulated without any thermal degradation (Wang, 2001; Watson, 2002; Howdle, 2003; Yang, 2004; Hao, 2004; Whitaker, 2005).

1.6 Cryogenic technology

1.6.1 Patent survey

The first cryogenic particle formation technology was patented in 1969 (Sauer, 1969). Virtually all of the techniques published and patented ever since take advantage of instantaneous freezing of a solution or suspension dispersed in a cryogenic fluid (Rogers, 2001). Inventions can be classified by the type of injection device (capillary, rotary, pneumatic, ultrasonic nozzle), location of nozzle (above or under the liquid level); and the composition of cryogenic liquid (hydrofluoroalkanes, N_2(l), Ar(l), O_2(l), organic solvents).

1.6.1.1 Spray freezing onto cryogenic fluids

Briggs and Maxwell (1973) invented the first process of spray freezing onto cryogenic fluid. The patent dates back to 1973, wherein the authors described a process of blending a solid biological product with sugars. The API and the carrier (mannitol, maltose, lactose, inositol or dextran) were dissolved in water and atomized above the surface of a boiling agitated fluorocarbon refrigerant. To enhance the dispersion of the aqueous solution a sonication probe was placed in the stirred refrigerant. Solid particles were sieved and lyophilized. Freon 12 (dichlorodifluoromethane) was found suitable for this purpose because its boiling point (T_b = -30 °C) is sufficiently low to cause instantaneous freezing, but not enough low to form an extensive "vapor barrier" around the droplets which would hinder fast freezing. Several APIs were blended in this manner including proteins and enzymes (luciferase, hexokinase, glucose-6-phosphate dehydrogenase (G-6-PDH), lactate dehydrogenase (LDH), pyruvate kinase; luciferin, bovine albumin, morpholinopropane sulfonic acid (MOPS), 2,6-dichlorophenol indophenol (DIP), nicotinamide-adeninine-dinucleotide (NAD) and its reduced derivative (NADH). In the following two patents, the authors completed the above list of APIs with blood serum, red blood cells, bacitracin, polymyxin B, tetracycline, chlorpromazine, maltase enzyme, testosterone, Vitamin C, cholesterol and gelatin (Briggs, 1975; 1976). Processed materials exhibited high biological activity, high homogeneity and adequate stability.

In 1980, Adams et al. patented a method similar to the one of Briggs and Maxwell with the slight difference that they used capillary nozzles to disperse the solution or suspension onto the surface of stirred halocarbon refrigerant (Adams, 1980; 1982) (Fig. 1.21). Blood plasma particles processed in Freon 12 ranged from 0.84 to 1.68 mm in diameter.

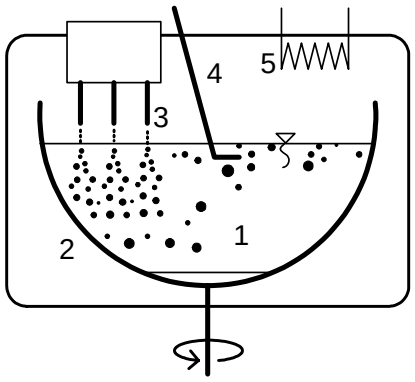

Fig. 1.21. Schematic diagram of the apparatus invented by Adams et al.
1. Refrigerant; 2. Rotated vessel; 3. Nozzles; 4. Wire screen; 5. Condenser.

Hebert et al. (1999) prepared microparticles of controlled release device by spraying the solution containing the pharmaceutical ingredients into cold nitrogen gas (Fig. 1.22). Particles were frozen partially in the gaseous phase and collected in the liquid phase at the bottom of the vessel where they solidified completely. In a second vessel liquid nitrogen was evaporated and residual organic solvent was removed by extraction.

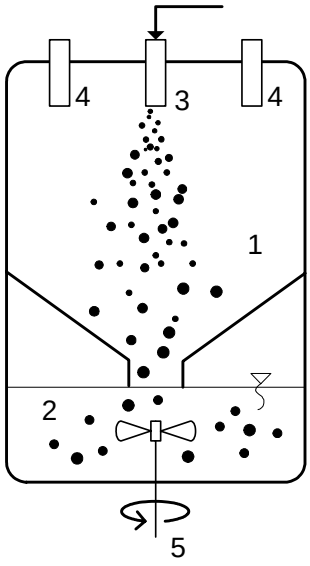

Fig. 1.22. Schematic diagram of the apparatus invented by Hebert et al.
1. Freezing vessel; 2. Extraction vessel; 3. Nozzle; 4.Liquified gas inlet; 5. Mixing device.

Gombotz et al. (1991) patented a similar process to prepare microparticles of biodegradable polymers wherein the solution of API is atomized directly into liquid non-solvent or in liquefied gas containing frozen non-solvent at a temperature below the melting point of the solution. The solvent in the microspheres then thaws and is slowly extracted by the non-solvent. However, it can be difficult to find a good solvent, which extracts exclusively the organic solvent, and residual organic traces are hard to remove. Previously, Gombotz et al. (1990) published another process, which consisted in atomizing

the solution or suspension of API into a liquefied gas and lyophilizing the frozen particles. Authors have described the formulation of zinc insulin, catalase, heparin, hemoglobin, dextran, superoxide dismutase (SOD), horse radish peroxidase (HRP), bovin serum albumin (BSA), glycine and testosterone. Particles ranged from 10 to 90 μm in diameter and kept 70 – 95 % of their initial biological activity. To achieve a mean diameter smaller than 10 μm, which is desirable in the case of injectable controlled drug delivery device, the lyophilized product was suspended in a non-solvent and exposed to ultrasonic energy. Owing to the porous structure and the great specific surface area of lyophilized products, particles were easy to disintegrate and micronize to the size range of 0.1-10 μm.

Lyophilization is a widespread process in pharmaceutical and food industry but rather expensive and time-consuming. Mumenthaler and Oyler used recirculated dry gas instead of vacuum to remove residual solvent from particles previously sprayed into cryogenic air (Mumenthaler, 1991; Oyler, 1993) (Fig. 1.23). During spray freezing cold gas is supplied on the top of the vessel around the spray nozzle. When spray freezing is over, frozen particles are fluidized by passing the gas through the bed. Solvent vapors are continuously condensed in a heat exchanger. The temperature of dry gas must be carefully controlled to supply the heat of sublimation without melting the frozen particles.

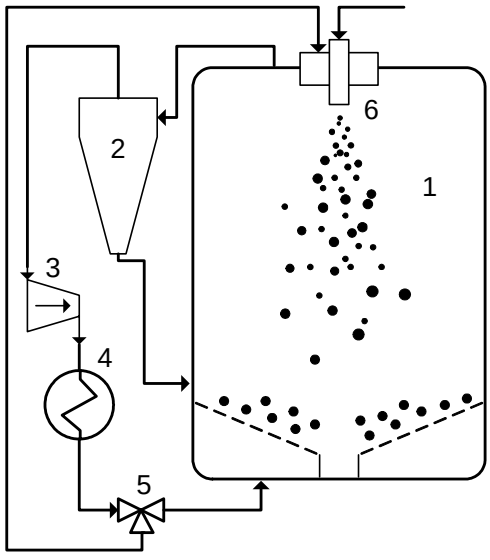

Fig. 1.23. Schematic diagram of the apparatus invented by Oyler.
1. Freezing and drying vessel; 2.Cyclone; 3. Turbine; 4.Heat exchanger; 5.Three-way valve; 6. Nozzle.

1.6.1.2 Spray freezing into cryogenic fluids

More intense atomization can be achieved by submerging the nozzle into the cryogenic substance. Due to the liquid-liquid collision, atomization beneath the surface of the cryogen results in smaller droplets which freeze much faster.

In 1969, Harold A. Sauer patented the first method using submerged atomization device (Sauer, 1969). Solution was injected in liquid refrigerant through a heated nozzle at the bottom of the vessel (Fig. 1.24). At the end of the atomization process, frozen droplets floating on the surface were collected in a spherical screen and dried in cold air or nitrogen gas. Residual moisture was removed under reduced pressure.

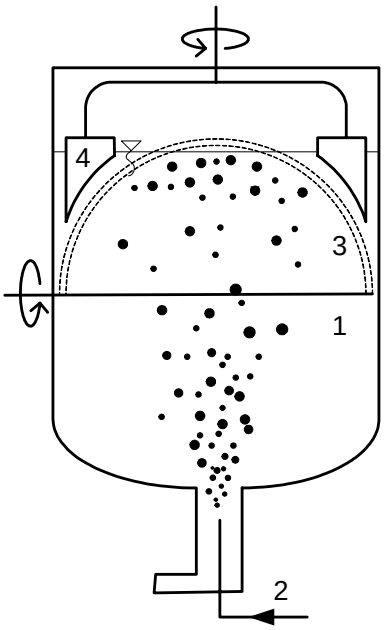

Fig. 1.24. Schematic diagram of the apparatus invented by Harold A Sauer.
1. Freezing and drying vessel; 2. Nozzle; 3. Screen hemisphere; 4 .Mixer paddle.

The method developed by Dunn (1972) involves two immiscible halocarbon refrigerants. The boiling point of the denser refrigerant must be slightly above the melting point of the solvent while that of the lighter one is lower. Solution is dispersed through a heated nozzle in the denser phase from which rising solution droplets step in the lighter refrigerant and solidify (Fig. 1.25). Frozen particles floating on the surface of the upper refrigerant are collected and freeze-dried. The authors described the precipitation of aluminum sulphate in various Freon-based cryogenic systems.

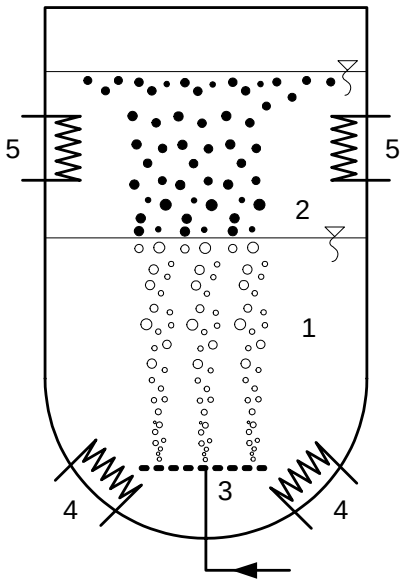

Fig. 1.25. Schematic diagram of the apparatus invented by Dunn et al.
1. Denser refrigerant (Injection zone) ; 2. Lighter refrigerant (Freezing zone); 3. Atomization device; 4 Heating coil; 5. Cooling coil.

In a more recent patent Williams et al. (2002) describe a method called Spray Freezing into Liquid (SFL) which, due to an insulating nozzle, enables injection into extremely cold liquids or liquefied gases without any nozzle blockage (Fig. 1.26). Unlike the process of Dunn et al., in SFL process, atomization and freezing occur simultaneously in the same cryogenic liquid which results in smaller droplet size and faster freezing. The benefits of small particle size were discussed in the chapter 1.3.1. However, small droplet (particle) size not only increase dissolution rate of processed powders but increase the rate of freezing during the preparation. Ultra rapid freezing hinders the phase separation and the crystallization of the pharmaceutical ingredients leading to intimately mixed, amorphous drug-carrier solid dispersions and solid solutions.

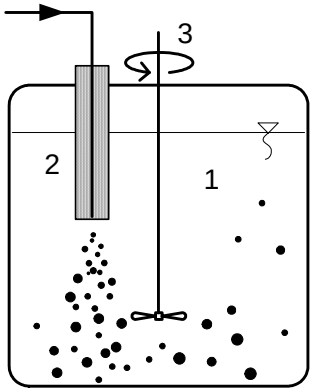

Fig. 1.26. Schematic diagram of the apparatus invented by Williams et al.
1. Liquified gas; 2. Insulating nozzle; 3. Propeller stirrer.

In addition to the small particle size (10 nm – 10 μm) and the glassy state, SFL prepared solid dispersions exhibited several advantageous properties including great specific surface area (>100 m^2/g), porous structure, improved wettability, low residual solvent content and high biological activity (Williams, 2002; Rogers, 2002a, 2002b, 2003; Yu, 2002, 2004; Hu, 2003, 2004, Vaughn, 2005; Leach, 2005).

Cryogenic technologies were found particularly advantageous for the preparation of injectable microspheres of biologically active proteins and rapidly dissolving formulations of poorly water soluble APIs (Table 1.10).

Table 1.10. Summary of active compound-carrier systems prepared by cryogenic technologies.

Active substance	Excipient	Solvent	Observation	References
NAD, NADH, Luciferase, Luciferin, Hexokinase, G-6-PDH, LDH, Pyruvate kinase, Bovine albumin, MOPS, DIP	Mannitol, Maltose, Lactose, Inositol, PEG	Water (KCl, $NaHCO_3$)	Embedded substrates with high biological activities	Briggs, 1973
Blood serum	Citric acid	Water	Embedded substrates with high biological activities	Briggs, 1975; Briggs, 1976;
Maltase enzyme	Inositol, Mannitol			
Testosteron	Sodium monoglutamate			
Vitamin C	Inositol			
Cholesterol	SDS	Water/Ethanol		
SOD, HRP, Mitomycin C, Etoposide, Hemoglobin	PLA PLGA	DCM	Microspheres MPS[b] = 30 - 50	Gombotz, 1990
Carbamazepine	SDS	Water/THF	Solid solution MPS=5.06-7.11 SSA[c]=12.81-44.44	Williams, 2002; Rogers, 2002a; Yu, 2002;
Danazol	PVA (22000) Poloxamer 407 PVP K15			
Insulin	Tyloxapol Lactose Trehalose	Water		
Danazol	HP-β-CD	Water/THF	Solid solution MPS=7; SSA=113.5	Williams, 2002; Rogers, 2002b;
Danazol	PVA (22000) Poloxamer 407 PVP K15	Water/THF Water/Ethyl acetate[a] Water/DCM[a]	Solid solution MPS=6.52-16.75 SSA=8.9-83.06	Williams, 2002; Rogers, 2003;
Carbamazepine	Poloxamer 407 PVP K15	Water/THF Acetonitrile	Solid solution MPS=0.68-7.06 SSA=3.88-13.3	Williams, 2002; Hu, 2003
Salmon calcitonin, Tyloxapol	Lactose	Water	Solid solution MPS=5.06-10.49 SSA=11.04-19.16	Williams, 2002;
Danazol	Poloxamer 407	THF		
Triamcinolone acetonide	Poloxamer 407 PVP K15			
Danazol	PVP K15	Acetonitrile DCM	Solid solution SSA=28.5-117.5	Hu, 2004
Bovine serum albumin		Water (phosphate buffer)	SSA=19.2-97.7 Protein microparticles, high biological activities	Yu, 2004
Danazol	PVP K15	Acetonitrile	Solid solution MPS=3.5 SSA=52.2	Vaughn, 2005
Bovine serum albumin			Encapsulated protein nanoparticles	Leach, 2005

[a] Emulsion.; [b] Mean particle size (μm); [c] Specific surface area (m^2/g)

1.7 Excipients

1.7.1 *Polyethylene Glycol (PEG)*

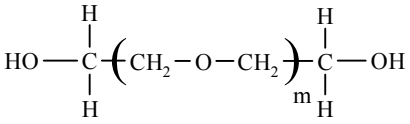

Fig. 1.27. Molecular structure of PEG.

Solubility: *all grades of PEG are soluble in water; liquid PEGs are soluble in acetone, alcohols, benzene; solid PEGs are soluble in acetone, DCM, EtOH, MeOH, DMF, slightly soluble in aliphatic hydrocarbons.*

Applications: *solubilizing and wetting agent, film coatings, micro-encapsulation, lubricanting agent, plasticizer.*

Polyethylene glycols (Fig. 1.27) are synthetic polymers obtained by reacting ethylene glycol with ethylene oxide. PEG 200 – 600 (average molecular weight) are liquids; PEG 1000 – 4000 range in consistency from pastes to waxy flakes; PEG 6000 and higher grades are solid (Kibbe, 2000). PEGs with average molecular weights between 3000 and 20000 are widely used in particular to form solid dispersions. These stable, non-irritant hydrophilic substances were found to improve the dissolution kinetics of poorly water soluble compounds owing to their high aqueous solubility and their ability to hinder crystallization of incorporated APIs.

Moneghini et al. evaluated the GAS technique for preparation of carbamazepine – PEG 4000 solid dispersions (Moneghini, 2001; Kikic, 2002). Formulations with D/P ratios of 5:1, 2:3 and 1:11 were precipitated from acetone solution using $scCO_2$ antisolvent. Authors succeeded in reducing particle size (from 284 to 31 μm) and improving considerably the dissolution kinetics of embedded carbamazepine. However, XRD studies revealed that crystalline drug was present even at low drug loadings and both polymorphs were detectable.

Ye (2000) used RESS technology to prepare solid dispersion of PEG 8000 – lidocaine in an attempt to increase the dissolution rate of this latter. Drug and excipient mixed in different weight ratios were dissolved in $scCO_2$ at 7100 psi (~ 490 bar) and 65 (75) °C and expanded to atmospheric pressure through a heated restrictor. DSC and

dissolution studies revealed that formulations with 20-40 wt. % lidocaine were in the eutectic region while those with 70-80 wt. % drug contained amorphous excipient. The dissolution rates measured in these regions were among the highest.

Drug-PEG solid dispersions were prepared by PGSS as well. Kerc et al. (1999) have increased the dissolution rate of three poorly water soluble APIs: nifedipine, felodipine and fenofibrate by using PGSS process. The authors have studied the effect of pre-expansion conditions; pressure was varied in the range of 100-200 bar, operating temperature between 65 and 185 °C, according to the melting point of the processed drug.

Jung et al. (1999) prepared solid dispersions of the antifungal agent, itraconazole and various polymers by spray-drying method. Two pH-dependent (AEA and Eudragit E100) and four pH-independent polymers (Poloxamer 188, PEG 20000, PVP, HPMC) were compared. Dissolution tests in simulated gastric juice revealed that PEG 20000 was the best pH-independent solubilizer agent.

1.7.2 Poloxamer

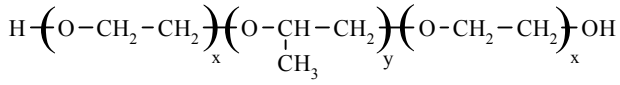

Fig. 1.28. Molecular structure of Poloxamer.

Solubility: *soluble in EtOH, water; mostly soluble in iPrOH, propylene glycol*

Applications: *solubilizing and wetting agents, emulsifying and dispersing agents, tablet lubricant, controlled release in drug delivery, artificial skin.*

Table 1.11. Properties of the different grades of Poloxamer (Kibbe, 2000).

Poloxamer	x	y	MW g/mol	T_m °C
124	12	20	2090-2360	16
188	80	27	7680-9510	52-57
237	64	37	6840-8830	49
338	141	44	12700-17400	57
407	101	56	9840-14600	52-57

Poloxamers are polyoxyethylene-polyoxypropylene-polyoxyethylene block co-polymers (Fig. 1.28) synthesized by sequential addition of propylene oxide and ethylene oxide monomers in the presence of an alkaline catalyst (NaOH or KOH) (Schmolka, 1977).

Poloxamer is a collective noun that covers more than 50 different amphiphilic non-ionic surfactants, sold under different names: Pluronic®, Synperonic®, Lutrol®, Monolan®. Due to their ability to form both solid dispersion and hydrophilic coating they are probably the most widely used solubilizing and emulsifying agents (Moghimi, 2000). Poloxamers are adsorbed owing to their hydrophobic polypropylene oxide (PPO) block on the surface of drug particles inhibiting the further growth and stabilizing them in aqueous solution due to their hydrophilic polyethylene oxide (PEO) arms.

Poloxamer 407 was one of the most widely used excipients in SFL. Alone or mixed with PVP K15 and PVA 22000, Poloxamer 407 improved significantly the dissolution rate of freeze-dried carbamazepine, danazol and triamcinolone acetonide formulations (Williams, 2002; Rogers, 2002a; Yu, 2002; Hu, 2003). The amount of danazol dissolved from SFL prepared solid dispersion was 93 % after 2 min and 100 % after 5 min whereas only 53 % of bulk drug was dissolved within 5 min (Williams, 2002; Rogers, 2003). SFL micronized carbamazepine displayed rapid dissolution profile, too. More than 90 % was achieved within 10 min whereas only 5 % of carbamazepine was dissolved in 20 min from bulk drug (Hu, 2003). Triamcinolone acetonide showed similar dissolution kinetics: 90 % dissolved in 10 min (Williams, 2002).

York et al. reported a series of experiments to demonstrate the feasibility of SEDS (York, 2001). A selective enzyme inhibitor (COX-2) was coprecipitated with Poloxamer 237 from DCM solution (Table 1.9). Operating parameters varied in the following ranges: pressure: 75-100 bar; temperature: 35-70 °C; solution flow rate: 0.1-0.2 ml/min; solution concentration: 1.0-3.0 w/v. The crystallinity of embedded drug was proportional to the drug content. The relationship was nearly linear in the case of Poloxamer 237. The amorphous formulation containing 20 wt. % API was stored for 13 months in a sealed glassy container under ambient temperature in the dark. DSC measurements showed no change in crystallinity level suggesting that Poloxamer 237 has stabilized the amorphous API. However, amorphous solid dispersion was obtained only at low D/P ratio (1:4), precipitation was difficult and the yield was extremely low (4 %). In spite of diluted feed solutions and low solution flow rates, particles were clustered or agglomerated.

Poloxamers are known to undergo both photo- and thermally induced oxidative degradation when exposed to light, atmospheric oxygen, elevated temperatures, high pressures or moisture during processing or storage (Moghimi, 2000). Edwards et al. (1999) suggested that SCF fractionation at 160 atm and 40 °C may cause cleavage of Poloxamer

188 polymer producing a mixture of intact surfactant and monomers. The current methodology of the United States Pharmacopeia (USP) does not take into account the presence of polymer fractions (monomers, PPO or PEO homopolymers) and their in vivo activities are not studied either.

1.7.3 Polyvinylpyrrolidone (PVP)

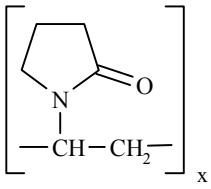

Fig. 1.29. Molecular structure of PVP.

Solubility: *soluble in acids, EtOH, MeOH, $CHCl_3$, DCM, ketones, water insoluble in CCl_4, ethyl ether.*

Applications: *binder in wet-granulation processes, disintegrant, solubilizing,- wetting,- coating,- suspending,- stabilizing and viscosity-increasing agents.*

PVP is a synthetic polymer consisting essentially of linear 1-vinyl-2-pyrrolidone (Fig. 1.29). The different grades of PVP are characterized by their viscosity in aqueous solution, relatively to that of water, expressed as a K-value, ranging from 10 to 120. The water soluble grades are obtained by free-radical polymerization of vinylpyrrolidone in water or isopropanol. The pyrrole ring contains a ternary amide N that can be protonated below pH 1.

Table 1.12. Properties of the different grades of PVP (Kibbe, 2000).

K-value	Approximate x	Approximate MW (g/mol)
12	20	2500
15	70	8000
17	90	10 000
25	270	30 000
30	450	50 000
60	3 600	400 000
90	9 000	1 000 000
120	27 000	3 000 000

PVP is widely used as excipient, particularly in oral tablets and solutions. It is considered as essentially non-toxic as it is not absorbed from the GI tract or mucous

membranes. Additionally, several authors have observed the inhibition of crystal growth by PVP (Simonelli, 1970; Sekikawa, 1978, 1979; Sarkari, 2002). One of the features that inhibit crystal growth and help to stabilize the amorphous API is the inter-molecular H-bonding between PVP and drug molecules (Sekizaki, 1995; Taylor, 1997; Serajuddin, 1999; Forster, 2001; Sethia, 2004). Each pyrrole ring contains two H-acceptor groups: a ternary amide (=N–) and a carbonyl (>C=O) group of which the tertiary N is not favoured due to the steric hindrance (Forster, 2001; Sethia, 2004). H-bonding not only decreases molecular mobility of embedded drug but increases stability by limiting the number of H-bonding sites available to water (Jans Frontini, 1996). Since water is a potential plasticizer, it decreases the T_g and results in crystallization of the API (Hancock, 1994). Forster et al. (2001) confirmed this relationship between the degree of H-bonding and shelf life of amorphous drug-carrier systems.

PVP polymers were successfully used in both supercritical (York, 2001; Corrigan, 2002; Sethia, 2004) and cryogenic particle formation processes (Williams, 2002; Rogers, 2002a, 2003; Yu, 2002; Hu, 2003, 2004; Vaughn, 2005). Although dissolution of PVP is slightly hindered by its low diffusivity in water, it was proved to be an excellent solubilizing agent (Sarkari, 2002). The intrinsic dissolution rate of GAS processed carbamazepine/PVP K30 was 4 times higher than bulk carbamazepine (Sethia, 2004). SFL prepared formulations showed even higher dissolution rates. Formulated drugs were fully dissolved within 10 min regardless of the solubility of bulk drug. The amorphous nature of freeze-dried formulation is of great importance. Hu et al. (2004) studied the effect of D/P ration on SFL micronized danazol/PVP K15 powder. XRD was used to determine the crystallinity of incorporated drug. However, all SFL formulations exhibited a diffuse background XRD pattern typical of amorphous compounds. Unlike conventional methods, SFL provides totally amorphous solid solutions with only 9 wt. % PVP. It was also evident, that from the point of view of dissolution rate, there is no use to add more than 25 wt. % PVP. Dissolution profiles of formulations with 25, 33, 50 and 66 wt. % PVP K15 were virtually identical and could not be further improved (95 % at 2 min and 100 % at 10 min). 25 wt. % PVP K15 was proved to be sufficient to stabilize the amorphous danazol, too. XRD patterns and dissolution profiles showed no significant differences between the initial and the one month samples, stored in glass vials between -5 and 40 °C.

1.7.4 Eudragit

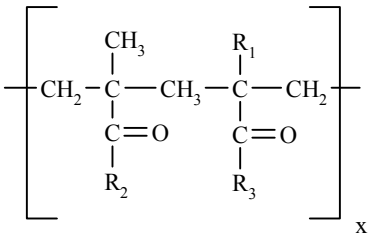

Fig. 1.30. Molecular structure of Eudragit.

Solubility: *soluble in aqueous EtOH, MeOH, iPrOH, and in CH_3Cl, DCM, acetone, ethyl acetate.*

Applications: *coating and solubilizing agents, colon targeting and sustained release drug delivery.*

Table 1.13. Properties of Eudragit polymers.

	Character	R_1	R_2	R_3	MW g/mol
E	Cationic	CH_3	C_4H_9 or $OCH_2CH_2N(CH_3)_2$ or CH_3 1:2:1		150000
L	Anionic	CH_3	OH or CH_3 1:1		135000
S	Anionic	CH_3	OH or CH_3 1:2		135000
RL	Neutral salt	H or CH_3	$OCH_2CH_2N(CH_3)_3^+Cl^-$	OCH_3 or OC_2H_5 1 : 5 : 5	150000
RS	Neutral salt	H or CH_3	$OCH_2CH_2N(CH_3)_3^+Cl^-$	OCH_3 or OC_2H_5 1 : 10 : 10	150000
NE	Neutral	H	OCH_3	OC_2H_5	800000

Eudragits are synthetic aminoalkylmethacrylate copolymers (Fig. 1.30) used since 1954 as enteric coating agents for solid oral formulation. The different grades listed in Table 1.13 cover the whole pH range prevailing in the GI tract. Eudragit E is a cationic copolymer based on dimethylaminoethyl methacrylate and neutral methacrylates. It becomes water soluble via salt formation with acids, thus providing gastrosoluble film coatings. L and S grades are soluble in the intestines and hence provide enteric properties for drugs that irritate the stomach or undergo degradation at low pH. RL and RS-type Eudragits consiste of acrylate and methacrylates with quaternary ammonium groups as functional groups. NE-type Eudragit is an ethylacrylate methylmethacrylate copolymer with neutral ester groups. RL-types are highly permeable, RS-types are poorly permeable and NE-types are swellable and permeable. Eudragit E is soluble below pH 5.5 while Eudragit L is soluble above pH 5.5, the other grades are pH independent.

Although, Eudragits were originally developed for protective coatings several authors have pointed out their ability to increase the solubility and dissolution rate of poorly water soluble APIs (Hamaguchi, 1995a, 1995b; Susuki, 1996). Jung et al. (1999) prepared solid dispersion of itraconazole and several polymers in an attempt to mask its hydrophobic character. The spray-dried itraconazole/Euragit E100 formulation showed a 141.4-fold increase in solubility and 70 times higher dissolution rate in pH 1.2 simulated gastric juice.

Juppo et al. (2003) used SEDS technology to prepare solid dispersion of a model drug and Eudragit E polymer. Drug-carrier particles were precipitated from DMSO/acetone (3:7) solvent mixture at 80 bar and 35 °C. CO_2 and solution flow rates ranged from 10 to 14 ml/min and from 0.1 to 0.2 ml/min, respectively. IR spectroscopic studies revealed a possible H-bonding between the –OH group of the drug and the carbonyl group of the polymer. As no peaks were seen in DSC thermograms, the authors concluded that both drug and polymer were amorphous. However, the extremely low precipitation yields (2-21 %) make doubts arise about the use of Eudragit in supercritical antisolvent processes.

Squillante et al. (2004) studied the feasibility of RESS to prepare sustained release devices of chlorpheniramine maleate embedded in Eudragit polymers. Among the different grades listed in Table 1.13 only RS and RL grades exhibited a reasonable solubility in $scCO_2$ suggesting that the other grades can be processed by any supercritical antisolvent process.

Wang et al. (2004) decribed the coating (encapsulation) of silica nanoparticles by Eudragit RL polymer using SAS technology. Experiments were carried out in the partly miscible region at 82.7 bar and 32 °C in acetone solution. Particles were agglomerated, but low yield was not reported.

1.8 Model compound

Our research concerns a new orally administered poorly water soluble API used in the treatment of type II diabetes. LM4156 belongs to a new class of diabetes drugs, the dual peroxisome proliferative activator receptor (PPAR) agonists, collectively known as the glitazars. The molecular structure of LM4156 is shown in **Hiba! A hivatkozási forrás nem található.**. Being a Class II API, LM4156 has high biological activity and high permeability but its bioavailability is limited because of its low aqueous solubility and low dissolution rate. In ultra pure water at ambient temperature its solubility is 1.64 mg/L which increases with pH and temperature (Table 1.14). Solubility enhancement with pH can be attributed to the dissociation of carboxyl group (pKa 4.9).

Table 1.14. Solubility of LM4156 in various solvents.

Solvent	Temperature (°C)	Solubility (mg/L)
Ultra pure water	25	1.64
Ultra pure water	37	3.01
pH 7.4 phosphate buffer	37	240.13
EtOH	35	21.45
EtOH / THF (50:50 v/v %)	35	203.10
THF	35	438.40
EtOH / $CHCl_3$ (50:50 v/v %)	35	145.32
$CHCl_3$	35	223.90
DCM	35	77.20
DMSO	35	649.30
NMP	20	800.00

XRD and differential scanning calorimetriy studies revealed that LM4156 has two polymorphic forms (Neuenfeld, 2000). The higher melting form (A) is the thermodynamically stable one at all temperatures (monotropic system). As seen in **Hiba! A hivatkozási forrás nem található.**, LM4156 contains several active groups with differing H-bonding abilities. Computer simulation using GenMol software revealed a potential H-bonding between carboxylic hydrogen and the methoxy oxygen. Owing to this strong H-bonding chain, LM4156 is highly crystalline and the crystal growths of both polymorphs are preferred in one crystallographic direction, leading to acicular crystals. Having needle-shaped crystal, conventionally crystallized LM4156 has poor flow properties.

1.9 Objectives

The objective of this study is to enhance the dissolution rate of LM4156 by using biodegradable polymers and new particle formation technologies. Though the main purpose is to improve the dissolution kinetics, formulations have to meet stability (crystallinity, polymorphic purity), toxicological (residual solvent content), technological (particle morphology, flowability) and economical (precipitation yield) requirements. As a solid product, LM4156 has one amorphous state and two crystalline monotropic phases. Any form is involved, commercialized product has to meet requirements relating to chemical and physical stability. Thus, our goal is to prepare either a semi-crystalline formulation containing the stable polymorph and an excipient or an amorphous solid solution stabilized by the excipient. Residual solvent content is also determined for its inherent toxicity. Recommended values are taken from the current ICH guidance. To obtain an easy to handle product flow properties should be markedly improved as well. As mentioned in the previous chapter, LM4156 is highly crystalline and acicular shape is dominant in all conventional methods tested so far. For economical reasons, coprecipitation has to be carried out with a reasonably high yield. It is a crucial factor not only in antisolvent precipitation.

Our specific aims are:

1. to consider the feasibility of Supercritical Antisolvent (SAS), and Solution Enhanced Dispersion by Supercritical Fluids (SEDS) processes,
2. to develop and evaluate a new cryogenic particle formation process,
3. to compare different solvents and excipients,
4. to optimize the process parameters.

2. Supercritical Antisolvent (SAS)

2.1 Purposes of the study

Although, the SAS process was essentially used for preparing sustained release devices (Table 1.8), its ability to provide micronized particles of intimately mixed drug-carrier systems could be beneficial for poorly water soluble APIs. Basically, our research aims to evaluate the SAS process as a potential new way to prepare solid dispersions. The model drug, LM4156 was coprecipitated with the previously chosen excipients: Eudragit E and RL, Poloxamer 188 and 407, PEG 8000 and PVP K17 using different solvents: ethanol (EtOH), tetrahydrofuran (THF), dichloromethane (DCM), chloroform ($CHCl_3$), N-methyl-2-pyrrolidone (NMP), dimethylsulfoxide (DMSO) and their mixtures.

The purposes are:

1. to consider the feasibility of the SAS process,
2. to study the effect of excipient and solvent choice on final product.

2.2 Materials and methods of analysis

2.2.1 Materials

Table 2.1. Materials.

Material	Purity	Source
LM4156 (Lot PP017)		Merck Santé, France
Carbon dioxide	99.7 %	Air Liquide, France
Ethanol	99.8 %	Carlo Erba, Italy
Chloroform	99 %	Carlo Erba, Italy
Dichloromethane	99.95 %	SDS, France
Dimethylsulfoxide	99.5 %	SDS, France
N-methylpyrrolidone	99 %	Acros Organics, Belgium
Methanol	99.8 %	Carlo Erba, Italy
Tetrahydrofuran	99.9 %	Ried-de Haen, Germany
Potassium phosphate monobasic		Acros Organics, Belgium
Sodium phosphate dibasic dodecahydrate		Acros Organics, Belgium
Hydrochloric acid		Carlo Erba, Italy
Sodium chloride		Prolabo, France
Lutrol F68 (Poloxamer 188)		BASF, Germany
Lutrol F127 (Poloxamer 407)		BASF, Germany
Pluriol E 8005 (PEG 8000)		BASF, Germany
Kollidon 17 PF (PVP K17)		BASF, Germany
Eudragit E		RÖHM GmbH & Co., Germany
Eudragit RL		RÖHM GmbH & Co., Germany

2.2.2 Methods of analysis

2.2.2.1 X-ray powder diffraction (XRD)

Samples were ground in agate mortar prior to analysis. Ground samples were placed in the cavity of an aluminum sample holder and flattened with a glass slide. SAS 063 – 067 samples were analyzed at the University of Veszprém. Instrument specifications are:

Apparatus:	Philips Analytical X-Ray B.V. PW3710
Tube Anode:	Cu
Generator Tension:	50 kV
Generator Current:	40 mA
Wavelength Kα_1:	1.54056 Å
Wavelength Kα_2:	1.54439 Å
Intensity Ratio (α_2/α_1):	0,5
Divergence Slit:	1°
Receiving Slit:	0.2
Data Angle Range:	4.0100 – 39.9900 2θ°
Scan Step Size:	0.020 2θ°
Scan Step Time:	1.00 s

SAS 05 – 62, SAS 70 – 75 and SEDS samples were analyzed in CEREGE - CNRS UMR6635, Aix-en-Provence. Instrument specifications are:

Apparatus:	Philips Analytical X-Ray
Tube Anode:	Co
Wavelength Kα_1:	1.78896 Å
Intensity Ratio (α_2/α_1):	0.5
Data Angle Range:	4.0 – 47.0 2θ°
Scan Step Size:	0.020 2θ°
Scan Step Time:	2.00 s

Crystallinity was calculated on the basis of peak area at d = 8.44 Å according to the following equation:

$$Crystallinity = \frac{Peak\ \ area\ \ (sample)}{Peak\ \ area\ \ (raw\ \ drug)} \times \frac{100}{Drug\ \ content} \qquad \textit{Eq. 29}$$

2.2.2.2 Dissolution studies

Dissolution tests were carried out either in pH 7.4 phosphate buffer medium (6.4g Na_2HPO_4 $12H_2O$; 0.6g KH_2PO_4 and 5.85g NaCl dissolved in 1000 ml distilled water) or in pepsin-free simulated gastric fluid at pH 1.2 (~ 7 ml HCl; 2 g NaCl dissolved in 1000 ml distilled water). Dissolution tests of SAS 05, 11, 14, 22-25, 27 and 28, were also performed in pH 7.4 phosphate buffer with 10g/L SDS (Grange, 2004 internal report). 100 mg samples (equivalent to ~ 50 mg LM4156) were added to 1000 ml dissolution medium. Bath temperature and paddle speed were set at 37 ± 0.5 °C and 75 rpm. Aliquots of 10 ml were taken through a filtering rod at 5, 10, 15, 30, 45, 60 and 120 min, diluted to 50 ml and analyzed on Spectronic AquaMate 9423 AQA 2000E spectrophotometer (Thermo Spectronic, UK) at λ = 292.0 nm. Measurements were carried out in triplicate; error bars represent the standard error of the mean.

2.2.2.3 UV/VIS Spectroscopy

The drug content of formulations was determined using Spectronic AquaMate 9423 AQA 2000E UV/VIS spectrophotometer (Thermo Spectronic, UK). UV spectra of LM4156 showed three peaks at 212.0 nm, 257.0 nm and 292.0 nm. Poloxamer 188, 407 and PEG 8000 have no chromofor group. The absorbance of Eudragit E, RL and PVP K17 is negligible in this concentration range at 292.0 nm. 100 mg samples were dissolved in 50 ml ethanol, 300 μl of the stock solution was diluted to 50 ml with ethanol. Samples and solutions were weighed on analytical balance. Drug content was calculated from the absorbance measured at 292.0 nm.

2.2.2.4 Gas chromatography (GC)

Residual solvent analysis was carried out on a Hewlet Packard 8590 (Hewlet Packard, Germany) gas chromatograph. Approximately 100 mg samples were dissolved in 2 ml DMF (to analyze the concentration of dichloromethane) or DMSO (to determine the concentration of chloroform). Sample solutions (2.0 μl) were introduced by direct injection. The method of external standardization was used to calculate the residual solvent content.

Apparatus:	Hewlet Packard 5890 A (Hewlet Packard, Germany)
Column:	Chrompack Fused Silica 25 m x 0.53 mm, (Chrompack International, The Netherlands)
Coating:	Poraplot Q
Injector temperature:	260 °C
Detector temperature:	260 °C
Oven temperature:	210 °C
Detector type:	Flame ionization
Carrier gas:	Ar

2.2.2.5 Optical Microscopy

Particle size and morphology of SAS and SEDS prepared formulations were investigated using a Motic B2 optical microscope (Motic Paris, France).

2.2.2.6 Scanning Electron Microscopy (SEM)

SEM micrographs were taken using Philips XL30 ESEM (Philips Analytical Inc., The Netherlands) Environmental Scanning Electron Microscope. Samples were coated by gold before examination (cathode dispersion).

2.2.2.7 Specific surface area (BET surface)

Micromeritics ASAP 2010 (Micromeritics, USA) apparatus was used to determine BET surface areas. A known amount of powder was loaded into the sample cell and degassed at ambient temperature for at least 2 hours (P <5 Hgμm) prior to analysis. Specific surface area was calculated using the model of Brunauer, Emmett, and Teller (Brunauer, 1938).

2.3 Method of preparation

The schematic diagram of the SAS apparatus is shown in Fig. 2.1. About 2 g of the pharmaceutical ingredients (LM4156 and excipient) were dissolved in 25-50 ml solvent. Feed solution was dispersed through a capillary nozzle (125 μm ID) on the top of a thermostated ½ liter precipitation vessel (Top Industrie S.A., France) in a co-current $scCO_2$ stream. Feed solution was delivered by a reciprocating HPLC pump (Gilson 307, France). CO_2 was liquefied at 0-5 °C and pumped by a water-cooled membrane pump (Dosapro Milton Roy, France). Compressed liquid CO_2 and solution were both heated to working temperature (> 31 °C) before entering the precipitation vessel to obtain $scCO_2$. Injection of feed solution was only started when operating parameters i.e. pressure, temperature and CO_2 flow rate reached the steady state conditions. Particles were collected on the bottom (retained by a 0.1 μm filter) and rinsed with pure SCF for 30 min to to renew the content of the autoclave before the depressurization step. A cold trap (-20 °C) was installed between the heated expansion valve and the flow meter to condense solvent vapors. Pressure and CO_2 flow rate were manually controlled by adjusting the CO_2 metering pump and the expansion valve.

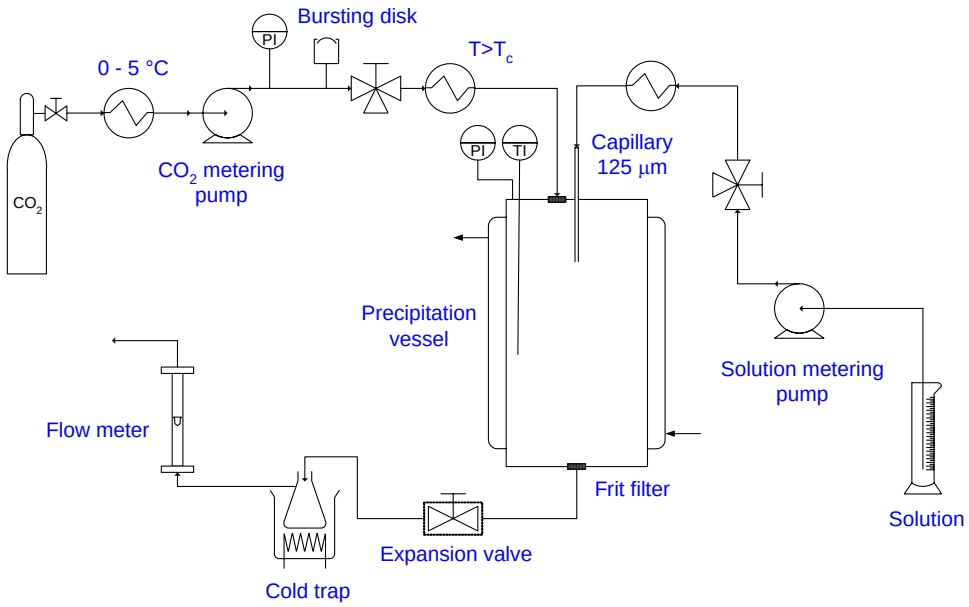

Fig. 2.1 Schematic diagram of the SAS apparatus.

2.4 Results and discussion

2.4.1 Preliminary studies

SAS crystallization is a molecular-level process in which the rate of solvent extraction controls the supersaturation profile and consequently, the crystallization kinetics. As the mechanism of this multi-step process is very complex empirical approach is likely to be the most convenient.

The first series of experiments were aimed to define the working domain of SAS process. The most important process parameters are: pressure (P), temperature (T), solution (B_S) and $scCO_2$ flow rates (B_{CO2}), concentration of solute in the feed solution (C), nozzle diameter and nature of solvent and excipient. Fargeot et al. have studied in depth the effect of these parameters, except the one of excipient, on SAS prepared LM4156 (Fargeot, 2003 and internal reports). These results were completed with our preliminary study involving pharmaceutical excipients as well. Having a multitude of parameters we limited ourselves to a few experiments, carried out from EtOH, THF, NMP, DMSO at B_S = 3 mL/min, B_{CO2} = 10 g/min, P = 80 – 120 bar, T = 35 – 45 °C and concentration of LM4156 and excipient C = 0.5 – 10 wt. %.

The ratio of **solution** (B_S) **and $scCO_2$ flow rates** (B_{CO2}) determines the solvent concentration in the vessel. Increasing solution/CO_2 ratio increases the solubility of the precipitated API and hence decreases the level of supersaturation and the yield of precipitation. On the other hand, larger nozzle velocity improves the intensity of mixing and dispersion of the solution. As a result of the superposition of these effects particle size was found to have a minimum with respect to B_S (Carretier, 2003). Bristow et al. (2001) observed similar dependence in SEDS process. The level of supersaturation had a maximum when plotted as a function of solution/CO_2 ratio. In the case of SAS prepared pure LM4156 Fargeot et al. (2003) observed a slight decrease in the particle size when B_S was increased from 1 to 5 mL/min at C = 1 wt. %. However, at C = 0.5 wt. %, solution flow rate did not affect the particle size at all. In this work, the effects of solution and $scCO_2$ flow rates were not studied. B_S and B_{CO2} were set to 3 mL/min and 10 g/min, respectively. These parameters allow adequate dispersion of the liquid solution with a maximum productivity using our laboratory scale apparatus.

Pressure and temperature are the most relevant parameters in controlling the product's physical properties. However, the roles of these parameters are hard to separate

from a third one, the density. Density is not an independent parameter, it is a function of operating pressure and temperature. The effects of these conditions are frequently disused together. For instance, the solvent strength of $scCO_2$, which is directly related to its density, can be modified by changing the operating pressure and temperature. It is known that the solubilities of high-boiling compounds increase with pressure, at constant temperature, in all cases. This can be explained by the shorter intermolecular distances which increase the solute-solvent interaction. The effect of temperature is more complex because of the crossover phenomena. When the solubility of a high-boiling compound is plotted as a function of pressure, isothermal curves cross each other twice. The intersection in supercritical domain is called (upper) crossover pressure point. At pressures above the crossover pressure, the solubility increases with temperature while at pressures below the crossover pressure, the solubility decreases with increasing temperature. In the crossover pressure point, the opposite effects of solute vapor pressure and solvent density on solubility compensate each other.

Liquid solvents enhance markedly the solubility of high-boiling compounds. On the other hand, high-boiling compounds are known to increase the bubble point pressure of the binary solvent-CO_2 system. Reverchon et al. (2000, 2002) pointed out the importance of solvent-CO_2 miscibility from the point of view of particle morphology. SAS prepared rifamicin, precipitated from the liquid phase of the two-phase system consisted of non-aggregated spherical particles ranging from 2.5 to 5 μm whilst those obtained in single phase fluid contained aggregated nanoparticles. Beyond the thermodynamic aspects, pressure and temperature have major influences on hydrodynamics. The viscosity of $scCO_2$ decreases with increasing temperature and increases with increasing pressure (Stephan, 1979). If the viscosity of bulk phase is lower, the liquid jet disintegrates more rapidly (Subramaniam, 1997). However, some authors found that mass transport due to diffusion has more influence on crystallization kinetics than jet breakup and hydrodynamics (Randolph, 1993; Thies, 1998; Rantakylä, 2002). Diffusion coefficient in turn is proportional to temperature and inversely proprtional to viscosity (Higashi, 2001). Owing to the complex relationship of these features, pressure and temperature may have contradictory effects on processed powders. For instance, increasing pressure may increase (Randolph, 1993; Shekunov, 1999) or decrease the particle size as well (Sze Tu, 1998; York, 1999). However, in most cases pressure does not have any significant effect (Bleich, 1994; Reverchon, 1999a; Magnan, 1999; Fargeot, 2003). The same behavior was observed for process temperature: higher temperatures may induce size reduction (Gao, 1998;

Fargeot, 2003) but in most cases size enlargement of particles was reported (Schmitt, 1995; Shekunov, 1998; Rantakylä, 2002). The particle size of LM4156 correlates with temperature rather than with pressure (Fargeot, 2003). Fargeot et al. reported decreasing particle size with increasing temperature. In this work, attempts were made to obtain particulate product from NMP, DMSO and DCM by increasing the operating pressure and temperature (120 bar, 45 °C) but the effects of these parameters were out of our scope.

Generally, **solute concentration** in the feed solution correlates well with mean particle size and size distribution: both increase with increasing concentration (Reverchon, 1998, 1999, 2000, 2002; Fargeot, 2003). In some cases, concentration affects particle morphology, too. For example, below a certain concentration (2-3 wt. %) L-PLA forms spherical particles while above this concentration authors observed fibrous network (Randolph, 1993; Bodmeier, 1995; Taki, 2001; Sze Tu, 2002). Taki et al. (2001) attributed this phenomena to the higher viscosity of the polymer solution which has a stabilizing effect on the liquid jet and results in poor mixing characteristics. As shown in Fig. 2.2 particle size of LM4156/Poloxamer 188 formulation increased considerably when concentration increased from 2 to 10 wt. % but it had no effect on the morphology. Below 2 wt. % pharmaceutical ingredients were washed out by the solvent-CO_2 mixture leaving an empty vessel behind.

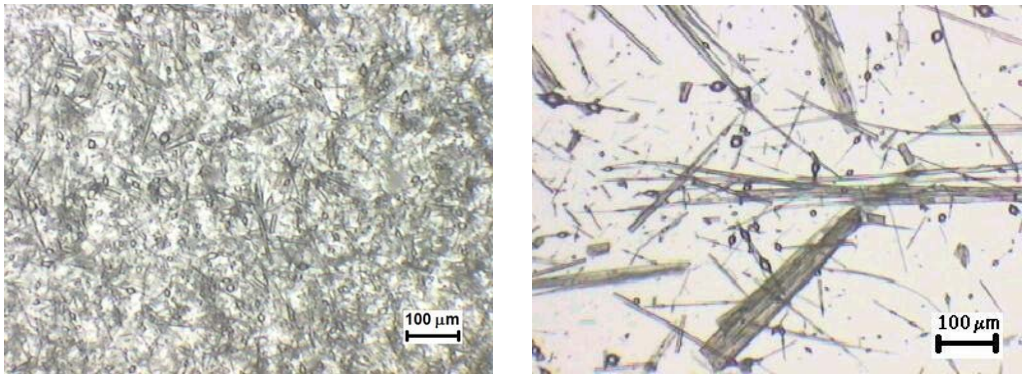

(a) *(b)*

Fig. 2.2 Optical micrographs of LM4156/Eudragit E from THF solution at 80 bar, 35 °C, (a) 2 wt.%, (b) 10 wt. %

The composition of **liquid solvent** was also found to affect considerably the size, morphology and yield of particles as well as the polymorphic form (Reverchon, 1999a, 1999b, 2002; Sze Tu, 2002; Fargeot, 2003; Badens, 2004). This can be attributed to the different densities, viscosities, solvent strengths, solvent-solute interactions and solvent-

CO_2 miscibility limits (bubble point pressure curves). Sze tu et al. (2002) studied the effect of liquid solvent on ASES prepared para-hydroxybenzoic acid (p-HBA). P-HBA powders precipitated from MeOH, acetone and ethyl acetate consisted of rhomboidal platelets, needle-like and rod-like particles, respectively. The authors concluded that the weaker the solvent, the larger the mean particle size and the poorer the crystallinity. The results of Reverchon et al. (1999a, 1999b, 2002) confirmed the influence of liquid solvent on precipitation yield and crystal habit. When rifampicin was precipitated from NMP, MeOH or DCM, tightly networked nanoparticles were obtained while needle-like crystals were formed from ethyl acetate solution (Reverchon, 1999b). Precipitation yield varied in a wide range depending on solute and liquid solvent. For example, DMSO gave the best yield in rifampicin crystallization, while in the case of amoxicillin and tetracycline DMSO extracted each antibiotics from the precipitation chamber (Reverchon, 1999b, 1999c). Fargeot et al. succeeded in modifying the crystal habit of LM4156 and control the polymorphic form by using different solvents (Fargeot, 2003; Badens, 2004). Conventionally crystallized LM4156 has a needle-like shape which was observed for SAS prepared drug from ethyl acetate, acetonitrile, EtOH, DCM and THF, as well. SCF processed LM4156 from DMF, DMSO and NMP solutions led to discrete rectangular platelets, aggregated irregular particles and aggregated microparticles, respectively. In the case of SAS prepared drug-carrier powders, yield and polymorphic purity were definitely related to the composition of liquid solvent. In some cases EtOH and THF have extracted up to 70 % of the injected APIs. Poor yield implies strong solute-solvent interactions. Liquid solvent had major influences on polymorphic purity as well, but this stochastic-like relationship will be discussed in chapter 2.4.2.3.

Although pure LM4156 was successfully precipitated from NMP and DMSO under these working conditions (Fargeot, 2003), coprecipitations of drug-polymer composites from these solvents were always hindered by filter blockage. In all cases, an amorphous film was observed on the bottom suggesting that our working point was in the two-phase region and that precipitation occurred in the liquid phase (Reverchon, 2000, 2002).

P-x isotherms of binary systems composed of CO_2 and solvents, used in this work, are shown in Fig. 2.3 - Fig. 2.5. Experimental data from the indicated references were correlated with Peng-Robinson EOS (Eq 13) using the van der Waals one fluid mixing rule. Solid lines represent the calculated values. Optimized binary interaction parameters are listed in Table 2.2. As experimental data for THF + CO_2 and $CHCl_3$ + CO_2 systems were not available at 308 K, k_{12} and l_{12} were estimated using an interpolation polynom.

Parameter fitting was performed choosing the average absolute relative deviation (AARD) as objective function. Eq 30 was used for CO_2 + $CHCl_3$, EtOH and THF systems and Eq 31 was used for CO_2 + DMSO, NMP and DCM systems.

At P = 80 bar, T = 35 °C, x_{DMSO} = 0.1567 and x_{NMP} =0.1205 (B_S = 3 mL/min, B_{CO2} = 10 g/min) we are closer to the bubble point pressure curve for DMSO + CO_2 and NMP + CO_2 mixtures than for any other system (Fig. 2.3 - Fig. 2.5). The addition of a high-boiling component (model compound, excipient, etc.) could shift the bubble point pressure over the working point leading to a two-phase system (Reverchon, 2000, 2002).

$$AARD = \frac{100}{NDP}\sum_{i=1}^{NDP}\left[\frac{\left|P_{calc} - P_{\exp}\right|}{P_{\exp}} + \frac{\left|y_{calc} - y_{\exp}\right|}{y_{\exp}}\right]_i \qquad \textit{Eq. 30}$$

$$AARD = \frac{100}{NDP}\sum_{i=1}^{NDP}\left[\frac{\left|P_{calc} - P_{\exp}\right|}{P_{\exp}}\right]_i \qquad \textit{Eq. 31}$$

Table 2.2. Binary interaction parameters (Peng-Robinson EOS, vdW II mixing rules).

System	T [K]	k_{12}	l_{12}	AARD	Reference
EtOH + CO_2	308.11	0.0937	0.0168	2.4089	Chang, 1997
DCM + CO_2	308.2	0.0617	-0.0255	1.4739	Tsivintzelis, 2004
DMSO + CO_2	308.2	0.0335	-0.0469	0.8945	Rajasingam, 2004
NMP + CO_2	308.2	0.0331	-0.0318	0.9237	Rajasingam, 2004
$CHCl_3$ + CO_2	303.15	0.0402	-0.0221	3.6020	Scurto, 2001
$CHCl_3$ + CO_2	308.15	0.0401	-0.0221	-	This work
$CHCl_3$ + CO_2	313.15	0.0385	-0.0236	2.5857	Scurto, 2001
$CHCl_3$ + CO_2	323.15	0.0327	-0.0289	1.7475	Scurto, 2001
$CHCl_3$ + CO_2	333.15	0.0267	-0.0328	1.4016	Scurto, 2001
THF + CO_2	298	0.0174	0.0182	0.6040	Lazzaroni, 2005
THF + CO_2	308.15	0.0175	0.0085	-	This work
THF + CO_2	313	0.0142	0.0023	0.7742	Lazzaroni, 2005
THF + CO_2	333	-0.0233	-0.0360	1.5825	Lazzaroni, 2005

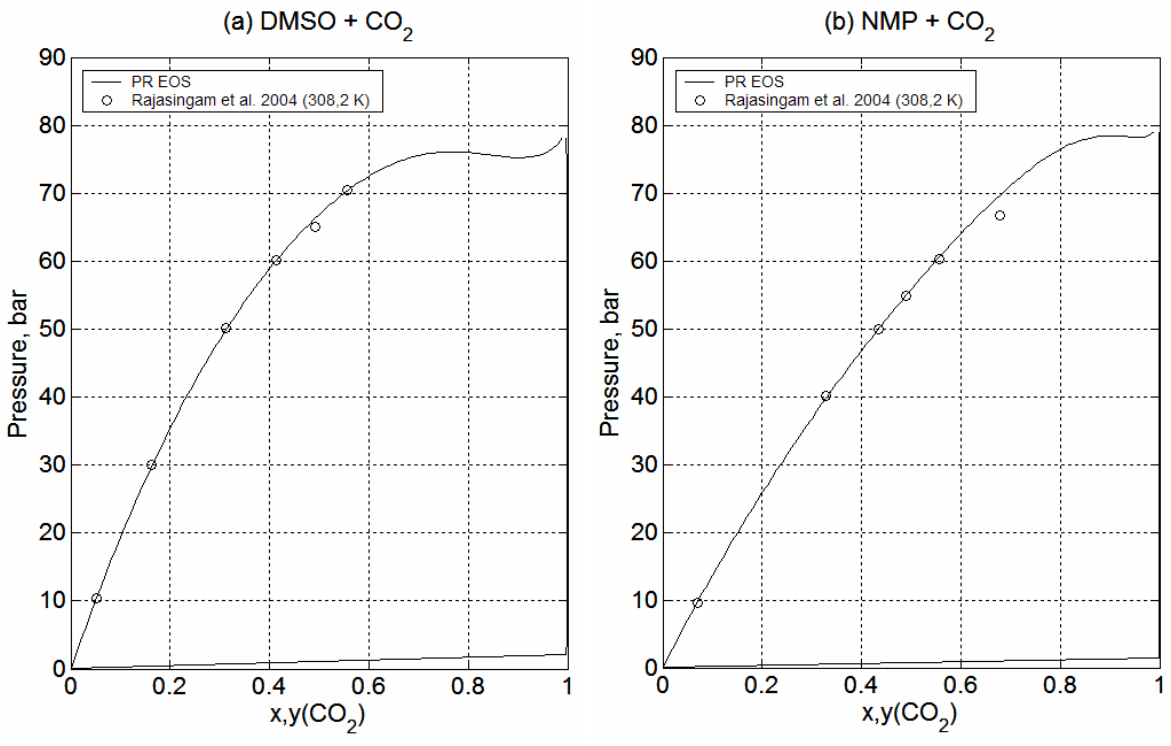

Fig. 2.3. Phase diagrams of (a) DMSO + CO_2 and (b) NMP + CO_2 systems.

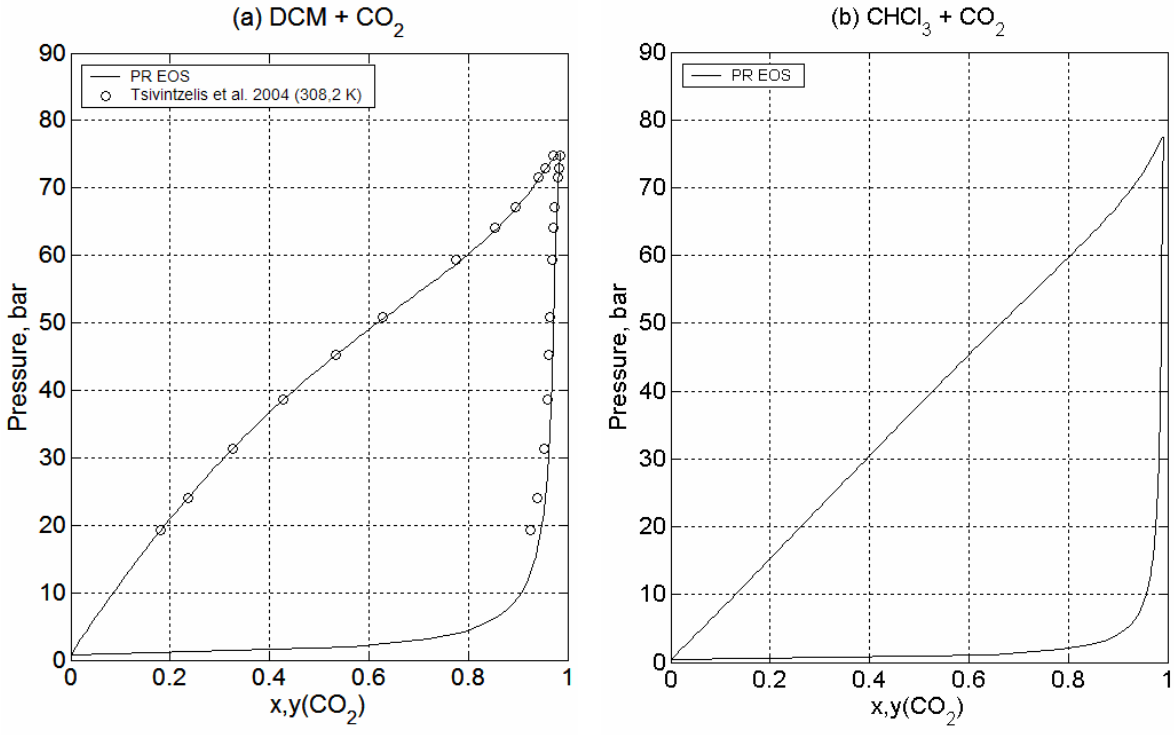

Fig. 2.4. Phase diagrams of (a) DCM + CO_2 and (b) $CHCl_3$ + CO_2 systems.

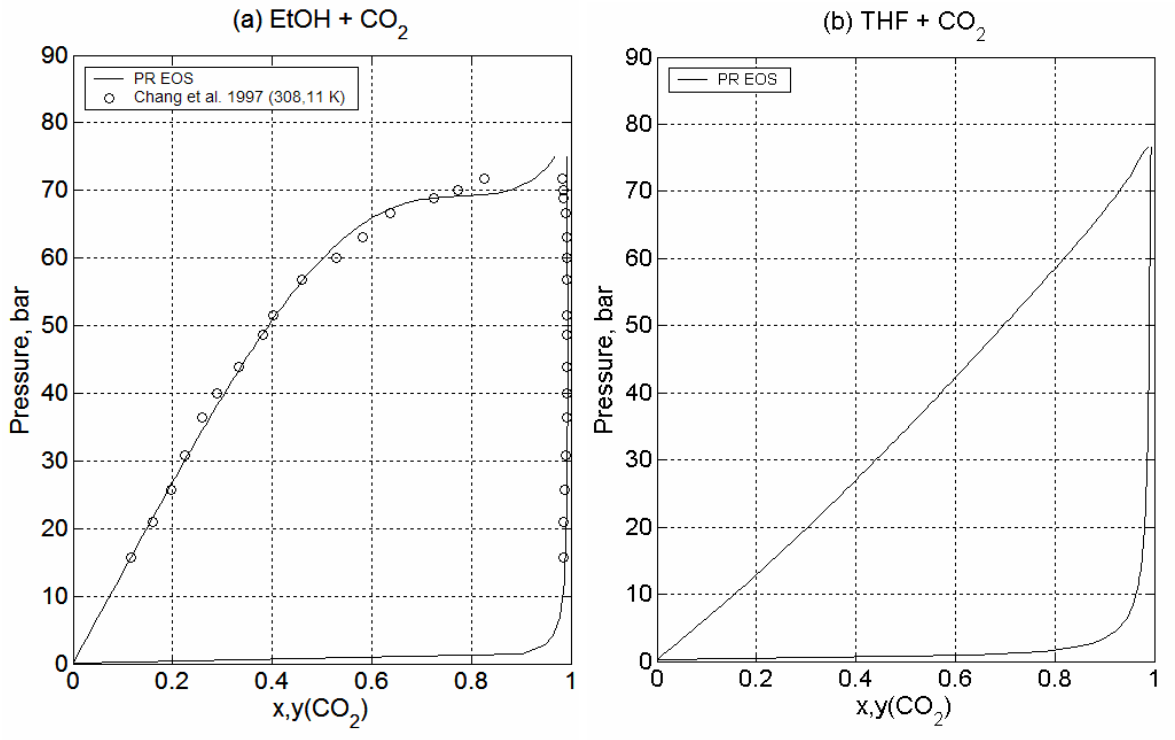

Fig. 2.5. Phase diagrams of (a) EtOH + CO_2 and (b) THF + CO_2 systems.

Beneath the liquid solvent, **excipient** has to be carefully chosen, as well. Polymers can considerably increase viscosity and turn single phase into two-phase system. On the other hand $scCO_2$ is known to penetrate in polymers and lower their glass transition temperatures (Shieh, 1996; Mawson, 1997b; Condo, 1994). Polymers with low T_g can only be processed by SCF antisolvent processes when conditions allow primary heterogeneous nucleation. In the precipitation process of a drug-carrier system, drug particles provide heteronuclei for the precipitation of polymer (Wang, 2003). In the absence of constantly renewing heteronuclei, these polymers form a film on the bottom of the vessel and block the outlet filter. Our results were consistent with previous studies and confirmed that these polymers precipitate as a film without the API (Juppo, 2003, York, 2001). This phenomena was observed for drug-carrier systems with low **D/P ratios** (< 1:2), as well.

Owing to the relatively great number of operating parameters (P, T, B_{CO2}, B_S, C_D, C_E, solvent, excipient, nozzle diameter, etc.) our parameter optimization does not pretend to be exhaustive. In this work we focused mainly on the effect of excipient and solvent and tried to find the condition that allow the most candidates to be tested.

Based on the work of Fargeot et al. and our preliminary study the following working conditions were chosen: P = 80 bar, T = 35 °C, B_S = 3 ml/min, B_{CO2} = 10 g/min, C_D = C_E = 2 wt. %, nozzle diameter: 125 μm (Fargeot, 2003 and internal reports).

Investigated solvents were: EtOH, THF, $CHCl_3$, DCM, and binary solvent mixtures of EtOH/THF and EtOH/$CHCl_3$ in the ratio of 50:50 v/v. It must be emphasized that this work is not exhaustive in terms of parameter optimization. Further studies have to be done to find the optimal conditions and fully understand the mechanism of SAS crystallization.

2.4.2 The effect of solvent and excipient choice on SAS prepared powders

2.4.2.1 Particle morphology

Particle morphology and particle size were defined on a visual basis (Fig. 2.6 and Fig. 2.7). Microscopy pictures of SAS prepared pure LM4156 showed long acicular crystals (Fig. 2.6a) similar to those prepared by cooling crystallization. SCF-processed drug-carrier particles were unusually long. SAS prepared formulations containing LM4156 combined with PEG 8000, Eudragit E, RL, Poloxamer 188 or 407 formed a thick cottony layer on vessel wall. Optical and SEM micrographs showed needle-shaped crystals varying from one to several mm in length (Fig. 2.6 b – e and Fig. 2.7a - e).

In most cases, crystals were partly covered by polymer spheres (~ 50 μm in diameter) suggesting that the nucleation of the active substance was much faster than the precipitation of the excipient (Fig. 2.6f and Fig. 2.7f). This particle morphology confirmed the theory of heterogeneous nucleation of polymers on the surface of drug crystalls. LM4156/Eudragit E particles showed similar shape, but unlike other excipients, Eudragit E succeeded in decreasing particle size by coating the drug nuclei and hindering their growth (Fig. 2.6g). Microscopy pictures showed completely encapsulated drug particles (~10 μm in diameter) and a few intact acicular crystals (< 80 μm in length). However, these formulations had poor flow properties that may cause processing difficulties on industrial scale.

Poloxamer 188 and 407 formulations from DCM solution consisted of aggregated acicular particles of around 1 mm in length (Fig. 2.6d and Fig. 2.7c - d). Although, needle-like shape was still dominant spherical coating was not observed.

The morphology of LM4156/PVP K17 particles was very different from those observed for the other polymers. Coprecipitations in chlorinated solvents led to a relatively dense amorphous film-like precipitate which broke up into irregular particles with high apparent densities and good flowabilities (Fig. 2.6h and Fig. 2.7g - h). Disparate morphology of these formulations might be attributed to the higher T_g of PVP K17.

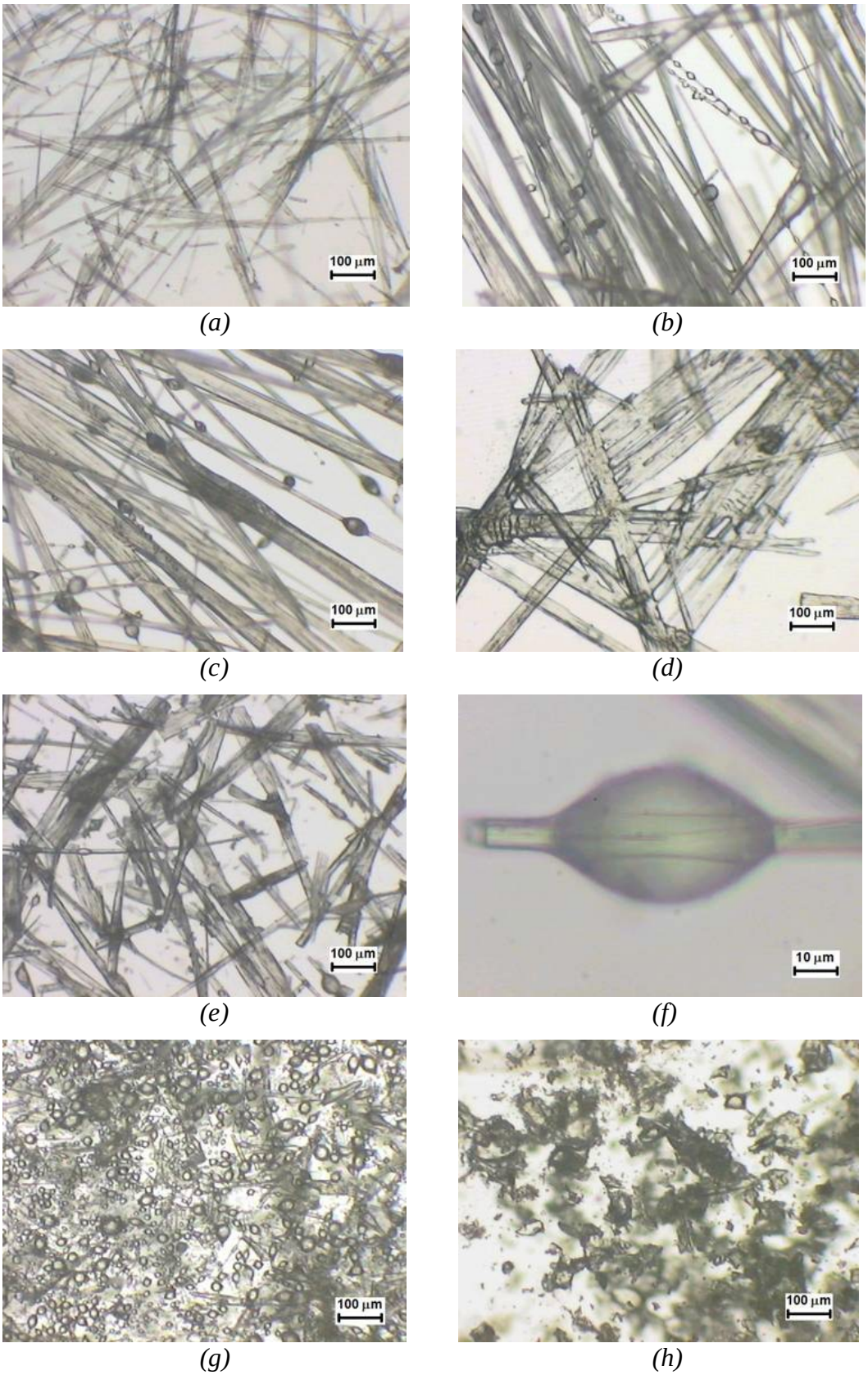

(a) *(b)* *(c)* *(d)* *(e)* *(f)* *(g)* *(h)*

Fig. 2.6 Optical micrographs of (a) SAS prepared LM4156 (SAS 74, $CHCl_3$), (b) LM4156/Eudragit RL (SAS 57, EtOH/$CHCl_3$), (c) LM4156/Poloxamer 188 (SAS 54, EtOH/$CHCl_3$), (d) LM4156/Poloxamer 407 (SAS 37, DCM), (e) LM4156/PEG 8000 (SAS 66, $CHCl_3$), (f) Typical polymer coating, (g) LM4156/Eudragit E (SAS 40, EtOH/THF), (h) LM4156/PVP K17 (SAS 52, EtOH/$CHCl_3$).,

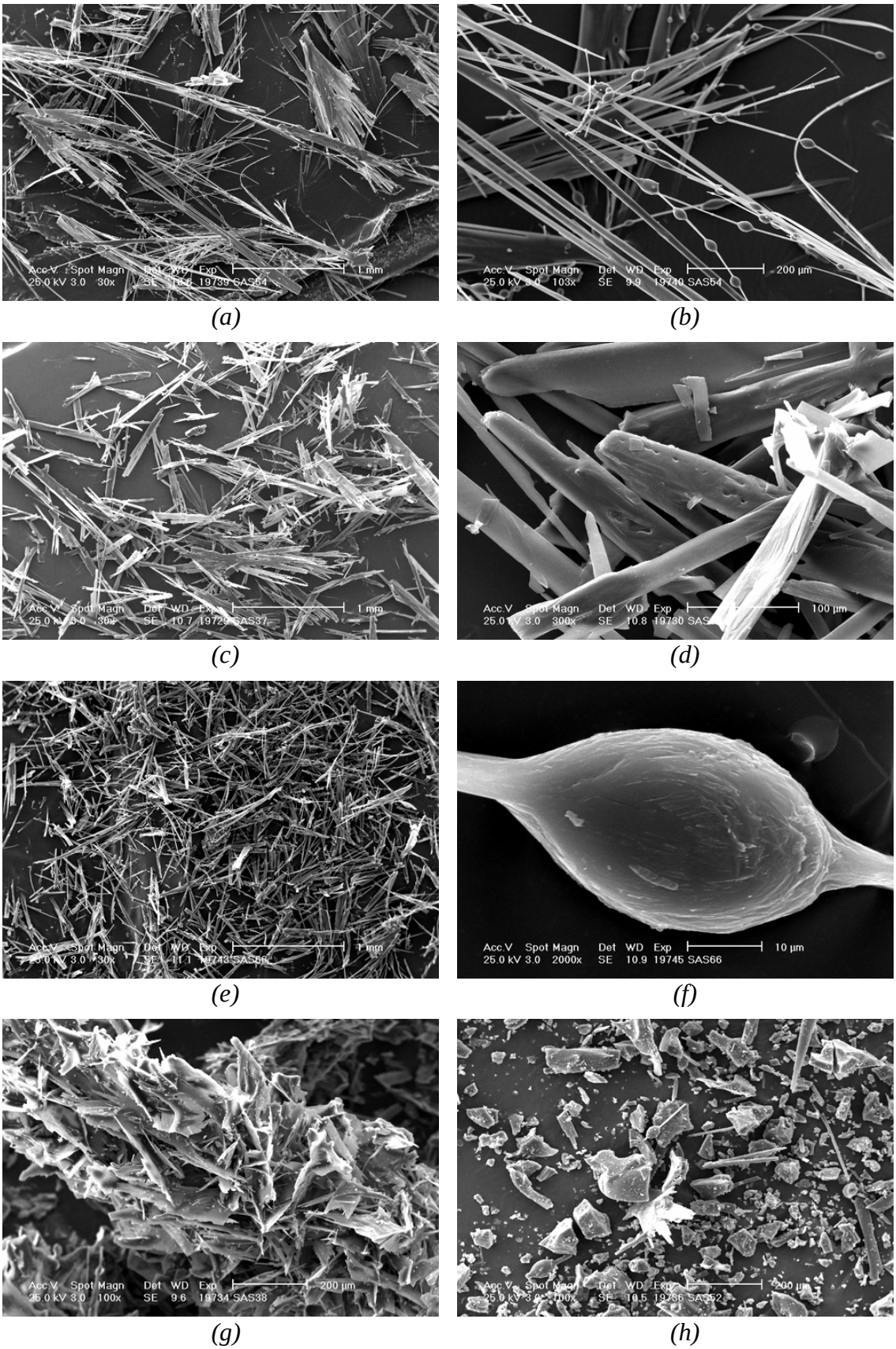

(a) *(b)*

(c) *(d)*

(e) *(f)*

(g) *(h)*

Fig. 2.7 SEM micrographs of (a-b) LM4156/Poloxamer 188 (SAS 54, EtOH/$CHCl_3$), (c-d) LM4156/Poloxamer 407 (SAS 37, DCM), (e-f) LM4156/PEG 8000 (SAS 66, $CHCl_3$), (g) LM4156/PVP K17 (SAS 38, DCM), (h) LM4156/PVP K17 (SAS 52, EtOH/$CHCl_3$),

2.4.2.2 Precipitation yield and drug content

Precipitation yield is the percentage of recovered drug with respect to the amount delivered with the liquid solution. Precipitation yield varied between 28 and 93 % (Table 2.3). Compared to other supercritical antisolvent techniques these values are rather promising (York, 2001; Juppo, 2003; Jung, 2003). Material loss can be partly decreased by improved filtration of the outlet stream and more careful collection of the particles retained in the precipitation vessel. The effect of these factors may be reduced by scale-up. Jung et al. (2003) have studied the scale-up of SAS process. Inulin was precipitated from NMP at three different scales: lab-scale (vessel volume, V = 0.5 l; mass of processed drug, m = 2 g), pilot plant scale (V = 4 l; m = 20 g) and commercial scale (V = 50 l; m = 200 g). Particle recovery yield was found to increase considerably with scale: from 61 % to 97 % when capacity was multiplied by 100.

Table 2.3. Yield (%) of SAS-prepared powders.

Solvent	Pure LM4156	Excipient					
		Eudragit E	Eudragit RL	Poloxamer 188	Poloxamer 407	PVP K17	PEG 8000
THF	72	75	~ 35	~ 35	~ 35	55	~ 35
EtOH / THF	47	62	32	48	70	~ 30	67
EtOH	36	-	-	28	38	~ 30	~ 30
EtOH / $CHCl_3$	66	75	66	68	62	56	80
$CHCl_3$	91	82	93	88	86	-	87
DCM	87	~ 85	86	65	72	70	73

However the major part of material loss arises from the fact, that pharmaceutical ingredients are not completely insoluble in $scCO_2$-solvent systems. Hence these latter dissolve and wash out a part of these ingredients. The difference in average yields and the presence of the pharmaceutical ingredients in the cold trap at the end of the precipitation process seem to confirm this theory. In this case study, non-chlorinated solvents, EtOH, THF and their mixture exhibited such co-solvent behavior. This phenomenon was previously observed in SEDS technology by several authors and is considered as the main source of loss in precipitation processes using SCF antisolvents (York, 2001; Juppo, 2003). York et al. (2001) have reported yields ranging from 4 to 96 % for drug/PVP K17 and drug/Poloxamer 237 composites precipitated from EtOH/$CHCl_3$ and DCM solutions. Juppo et al. (2003) obtained even lower yields, reported values for drug/Eudragit E and drug/mannitol solid dispersions were in the range of 2-21 % and 35-84 %, respectively.

It seems that chlorinated solvents do not increase the solubility of LM4156 to such extent. The highest yield was obtained from $CHCl_3$, between 82 and 93 %.

As the feed solution contained both ingredients in equal quantities a drug content of 50 wt. % is expected. However, drug content in SAS formulations ranged from 36.7 to 60.3 wt. % (Table 2.4) suggesting that the two ingredients exhibit different solubilities in different CO_2-solvent systems. Low D/P ratios were typically observed from $CHCl_3$, EtOH/$CHCl_3$ and EtOH/THF. York and co-workers (2001) have observed similar deviations in effective drug content in SEDS prepared formulations.

Table 2.4. Drug content (wt. %) of SAS-prepared powders.

Solvent	Excipient					
	Eudragit E	Eudragit RL	Poloxamer 188	Poloxamer 407	PVP K17	PEG 8000
THF	47.7	51.3	50.3	55.1	47.6	47.3
EtOH / THF	36.7	60.3	45.9	43.1	41.3	39.7
EtOH	-	-	40.1	53.9	51.6	50.2
EtOH / $CHCl_3$	43.2	47.3	46.0	49.4	43.6	42.6
$CHCl_3$	49.3	42.2	41.8	47.5	44.4	46.9
DCM	50.3	43.1	49.8	53.5	57.9	50.4

2.4.2.3 Crystallinity and polymorphic purity

XRD measurements were performed to determine the polymorphic purity and calculate the crystallinity of embedded LM4156. Drug crystallinity plays a key role in aqueous solubility and stability of solid dosage forms. The amorphous state of an API is generally more soluble than its crystalline counterpart. However amorphous solids were long time considered unsuitable for pharmaceutical application for their susceptibility to undergo phase transformation during storage (Debenedetti, 2002).

The proportion of crystalline to amorphous LM4156 ranged from 4 to 100 % (Table 2.5). Although polymorphism and crystallinity were likely to depend both on solvent and excipient, crystallinity was more affected by the polymer. Excipients with low glass transition temperatures (PEG 8000, Poloxamer 188 and 407) contained higher fraction of crystalline drug typically between 58 and 100 % while coprecipitations with PVP K17 and Eudragit E resulted in amorphous solid dispersions with low degrees of crystallinity (4 - 48 %). These results seem to be consistent with previous studies suggesting that PVP and Eudragit E can inhibit crystallization of active substances (chapter 1.7.3 and 1.7.4). York et al. (2001) studied the crystallinity of indomethacin/PVP K17 and drug/Poloxamer 237

formulations as a function of drug loading. Indomethacin was totally amorphous below 62 wt. %, the corresponding value for Poloxamer 237 was much lower; crystalline phase was detectable and showed linear increase over 20 wt. % drug.

Table 2.5. Crystallinities (%) of SAS prepared formulations.

Solvent	No excipient	Excipient					
		Eudragit E	Eudragit RL	Poloxamer 188	Poloxamer 407	PVP K17	PEG 8000
THF	100	38	46	> 100	69	40	67
EtOH / THF	92	26	96	> 100	47	25	38
EtOH	100	-	-	83	75	22	46
EtOH / $CHCl_3$	92	33	61	> 100	> 100	27	58
$CHCl_3$	100	41	> 100	77	99	4	51
DCM	100	48	45	72	61	18	72

Polymorphic purity is listed in Table 2.6. The higher melting form is always dominant notwithstanding that in most cases the metastable form is also present. The lower melting form B is detectable owing to the characteristic peaks at d = 13.23 and 10.20 Å (Appendix C). Contrary to what we expected there was no overall tendency in polymorphic purity. Apart from Eudragit RL and PEG 8000 which always resulted in pure form A and mixture of the two polymorphs, a stochastic-like relationship was observed between polymorphic purity and chosen solvent and polymer. Polymorphism is known to depend on both thermodynamic and kinetic factors. The effects of temperature, pressure, liquid solvent and level of supersaturation was widely studied but no information is available on the effect of excipients (Beach, 1999; Tong, 2001; Kordikowski, 2001; Shekunov, 2002; Yeo, 2003; Gosselin, 2003; Fargeot, 2003; Badens, 2004; Rehman, 2004). No doubt both solvent and polymer affect polymorphism but this dependence is not completely understood and further experiments are needed to make it clear.

Table 2.6. Polymorphic purities of SAS prepared formulations.

Solvent	No excipient	Excipient					
		Eudragit E	Eudragit RL	Poloxamer 188	Poloxamer 407	PVP K17	PEG 8000
THF	A (B)	A & B	A	A	A	A & B	A & B
EtOH / THF	A & B	A	A	A & B	A & B	A & B	A (B)
EtOH	A & B	-	-	A	A & B	A	A (B)
EtOH / $CHCl_3$	A	A	A	A (B)	A (B)	A	A (B)
$CHCl_3$	A	A (B)	A	A & B	A & B	A & B	A (B)
DCM	A (B)	A (B)	A	A	A	A & B	A (B)

A: Form A; A (B): Form A containing a few Form B; A & B: nearly stoichiometric mixture of the two polymorphs;

2.4.2.4 Specific surface areas

Specific surface areas of raw drug and three representative SAS powders are listed in Table 2.7. SAS 54 and 37 powders consisted of acicular drug crystals with and without spherical polymer coating. SAS 52 is a typical LM4156/PVP K17 solid dispersion with dense irregular particles. However processed powders exhibited low specific surface areas. Measured values did not reach the lower measuring limit of the instrument (1 m^2/g).

Table 2.7 Surface areas of SAS powders.

Run	Excipient	Solvent	Specific surface area (m^2/g)
Raw drug	-	-	0.7[a]
SAS 37	Poloxamer 407	DCM	< 1
SAS 52	PVP K17	EtOH/$CHCl_3$	< 1
SAS 54	Poloxamer 188	EtOH/$CHCl_3$	< 1

[a] Measured at the University of Veszprém (see chapter **Hiba! A hivatkozási forrás nem található.**)

2.4.2.5 Residual solvent

The residual solvent content was determined by gas chromatography analysis. Only powders prepared in $CHCl_3$, EtOH/$CHCl_3$ and DCM solutions were considered. Residual solvents in powders from THF, EtOH and EtOH/THF were not assessed because of their low yield. Among the solvents of interest, $CHCl_3$ and DCM are Class 2 solvents with permitted daily exposure (PDE) of 0.6 and 6 mg; EtOH belongs to the third and less toxic solvent class with a PDE of 50 mg (FDA, 1997). The concentrations of Class 2 solvents in pharmaceutical products are limited because of their inherent toxicity. Some of these solvents like $CHCl_3$ are animal carcinogens without adequate evidences of carcinogenicity in humans. Although current requirements can be met using conventional technologies, there is a clear tendency in pharmaceutical industry to replace Class 2 solvents or limit their application i.e.: to avoid them in the final stages of manufacturing. Two options are available when setting limits of Class 2 solvents: Option 1 may be applied if the daily dose is not known or fixed. This option assumes a high dose (10 g/day) that is rarely exceeded. Option 2 takes into account the daily dose or the maximum administered daily mass of a drug product, if the drug is not regularly administered. The maximum allowed daily dose is approximately 400 mg for LM4156, which means 800 mg together with the inactive pharmaceutical ingredient. According to the Eq. 27, limits of $CHCl_3$ and DCM are 750 and 7500 ppm, under Option 2.

$$Conc\ (ppm) = \frac{1000 \times PDE\ (mg/day)}{Dose\ (g/day)} \qquad \textit{Eq. 32}$$

Solvents in Class 3 are less toxic in short-term studies and negative in genotoxicity studies. Their presence in pharmaceutical products is acceptable without justification below 5000 ppm (under Option 1). The residual amount of EtOH was not determined in this work.

Results of gas chromatography studies are shown in Table 2.8. With some exception all formulations meet ICH requirements. In the case of PVP K17 and PEG 8000 (precipitated from $CHCl_3$ solution), longer solvent stripping is recommended. PVP K17 formulations were characterized by high apparent density and low crystallinity which makes solvent stripping more difficult. In addition, the precipitation processes of PVP formulations were frequently perturbed because the polymer has partly blocked the outlet filter.

Table 2.8. Residual solvent level (ppm).

Solvent	Limit		Excipient					
	Option 1	Option 2	Eudragit E	Eudragit RL	Poloxamer 188	Poloxamer 407	PVP K17	PEG 8000
DCM	600	7500	515	4872	765	804	13500	233
$CHCl_3$	60	750	ND	201	341	132	28600	826
$CHCl_3$ ($EtOH/CHCl_3$)	60	750	57	350	52	89	3240	441

ND: Not detectable, Detection limit is 5 ppm.

Residual DCM contents were consistent with published works on SCF processed pharmaceutical products. Bitz et al. (1996) compared spray-drying, solvent evaporation and ASES processes. L-PLA and L-PLA/tetracosactide powders contained 5283 and 758.3 ppm DCM after 4 hours of drying at a CO_2 flow rate of 6 kg/h. As residual solvent content exceeded recommended limits, authors used vacuum drying. Residual DCM concentration in pure and drug loaded particles decreased to 5.9 and 2 ppm after 3 days of drying under reduced pressure. Ruchatz et al. (1997) pointed out that there is no need for additional drying procedures when using ASES process. $ScCO_2$ was circulated through the precipitation vessel for 5 hours at high flow rates (2 – 11 kg/h). The lowest DCM concentration in L-PLA particles (71.47 ppm) was achieved at the highest CO_2 flow rate: 11 kg/h. Jung et al. (2003) concluded that reducing the residual solvent content in a SCF extraction equipment may be more efficient than in a precipitation vessel. The decrease of

residual solvent content was very slow when its extraction was carried out in the precipitation vessel. Residual NMP concentrations between 3 and 5 % were reported. Residual $CHCl_3$ content was not previously reported in the literature of SCF particle engineering.

2.4.2.6 Dissolution

Dissolution tests were carried out on SAS prepared formulations from DCM, $CHCl_3$ and EtOH/$CHCl_3$ (50:50 v/v). Approximately 30 % of raw drug were dissolved within 5 min and this value increased to 85 % after two hours. In spite of the larger particle size, SAS formulations exhibited higher dissolution rate compared to raw drug and physical mixtures. PEG 8000 formulations showed only a slight improvement: 1.4 fold higher drug concentration was measured compared with raw drug within 5 min (Fig. 2.8). Dissolution curves of PVP formulations showed the steepest initial slope, more than two times higher than raw drug (Fig. 2.9). However, initial release rate of embedded LM4156 dropped considerably after 5 min. Poloxamer 188 and 407 formulations dissolved rapidly (1.3-2.0 fold increase), as well, but contrary to PVP K17 matrix, Poloxamers exhibited high dissolution rate throughout the whole test (Fig. 2.10 and Fig. 2.11). In pH 7.4 dissolution medium, both grades of Eudragit copolymers have decreased the rate of drug release (Fig. 2.12 and Fig. 2.13). In contrast, dissolution profiles of LM4156/Eudragit E in pepsin-free simulated gastric fluid showed significant improvement over raw drug (Fig. 2.14). Although, some formulations showed up to 3.5-fold higher dissolution rate, absolute values of LM4156 concentrations are still very low compared to pH-independent polymers at pH 7.4. Thus absorption of LM4156 in the intestine seems to be more favorable.

Moneghini et al. (2001) achieved better enhancement in the dissolution rate of carbamazepine with PEG 4000. GAS processed formulation exhibited approximately 6 times higher dissolution rate compared to raw drug which is attributable to the higher dissolution rate of the lower grade PEG. Perrut et al. (2005) have coprecipitated nifedipine and lidocaine with Poloxamer 188 (8:92 w/w). Dissolution profiles of RESS processed powders showed particularly high improvement which can be attributed to the high excipient content and small particle size. The results obtained in this work with PVP K17 are clearly better than previously published ones. Corrigan et al. (2002) did not observe any distinct improvement in dissolution rate of GAS processed hydrocortisone at 5 min using PVP excipient.

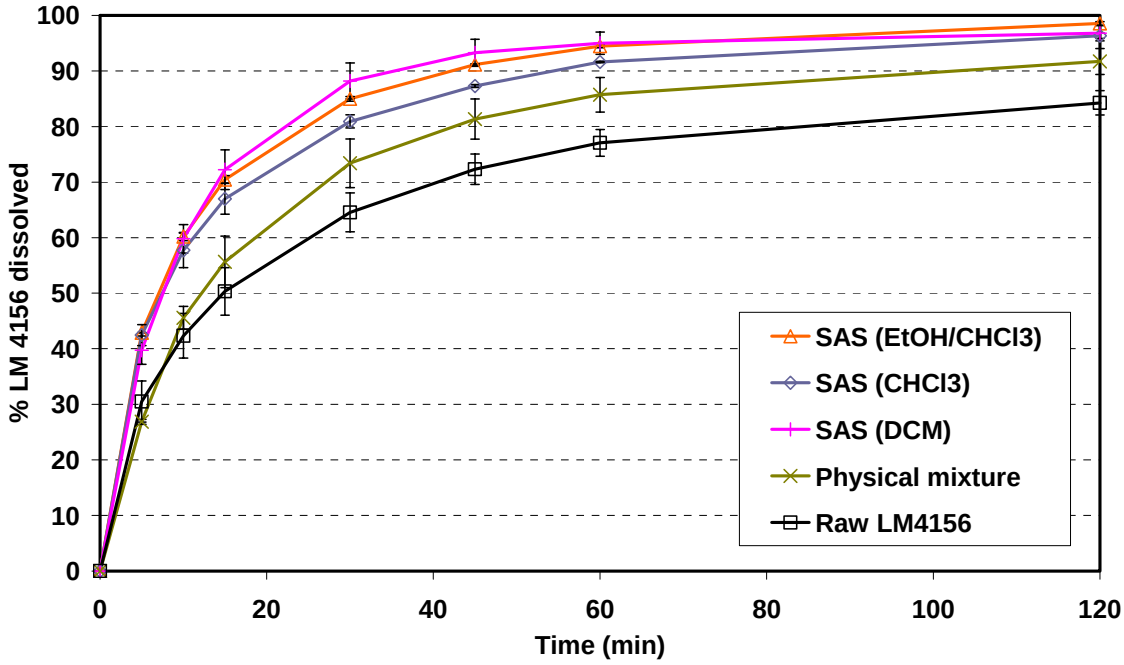

Fig. 2.8 Dissolution profiles of LM4156/PEG 8000 formulations at pH 7.4.

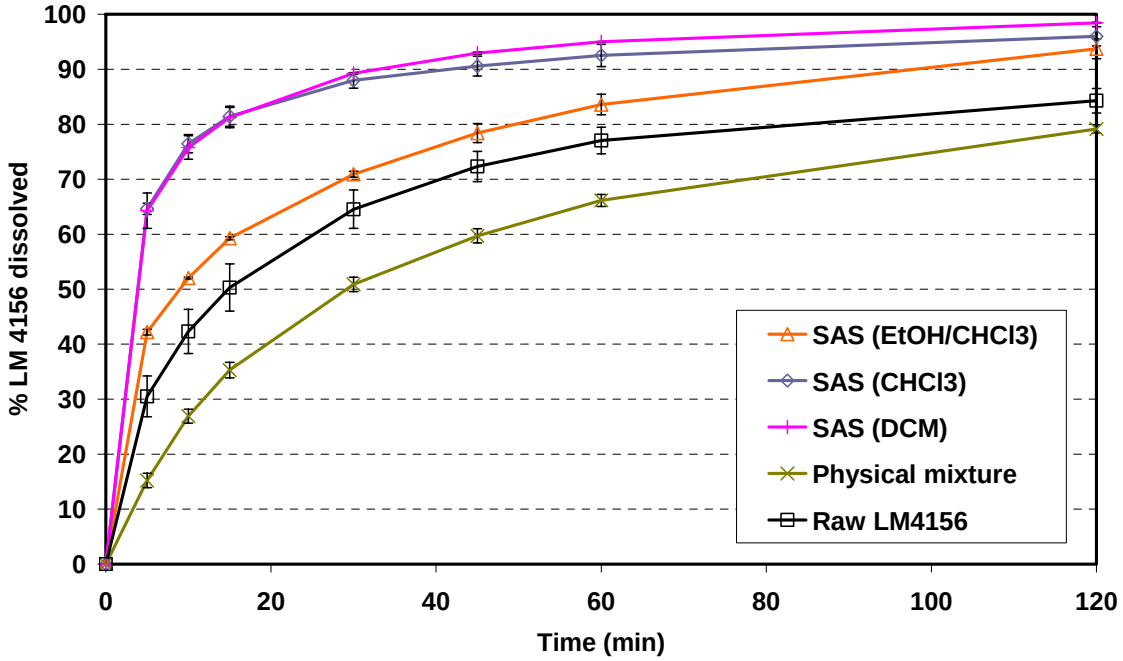

Fig. 2.9 Dissolution profiles of LM4156/PVP K17 formulations at pH 7.4.

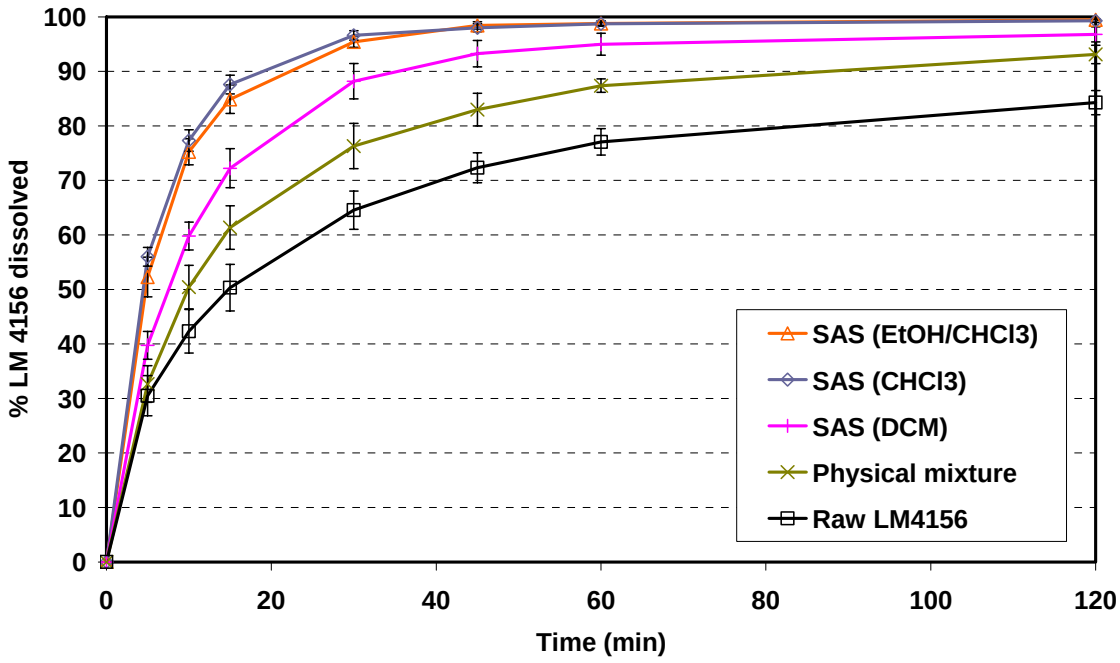

Fig. 2.10 Dissolution profiles of LM4156/Poloxamer 188 formulations at pH 7.4.

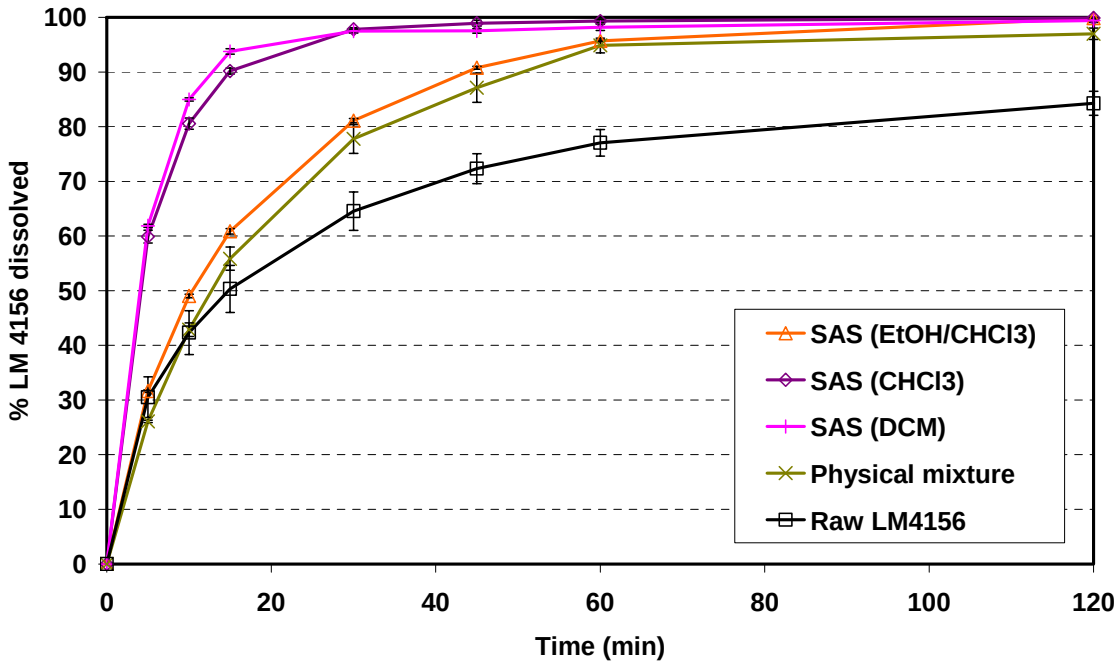

Fig. 2.11 Dissolution profiles of LM4156/Poloxamer 407 formulations at pH 7.4.

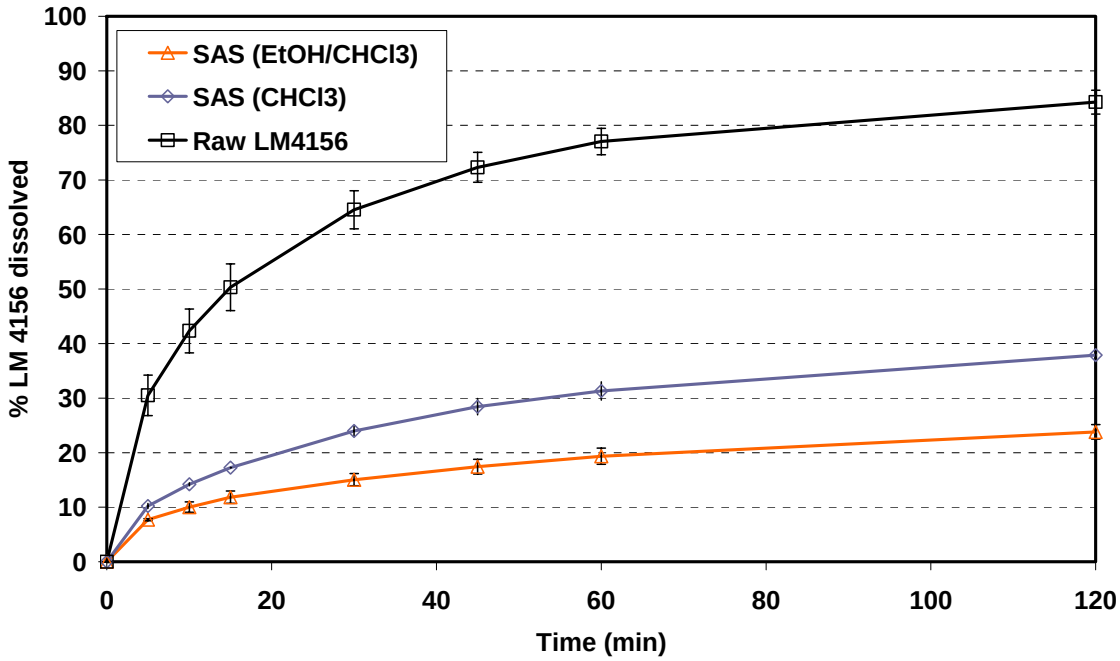

Fig. 2.12 Dissolution profiles of LM4156/Eudragit E formulations at pH 7.4.

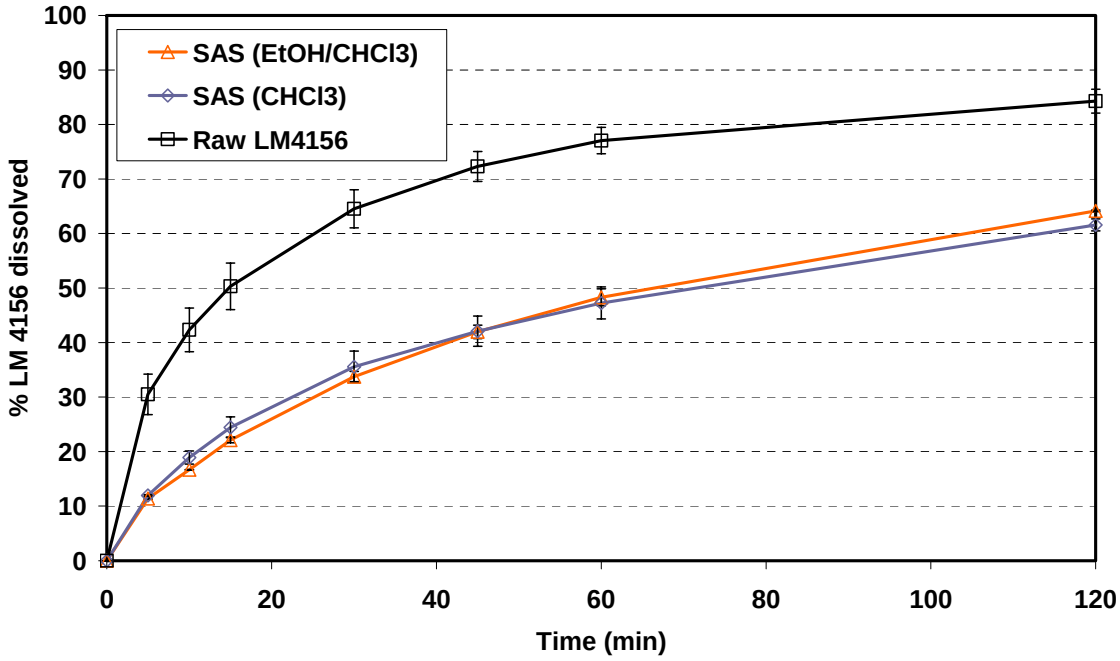

Fig. 2.13 Dissolution profiles of LM4156/Eudragit RL formulations at pH 7.4.

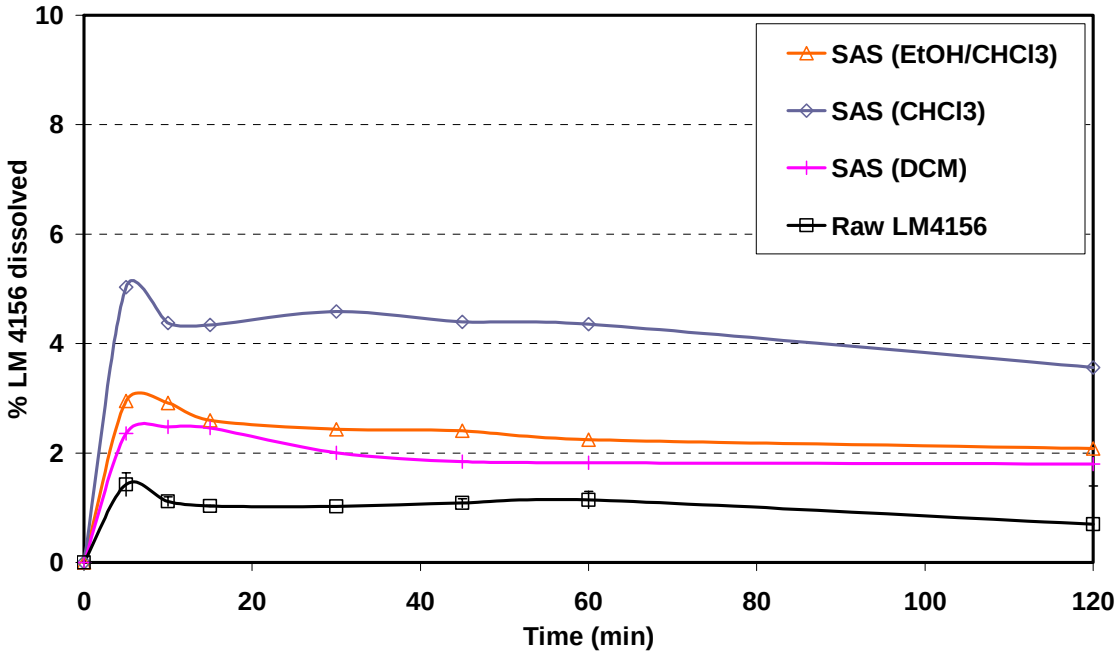

Fig. 2.14 Dissolution profiles of LM4156/Eudragit E formulations at pH 1.2.

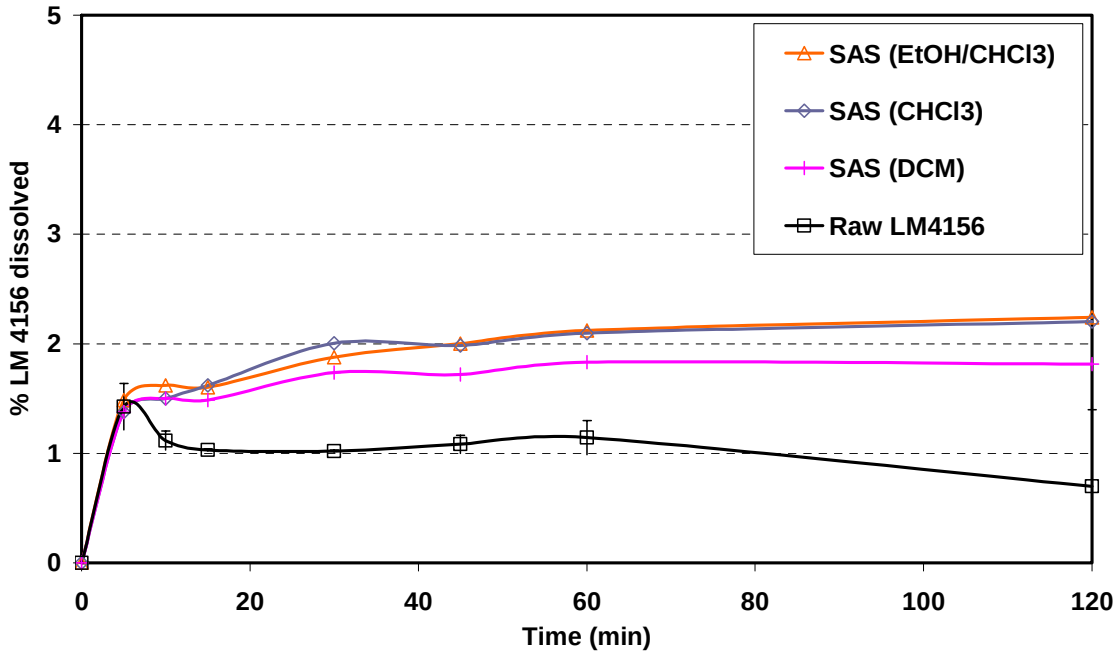

Fig. 2.15 Dissolution profiles of LM4156/Eudragit RL formulations at pH 1.2.

2.4.3 Other solvent systems

Our solvent-excipient screening revealed that SAS prepared PVP K17 formulation from $CHCl_3$ and EtOH/$CHCl_3$ solutions exhibited relatively high apparent density, high polymorphic purity and high amorphous content. Thus, further attempts were made to combine the benefits of EtOH and $CHCl_3$ by mixing them in a ratio of 20:80 v/v. To increase the yield (56 % from EtOH/$CHCl_3$ 50:50 v/v), drug and PVP K17 concentrations were increased in feed solution. Operating parameters and observations are listed in Table 2.9, B_S and B_{CO2} were set to 3 ml/min and 10 g/min, respectively.

Table 2.9. The effect of various solvent systems.

Run	Excipient	Solvent	P (bar)	T (°C)	C_D (wt. %)	C_E (wt. %)	Observation
76	PVP K17	EtOH/$CHCl_3$ 20:80	80	35	10	10	Filter blockage, yellow precipitate
77	PVP K17	EtOH/$CHCl_3$ 20:80	80	35	5	5	Filter blockage, film on the bottom
78	PVP K17	EtOH/$CHCl_3$ 20:80	100	35	10	10	Filter blockage, film on the bottom
47	PVP K17	EtOH/DCM 50:50	80	35	2	2	Filter blockage, fluctuant CO_2 flow
48	PVP K17	THF/DCM 50:50	80	35	2	2	Fluctuant CO_2 flow
68	-	MeOH/H_2O 99:1	200	40	1	0	Fluctuant CO_2 flow, No precipitate

However, experiments with concentrated feed solution containing 20 % v/v EtOH were not successful. Similar results were obtained with EtOH/DCM, THF/DCM solvent systems, too (run 47-48).

Rehman et al. (2004) investigated the effect of operating parameters and solvent choice on the degree of crystallinity and polymorphic composition of SEDS prepared terbutaline sulphate. Authors prepared all of the known crystal forms of the active substance, including two polymorphs, one monohydrate and the amorphous form. The highest amorphous content was obtained from MeOH/H_2O (99:1) solvent system at 250 bar and 45 °C. In spite of the milder working conditions (200 bar, 40 °C) we failed to precipitate LM4156 from MeOH/H_2O (99:1 v/v) solution (run 68 in Table 2.9). Precipitation vessel was absolutely clear as if no particle formation had occurred.

2.4.4 Static step (Maturation)

Freiss and Lochard have developed a three step process comprising 1, a supercritical antisolvent (SAS) precipitation of an API and a cyclodextrin-type host molecule; 2, a "maturation" or static step and 3; a solvent stripping step (Freiss, 2003a, 2003b, Lochard, 2003, 2004, Rodier, 2005). The main novelty of this process lies in the static step in which the co-crystallized powder is wetted and is held in $scCO_2$ for a few hours. Without water, maturation was not successful. The authors suggested that water plays the role of solvent that allows the drug-carrier mixture to realize a more intimate contact by dissolution and recrystallization (Rodier, 2005). Crystalline drug was hardly detectable in processed drug-carrier systems implying the formation of inclusion complexes. Owing to the hydrophilic nature of the CD host molecule unusually high drug concentrations were measured in the first hour: 10-fold higher than from raw drug after 20 hours.

Formulations prepared in $CHCl_3$ were further processed by the so called static step. 100 – 200 mg of samples were placed in the vessel which was afterwards filled with $scCO_2$ at 80 bar 35 °C and left under pressure for 6 hours. Dissolution tests were carried out in pH 7.4 buffer dissolution medium and results were compared to initial curves (Fig. 2.16 - Fig. 2.20).

Dissolution profiles showed no significant improvement due to the static step. LM4156/PVP K17 formulation exhibited worst dissolution kinetics because plasticized polymer made the processed powder more compact. Thus static step is likely to work only with cyclodextrin-type host molecules.

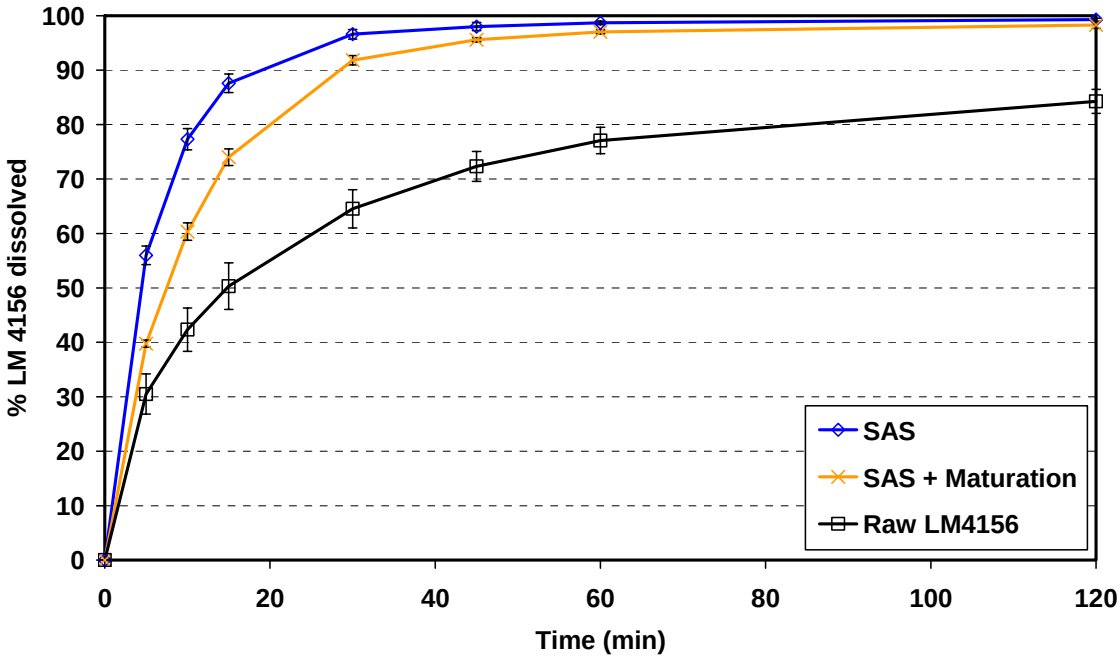

Fig. 2.16 Dissolution profiles of LM4156/Poloxamer 188 formulations before and after the static step.

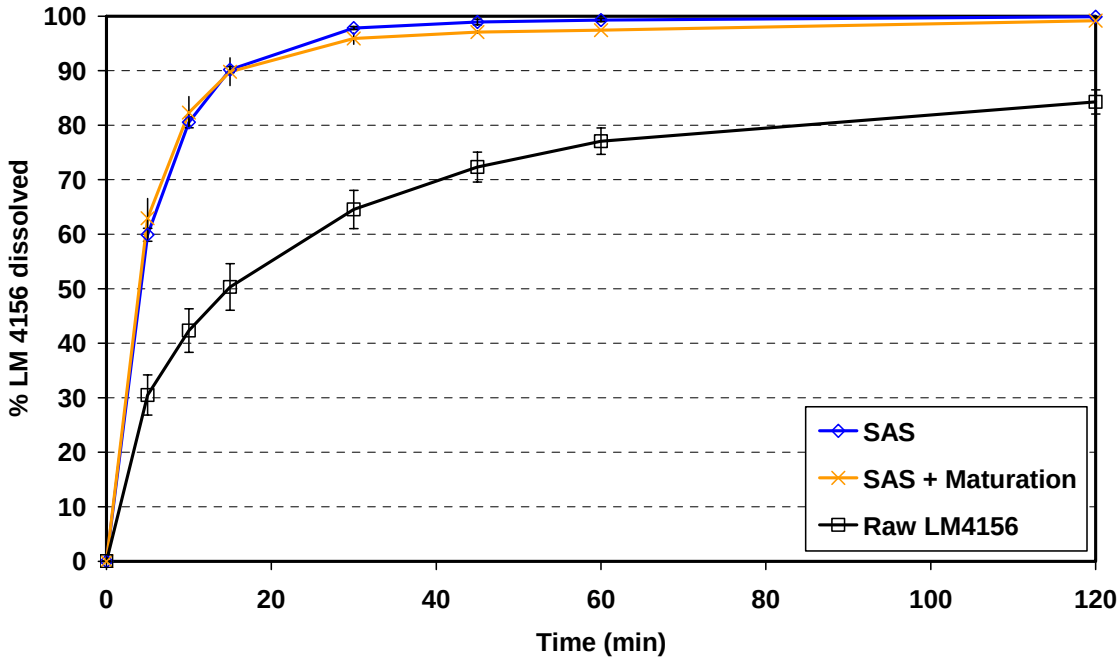

Fig. 2.17 Dissolution profiles of LM4156/Poloxamer 407 formulations before and after the static step.

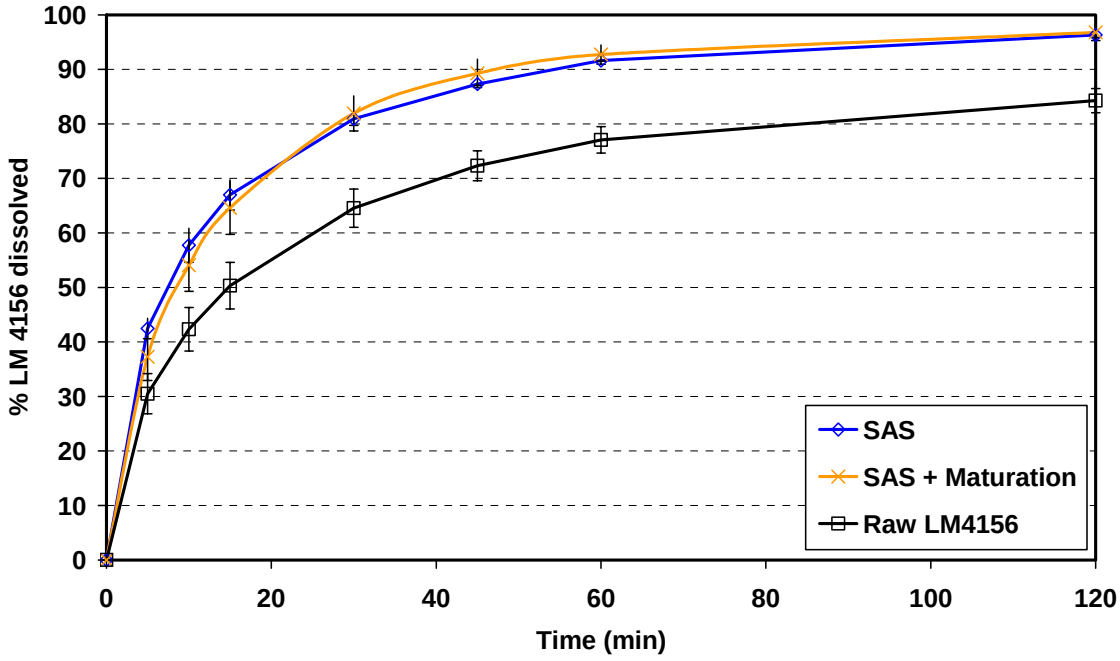

Fig. 2.18 Dissolution profiles of LM4156/PEG 8000 formulations before and after the static step.

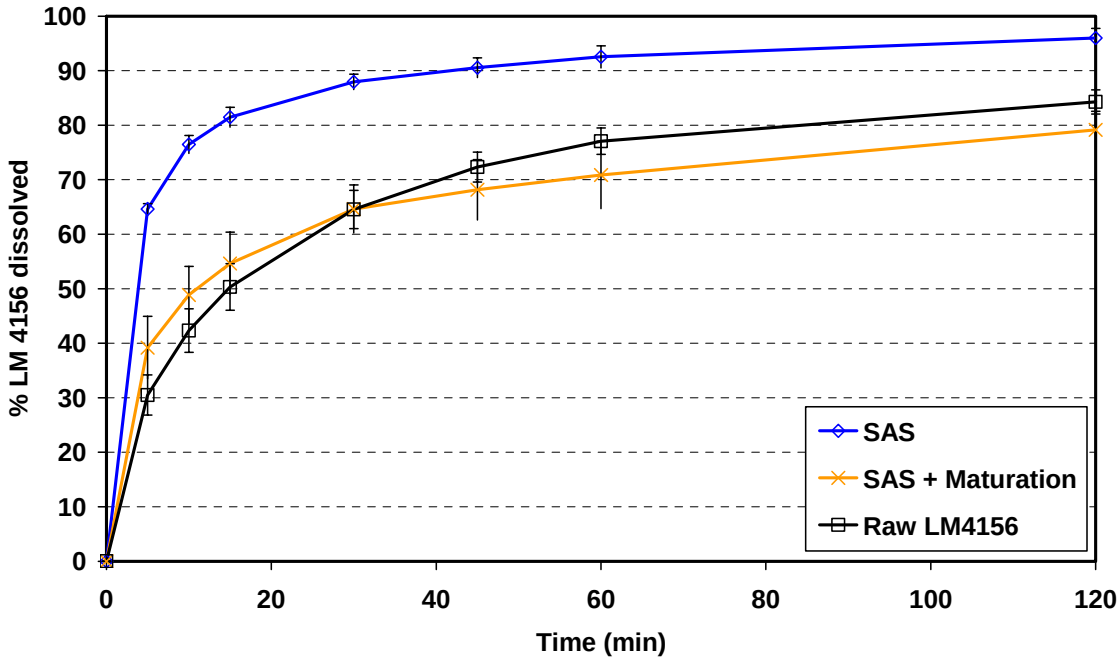

Fig. 2.19 Dissolution profiles of LM4156/PVP K17 formulations before and after the static step.

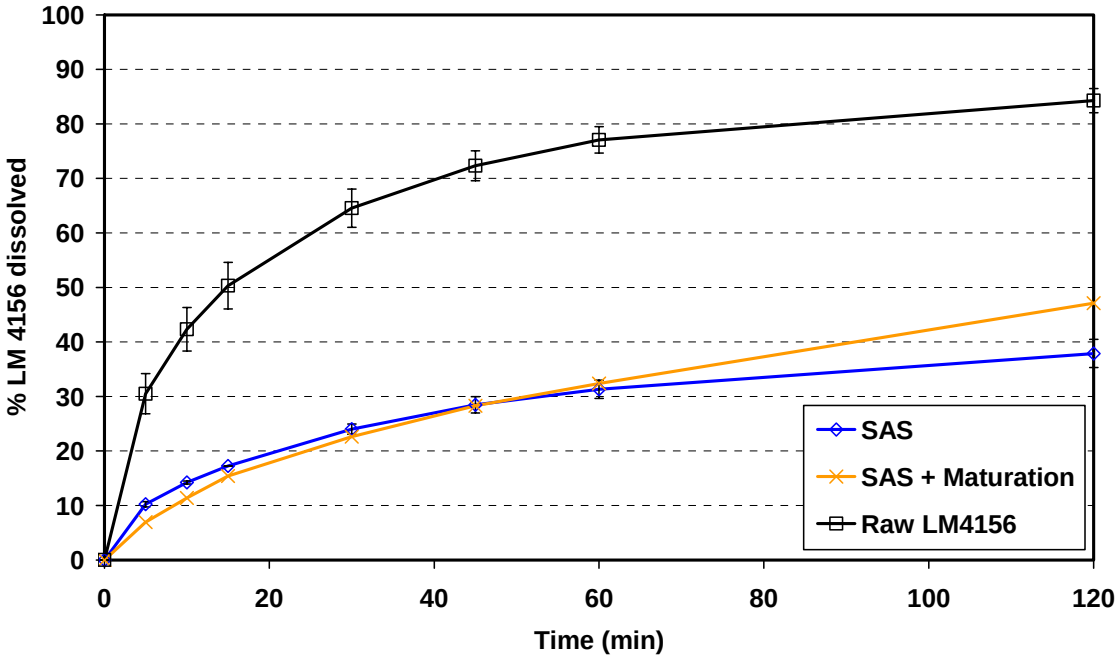

Fig. 2.20 Dissolution profiles of LM4156/Eudragit E formulations before and after the static step.

2.5 Conclusions

SAS process was proved to be a viable method to prepare rapidly dissolving semi-crystalline drug-carrier systems which satisfy requirements on polymorphic purity and residual solvent content. Table 2.10 provides a summary of the results. Some of the formulations showed more than 2 times higher dissolution rate compared to raw drug. However, in most cases, particle morphology of SAS prepared formulations was similar to raw material and particle size was unexpectedly large. The specific surface area of processed powders were close to the one of raw drug, as well. Needle-like crystals were similar to those prepared by conventional cooling crystallization. One possible theory to explain large particle size is the low level of supersaturation. The influence of solvent to CO_2 ratio was disccussed in chapter 2.4.1. Increasing solution/CO_2 ratio increases the solubility of the pharmaceutical ingredients and hence decreases the level of supersaturation. Thus, one could conclude that the concentration of organic solvent in the SCF phase was simply too high. However, this is not the case. Fargeot et al. (2003) studied the effect of solution flow rate on the shape and size of LM4156 crystals prepared by SAS. Drug was dissolved in acetonitrile and the resulting solution was injected at various flow rates (1, 3 and 5 ml/min) in scCO_2 at 80 bar and 35 °C. Scanning electron micrograms showed no significant differences in morphology or particle size when feed solution contained 0.5 wt. % drug. At higher drug concentration (1 wt. %) particle size decreased

slightly with increasing solution flow rate, nevertheless particles obtained at 5 ml/min were still very large, some of them measured 1 mm in length.

In most cases, needle-like crystals were partly covered by polymer spheres suggesting that the precipitation of these drug-carrier systems began with the nucleation of the active substance followed by the deposition of polymer coating around drug crystals. Thus, drug crystals played the role of heteronuclei in the precipitation process of the polymer (Juppo, 2003, York, 2001). Even though, encapsulation is supposed to slow down drug release from formulations, it can also improve dissolution rate owing to the reduced particle size, increased amorphous content and the presence of water-soluble surfactants. The size reduction was evident in the case of LM4156/Eudragit E formulations. Eudragit E coating succeeded in decreasing particle size to ~10 μm by hindering the growth of drug crystalls. Although, these formulations showed improved dissolution rates compared to raw drug and physical mixtures, the problem of unfavorable morphology and poor flowability was still unsolved.

Poloxamers and PVP K17 formulations showed disparate particle morphologies. Experiments with PVP K17 in chlorinated solvents led to irregular particles with high apparent densities, good flow properties and improved dissolution rates. The highest amorphous content was also measured in LM4156/PVP K17 solid dispersions. If it were not for the high residual solvent content and the low polymorphic purity, PVP K17 would be the most prosperous excipient. However, high density and glassy state which could be attributed to the higher melting and glass transition temperatures are responsable for high residual solvent content, too. Further attempts were made to evaluate various solvent systems but we failed to precipitate particulate product.

Aggregated needle-like crystals were obtained with Poloxamer 188 and 407 from DCM but polymer spheres were not observed. In spite of its acicular crystal habit, the flowabilities of these powders were rather good. Additionally, LM4156/Poloxamer 407 formulation exhibited high dissolution rate and high polymorphic purity. Although, its precipitation yield was not particularly high (72 %) it can be improved by scaling up the process. Obviously, all requirements can not always be fulfilled but SAS-prepared LM4156/Poloxamer 407 formulation from DCM solution satisfied the most important conditions concerning the polymorphic purity and residual solvent content and its improved dissolution rate was satisfying as well.

Table 2.10. Overview table of the physical properties.

	Solvent	Eudragit E	Eudragit RL	Poloxamer 188	Poloxamer 407	PVP K17	PEG 8000
Dissolution rate (pH 7.4)	$EtOH/CHCl_3$	★	★	★★	★	★★	★★
	$CHCl_3$	★	★	★★	★★★	★★★	★★
	DCM	★	★	★★	★★★	★★★	★★
Polymorphism	$EtOH/CHCl_3$	★★★	★★★	★★	★★	★★★	★★
	$CHCl_3$	★★	★★★	★	★	★	★★
	DCM	★★	★★★	★★★	★★★	★	★★
Flowability	$EtOH/CHCl_3$	★	★	★	★	★★★	★
	$CHCl_3$	★	★	★	★	★★★	★
	DCM	★	★	★★	★★	★★★	★
Apparent density	$EtOH/CHCl_3$	★	★	★	★	★★★	★
	$CHCl_3$	★	★	★	★	★★★	★
	DCM	★	★	★★	★★	★★★	★
Residual solvent	$EtOH/CHCl_3$	★★★	★★	★★★	★★	★	★★
	$CHCl_3$	★★★	★★	★★	★★	★	★★
	DCM	★★★	★	★★	★★	★	★★★

3. Solution Enhanced Dispersion by Supercritical Fluids (SEDS)

3.1 Purposes of the study

In chapter 2., possibilities and limitations of SAS process were studied in depth. Several SAS prepared formulations possessed adequate dissolution rate and satisfied requirements on residual solvent level and polymorphic purity, as well. However, particles were still very large and showed unfavorable morphology. To overcome these difficulties capillary nozzle was replaced by a coaxial nozzle (Hanna, 1995). In the SEDS process, the jet of feed solution is broken by the high velocity jet of $scCO_2$ which is supposed to provide higher supersaturation and direct control over powder properties (Beach, 1999). SEDS process was successfully used in preparation of respirable drug particles (Hanna, 1995; Beach, 1999; Rehman, 2004; Velaga, 2004).

3.2 Materials and methods of analysis

See chapter 2.2.

3.3 Method of preparation

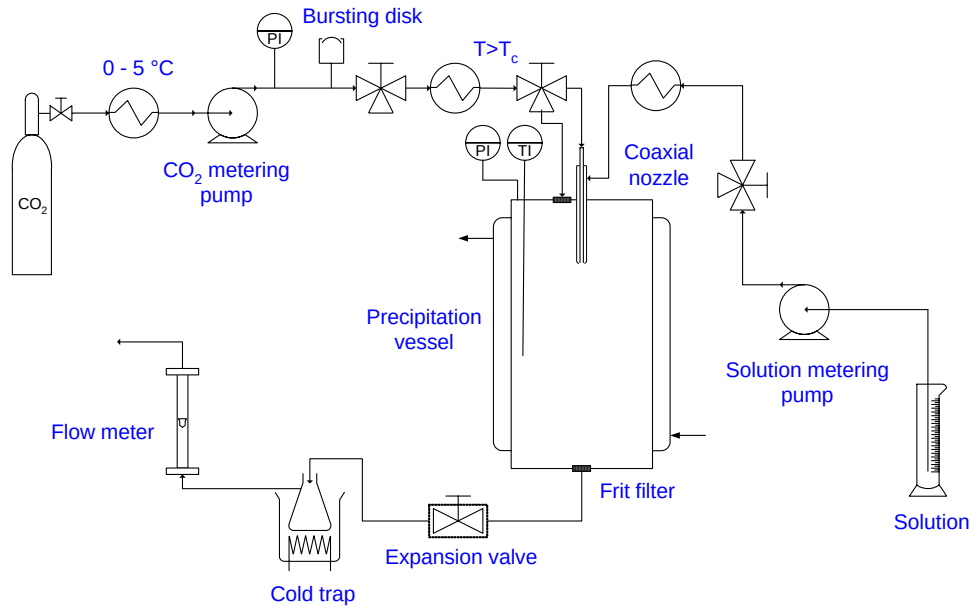

Fig. 3.1 Schematic diagram of the SEDS apparatus.

The method of preparation is the same as for the SAS process (chapter 2.3). The only difference is that in SEDS the capillary nozzle was replaced by a coaxial nozzle. $ScCO_2$ was delivered in the inner, the feed solution in the outer passage of the coaxial nozzle, comprising a capillary tube (250 μm ID, 1/16" OD) and a 3/16" stainless steel tube. During the solvent stripping $scCO_2$ was delivered through the SAS inlet, to achieve plug-flow conditions.

3.4 Results and discussion

DCM and $CHCl_3$ were chosen for SEDS experiments owing to the high yields achieved in SAS. Experiments were carried out under the same working conditions: P = 80 bar, T = 35 °C, B_S = 3 ml/min, B_{SCF} = 10 g/min, $C_D = C_E$ = 2 wt. %.

Table 3.1. Yield (%) of SEDS prepared pure LM4156 and formulations.

Solvent	Pure LM4156	Excipient					
		Eudragit E	Eudragit RL	Poloxamer 188	Poloxamer 407	PVP K17	PEG 8000
$CHCl_3$	84	70	80	80	78	-	75
DCM	80	74	78	65	75	-	75

Particle morphology and particle size were defined on a visual basis. Microscopy pictures of SAS and SEDS prepared powders showed no significant differences (Appendix A). Acicular drug crystals with polymeric spheres have formed again. Unlike SAS, in SEDS cottony precipitate covered the top of the vessel too, suggesting, that particle formation occurred in the whole volume due to the increased jet turbulence. However, contrary to what we expected, SEDS did not decrease but occasionally increased the particle size compared to SAS. Furthermore, dry powder containing PVP K17 could not be prepared. Experiments with PVP K17 in DCM, $CHCl_3$ and EtOH/$CHCl_3$ solutions resulted in filter blockage even at lower solution flow rate (B_S = 1 ml/min). Yields and drug contents are listed in Table 3.1 and Table 3.2. In most cases, values of precipitation yield were lower in comparison with SAS; drug contents were nearly the same.

Table 3.2. Drug content (wt. %) of SEDS prepared formulations.

Solvent	Excipient					
	Eudragit E	Eudragit RL	Poloxamer 188	Poloxamer 407	PVP K17	PEG 8000
$CHCl_3$	48.9	46.2	50.9	50.8	-	53.1
DCM	50.5	41.3	50.1	50.2	-	49.0

3.5 Conclusions

SEDS process was investigated as a potential method to prepare micronized powders having good flow properties. Drug-carrier systems were prepared in DCM and $CHCl_3$ solutions and compared to corresponding SAS formulations.

As expected, pneumatic nozzle provided more intense mixing. While in SAS only the lower part of the precipitation vessel was "used", in SEDS the whole vessel was covered by thick cottony layer consisting of needle-shaped crystals. However, in spite of the improved jet mixing, no significant difference was observed in morphology and size of particles prepared by the various methods. SEDS did not decrease but occasionally increased particle size compared to SAS. Thus, our attempt to reduce particle size using SEDS process has failed.

4. General Summary

SAS, SEDS and SF techniques were evaluated for their potential use in preparation of immediate release solid oral dosage forms. LM4156, a poorly water soluble active substance was coprecipitated with several excipients, including Eudragit E, Eudragit RL, Poloxamer 188, Poloxamer 407, PVP K17 and PEG 8000. Our aim was to prepare solid solution or solid dispersion of the above mentioned pharmaceutical ingredients in an attempt to improve the bioavailability of the active substance by increasing its dissolution rate. Though main purpose was to improve the dissolution kinetics, formulations had to meet stability (crystallinity, polymorphic purity), toxicological (residual solvent content), technological (particle morphology, flowability) and economical (precipitation yield) requirements. Thus, formulations were compared on the basis of these properties.

Owing to the different mechanisms of particle formation, powders exhibited different particle morphologies, crystallinities and dissolution rates. SF technology was proved to be a viable method for preparing fast-dissolving solid dispersions of various excipients in a wide range of D/P ratios. Due to the ultra-rapid freezing, much less excipient is needed to prepare molecularly dispersed solid solutions and the D/P ratio can be easily controlled by the feed solution. SF is a versatile and simple technique. Unlike conventional and supercritical methods, any kind of active substance and excipient can be processed in any kind of solvent without any considerable loss in yield or biological activity. Compared to other particle formation methods, particle recovery yield is unusually high, nearly 100%. SF does not require any special equipment and liquid solvent can be recovered easily from ice condenser. However, SF has some inherent limitations like time consumption of the freeze-drying process and long-term stability of amorphous solid dosage forms.

SCF antisolvent techniques are able to reduce particle size and residual solvent content in one step and allow a certain control over polymorphic purity and particle morphology. Additionally, these methods have several attractive features in terms of GMP requirements including light-, oxygen- and moisture-free environment in a totally enclosed equipment which is free from moving parts. Although, precipitation yield and amorphous content were proved to depend on solvent and excipient choice, occasionally very high yield and low crystallinity were achieved. SCF-processed formulations showed higher

crystallinities and lower dissolution rates in comparison with SF powders but SAS is more advantageous in terms of particle size and time consumption.

Among the polymers tested, Poloxamer 407 was found to be the most prosperous excipient regardless of the method of preparation. LM4156/Poloxamer 407 powders showed high polymorphic purity, high dissolution rate and low residual solvent content. In addition, SF prepared LM4156/Poloxamer 407 solid dispersion proved to be stable over a three month storage.

The experimental and theoretical results obtained in this work are summarized in the following points:

I. SAS, SEDS and SF technologies were evaluated in this thesis for their potential use in preparation of immediate release solid oral dosage forms. Both SAS and SF technologies were proved to be able to improve the dissolution kinetics of LM4156 and satisfy regulatory requirements.

II. Most SAS prepared powders consisted of needle-like crystals partly covered by polymer spheres suggesting that LM4156 and polymers had different rate and mechanism of nucleation. The precipitation process of these drug-carrier systems begun with the nucleation of the active substance followed by the deposition of polymer coating around drug crystals which provided heteronuclei for the precipitation of polymer which could not be processed alone.

III. In SAS technology, precipitation yield, crystallinity and residual solvent content varied over a wide range depending on the solvent and polymer involved. Non-chlorinated solvents (EtOH, THF and their mixtures) exhibited co-solvent behavior and washed out a part of the pharmaceutical ingredients leading to low yield.

IV. Crystalline excipients (PEG 8000, Poloxamer 188 and 407) contained a higher fraction of crystalline drug, typically between 58 and 100 %, while coprecipitation with the amorphous PVP K17 and Eudragit E resulted in semi-crystalline solid dispersions with low degrees of crystallinity.

V. With a few exceptions all formulations met ICH requirements on residual $CHCl_3$ and DCM content (under Option 2). In the case of PVP K17 and PEG 8000 (precipitated from $CHCl_3$ solution), longer solvent stripping is recommended. PVP K17 formulations were characterized by high apparent density and low crystallinity which makes solvent stripping more difficult. In addition, the precipitation

processes of PVP formulations were frequently perturbed as the polymer has partly blocked the outlet filter.

VI. The higher melting polymorph was always dominant notwithstanding that in most cases the metastable form was also present in SAS prepared powders. Contrary to what we expected, there was no overall tendency in polymorphic purity. Apart from Eudragit RL and PEG 8000, a stochastic-like relationship was observed between the polymorphic purity, solvent and polymer.

VII. The newly developed SF technology was proved to be a versatile method for preparing fast-dissolving solid dispersions and solid solutions. Unlike conventional and supercritical fluid techniques this new cryogenic particle formation method allows to prepare solid dispersions using a wide range of solvents and excipients with a wide range of drug/polymer ratio.

VIII. All freeze-dried formulations were composed of highly porous free-flowing spherical particles. Due to the high porosity, particles were easy to disintegrate and micronize but powders containing Eudragit or a high concentration of LM4156 were electrostatically charged and difficult to handle.

IX. Owing to the ultra-rapid freezing rate, SF prepared powders showed low crystallinities. While PVP K17 and Eudragit E formed totally amorphous solid solution, semi-crystalline formulations showed low crystallinities (< 5.76 %) and high polymorphic purities.

X. SF prepared powders showed improved dissolution kinetics. The higher dissolution rate can be attributed to the glassy state, high specific surface area and homogenous distribution of the active substance in the polymer matrix.

XI. Among the tested polymers, Poloxamer 407 was found to be the most prosperous excipient. LM4156/Poloxamer 407 powders were characterized by high polymorphic purity, high dissolution rate, adequate stability and low residual solvent content.

5. Future works

We may conclude that on laboratory scale, results were quite promising for both SAS and SF technologies. The next step is to scale them up and evaluate their technical and economical feasibilities. Although, these processes are subjects of R&D in companies and laboratories worldwide, they have only a few if any industrial application. The reason is the inherent technical difficulties. A commercial scale SAS pilot plant has to be equipped with high-throughput injection device, particle collection system, CO_2 and liquid solvent recycling systems. In the SF process, liquid solvent can be recovered from the ice condenser but appropriate injection, particle collection and the transfer of frozen materials to the freeze-dryer are challenging tasks.

Economical feasibility depends on capital investment costs, operation and maintenance costs. Although, a common belief is that supercritical fluid and cryogenic technologies are more capital intensive than conventional techniques, current trends are showing that they might become an alternative way in future foremost in the case of products of high market values.

References

Adams, T.H., Beck, J.P., Menson, R.C. Method and apparatus for making novel particulate compositions. Patent US 4,211,015, 1980.

Adams, T.H., Beck, J.P., Menson, R.C. Novel particulate compositions. Patent US 4,323,478, 1982.

Amidon, G.L., Lunnernas, H., Shah, V.P., Crison, J.R. A theoretical basis for a biopharmaceutic drug classification: the correlation of in vitro drug product dissolution and in vivo bioavailability. *Pharm. Res.* 12, 1995, 413–420.

Badens, E., Fargeot, C., Bosc, N., Veesler, S., Teillaud, E., Charbit, G. Polymorph control of drug in supercritical CO_2. *Proceedings of the European Conference on Drug Delivery and Pharmaceutical Technology,* Sevilla, 10-12 May, 2004, pp. 46.

Bausch, A., Hidber, P. Process for the manufacture of (sub)micron sized particles by dissolving in compressed gas and surfactants. Patent WO 99/52504, 1999.

Beach, S., Lathan, D., Sidgwick, C., Hanna, M., York, P. Control of the physical form of Salmeterol Xinafoate. *Org. Proc. Res. Dev.*, 3 (1999) 370-376.

Bender, E. Die Berechnung von Phasengleichgewichten mit der termischen Zustandsgleichung dargestellt an der reinen Fluiden Argon, Stickstoff, Sauerstoff und an ihren Gemischen. Habilitationsschrift, Ruhr-Universität Bochum, 1971.

Bertucco, A., Pallado, P., Benedetti, L. Formation of biocompatible polymer microspheres for controlled drug delivery by a supercritical antisolvent technique. *Proceedings of High Pres. Chem. Eng.,* Elsevier, (1996) 217-222.

Bertucco, A., Vaccaro, F., Pallado, P. Drugs encapsulation using a compressed gas antisolvent precipitation, *Proceedings of 4th Italian Conference on Supercritical Fluids and Their Applications,* CVES, Salermo, 1997, (I) pp. 327.

Bitz, C., Doelker, E. Influence of the preparation method on residual solvents in biodegradable microspheres. *Int. J. Pharm.* 131 (1996) 171-181.

Bleich, J., Kleinebudde, P., Müller, B. Influence of gas density and pressure on microparticles produced with the ASES process. *Int. J. Pharm.* 106 (1994) 77-87.

Bleich, J., Müller, B.W. Production of drug loaded microparticles by the use of supercritical gases with the aerosol solvent extraction system (ASES) process. *J. of Microencapsulation,* 13(2) (1996) 131-139.

Bodmeier, R., Wang, H., Dixon, D., Mawson, S., Johnston, K. Polymeric microspheres prepared by spraying into compressed carbon dioxide. *Pharm. Res.* 12 (1995) 1211-1217.

Briggs, A.R., Maxvell, T.J. Process for preparing powder blends. Patent US 3,721,725, 1973.

Briggs, A.R., Maxvell, T.J. Lyophilized biological products. Patent US 3,928,566, 1975.

Briggs, A.R., Maxvell, T.J. Method of preparation of lyophilized biological products. Patent US 3,932,943, 1976.

Bristow, S., Shekunov, T., Shekunov, B. Yu., York, P. Analysis of the supersaturation and precipitation process with supercritical CO_2. *J. Supercrit. Fluids,* 21 (2001) 257-271.

Brittain, H.G. Solubility of pharmaceutical solids, In: Physical characterization of pharmaceutical solids, New York, M. Dekker, 1995, pp. 321-386.

Brunauer S., Emmett P.H., Teller E. Adsorption of gases in multimolecular layers. *J. Am. Chem. Soc.*, 60 (1938) 309-319.

Brunner, G. Gas Extraction: An Introduction to Fundamentals of Supercritical Fluids and the Application to Separation Processes. Steinkopff, Darmstadt, 1994.

Bustami, R.T., Chan, H.K., Sweeney, T., Dehghani, F., Foster, N.R. Generation of fine powders of recombinant human deoxyribonuclease using the aerosol solvent extraction system. *Pharm. Res.,* 20(12) (2003) 2028-2035.

Cagniard de la Tour, C. *Ann. Chim. Phys.,* 21(2), 1822, 127, 178.

Caliceti, P, Salmaso, S., Elvassore, N., Bertucco, A. Effective protein release from PEG/PLA nano-particles produced by compressed gas anti-solvent precipitation techniques. *J. Controlled Release,* 94 (2004) 195-205.

Carretier, E., Badens, E., Guichardon, P., Boutin, O., Charbit, G. Hydrodynamics of supercritical antisolvent precipitation: Characterization and influence on particle morphology. *Ind. Eng. Chem. Res.*, 42 (2003) 331-338.

Chang, C.J., Day, C.-Y., Ko, C.-M., Chiu, K.-L. Densities and P-x-y diagrams for carbon dioxide dissolution in methanol, ethanol, and acetone mixtures. *Fluid Phase Equilibria,* 131 (1997) 243-258.

Charbit, G., Badens, E., Boutin, O. Methods of particle production. In: York P., Kompella U.B., Shekunov B.Y. Supercritical fluid technology for drug product development, Drugs and Pharmaceutical Sciences Vol 138, Marcel Dekker Inc., New York, 2004, pp. 159-212.

Charoenchaitrakool, M., Dehghani, F., Foster, N.R. Utilization of supercritical carbon dioxide for complex formation of ibuprofen and methyl-β-cyclodextrin, *Int. J. Pharm.,* 239 (2002) 103.

Chou, Y.H., Tomasko, D.L. GAS Recrystallization of polymer-pharmaceutical composite particles. *Proceedings of The 4th International Symposium on Supercritical Fluids,* Sendai (Japan), 11–14 May 1997, pp. 55-57.

Condo, P., Paul, D., Johnston, K. Glass transition behavior including retrograde vitrification of polymers with compressed fluid diluents. *Macromolecules,* 27 (1994) 365.

Conte, U., Conti, B., Giunchedi, P., Maggi, L., Spray dried polylactide microsphere preparation: influence of the technological parameters. *Drug Dev. Ind. Pharm.*, 20 (1994) 235-258.

Corrigan, O.I. Mechanisms of dissolution of fast release solid dispersions. *Drug Dev. Ind. Pharm.* 11 (1985) 697-724.

Corrigan, O.I. Retardation of polymeric carrier dissolution by dispersed drugs: factors influencing the dissolution of solid dispersions containing polyethylene glycols. *Drug Dev. Ind. Pharm.*, 12 (1986) 1777-1793.

Corrigan, O.I., Crean, A.M. Comparative physicochemical properties of hydrocortisone–PVP composites prepared using supercritical carbon dioxide by the GAS anti-solvent recrystallization process, by coprecipitation and by spray drying. *Int. J. Pharm.,* 245 (2002) 75-82.

Craig, D.Q.M., Newton, J.M. The dissolution of nortriptyline HCl from polyethylene glycol solid dispersions. *Int. J. Pharm.,* 78 (1992) 175-182.

Craig, D.Q.M. The mechanisms of drug release from solid dispersions in water-soluble polymers. *Int. J. Pharm.*, 231 (2002) 131-144.

Dirksen, J.A., Ring, T.A. Fundamentals of crystallization: Kinetic effects on particle size distributions and morphology. *Review. Chem. Eng. Sci.,* 46 (1991) 2389-2427.

Debenedetti, P.G., Tom, J.W., Yeo, S.D., Lim, G.B. Application of supercritical fluids for the production of sustained delivery device. *J. Cont. Rel.,* 24 (1993) 27-44.

Debenedetti, P.G., Tom, J.W., Jerome, R. Precipitation of poly(L-lactic acid) and composite poly(L-lactic acid)-pyrene particles by rapid expansion of supercritical solutions. *J. Supercrit. Fluids,* 7 (1994) 9-29.

Debenedetti, P.G., Roberts, C.J. Engineering pharmaceutical stability with amorphous solids, *AIChE Journal,* 48(6) (2002) 1140-1144.

Devereux, J.E., Newton, J.M., Short, M.B. The influence of density on the gastrointestinal transit of pellets. *J. Pharm. Pharmacol.*, 7 (1990) 500-501.

Doherty, C., York, P. The in-vitro pH-dissolution dependence and invivo bioavailability of frusemide-PVP solid dispersions. *J. Pharm. Pharmacol.,* 41 (1989) 73-78.

Dubois, J.-L., Ford, J.L. Similarities in the release rates of different drugs from polyethylene glycol 6000 dispersions. *J. Pharm. Pharmacol.*, 37 (1985) 494-495.

Dunn, E.B., Masavage, G.J., Sauer, H.A. Method of freezing solution droplets and the like using immiscible refrigerants of differing densities. Patent US 3,653,222, 1972.

Edwards, C.M., Gambaretto, G.P., Conte, L., Lowe, K.C. Evaluation of commercial and purified PLURONIC F-68 in a human blood neutrophil bioassay. *Art. Cells, Blood Subs. Immob. Biotech.,* 27 (1999) 171-177.

Elvassore, N., Bertucco, A., Caliceti, P. Production of protein-polymer micro-capsules by Supercritical Anti-solvent techniques, *Proceedings of The 5th International Symposium on Supercritical Fluids,* Atlanta, 8–12 April, 2000.

Elvassore, N., Bertucco, A., Caliceti, P. Production of insulin-loaded poly(ethylene glycol)/poly(l-lactide) (PEG/PLA) nanoparticles by gas antisolvent techniques. *J. Pharm. Sci.*, 90 (2001a) 1628-1636.

Elvassore, N., Bertucco, A., Caliceti, P. Production of protein-loaded polymeric microcapsules by compressed CO2 in a mixed solvent. *Ind. Eng. Chem. Res.,* 40 (2001b) 795-800.

Engwicht, A., Girreser, U., Müller, B.W. Critical properties of lactide-co-glycolide polymers for the use in microparticle preparation by the Aerosol Solvent Extraction System. *Int. J. Pharm.,* 185 (1999) 61-72.

Falk, R.F., Randolph, T.W., Meyer, J.D., Kelly, R.M., Manning, M.C. Controlled release of ionic compounds from poly (L-lactide) microspheres produced by precipitation with a compressed antisolvent. *J. Cont. Rel.,* 44 (1997) 77-85.

Falk, R.F., Randolph, T.W. Process variable implication for residual solvent removal and polymer morphology in the formation of gentamycin-loaded poly (L-lactide) microparticles. *Pharm. Res.*, 15(8) (1998) 1233-1237.

Fallingborg, J. Intraluminal pH of the human gastrointestinal tract, *Dan. Med. Bull.,* 46 (1999) 183–196.

Fargeot, C., Badens, E., Charbit, G., Bosc, N., Teillaud, E., Veesler, S. Cristallisation d'un prinicipe actif: comparaison des méthodes par voie liquide et supercritique. *Proceedings of The Cristal2,* Toulouse, 12-13 Novembre, 2003, pp. 55-60.

FDA, International Conference on Harmonisation, ICH Guidance on Impurities: Residual Solvents, Federal Register. 62(247) (1997) 67377-67388.

FDA, Draft – Guidance for Industry: Bioavailability and Bioequivalence Studies for Orally Administered Drug Products. U.S. Department of Health and Human Services, Food and Drug Administration, Center for Drug Evaluation and Research (CDER), July 2002.

Fenghour, A., Wakeham, W.A., Vesovic, V. The viscosity of carbon dioxide. *J. Phys. Chem. Ref. Data,* 27(1) (1998) 31-44.

Fischer, W., Müller, B.W. Method and apparatus for the manufacture of a product having a substance embedded in a carrier. Patent U.S. 5,043,280, 1991.

Forster, A., Hempenstall, J., Rades, T. Investigation of drug / polymer interaction in glass solutions prepared by melt extrusion. *Int. J. Vib. Spec.*, [www.ijvs.com] 5(2) (2001) 6.

Foster, N.R., Mammucari, R., Dehghani, F. Coprecipitation of pharmaceuticals using gas antisolvent technique. *Proceedings of The 8th Meeting on Supercritical Fluids,* Bordeaux (France) 14-17 April, 2002, p. (1) 321.

Frederiksen, L., Anton, K., van Hoogevest, P. Process for preparing a liposome dispersion at high pressure. Patent EP 0616801, 1994.

Frederiksen, L., Anton, K., van Hoogevest, P., Keller, H.R. Leuenberger H. Preparation of liposomes encapsulating water-soluble compounds using supercritical carbon dioxide. *J. of Pharm. Sci.,* 86(8) (1997) 921-928.

Freiss, B., Marciacq, F., Fages, J., Sauceau, M., Lochard, H., Letourneau, J.J., Joussot-Dubien, C. Method for preparing an interactive compound of an anilide derivative with a porous support by supercritical fluid. Patent WO 03/030867, 2003a.

Freiss, B., Marciacq, F., Fages, J., Sauceau, M., Lochard, H., Letourneau, J.J., Joussot-Dubien, C. Method for preparing a compound for interactive of active substances with a porous support using supercritical fluid. Patent WO 03/043604, 2003b.

Gallagher, P.M., Coffey, M.P., Krukonis, V.J., Klasutis, N. Gas anti-solvent recrystallization: New process to recrystallize compounds insoluble in supercritical fluids. In: Supercritical Fluid Science and Technology; K.P. Johnston, J.M.L. Penniger, ACS Symposium Series 406; American Chemical Society: Washington, DC, 1989.

Ganderton, D. Size reduction and classification. In: Unit process in pharmacy, Chapter 13, London, Heinemann Medical, 1968, pp. 190-216.

Gao, Y., Mulenda, T.K., Shi, Y.-F., Yuan, W.-K. Fine particles preparation of Red Lake C pigment by supercritical fluid. *J. Supercrit. Fluids*, 13 (1998) 369-374

Ghaderi, R., Artursson, P., Carlfors, J. A new method for preparing biodegradable microparticles and entrapment of hydrocortisone in DL-PLG microparticles using supercritical fluids. *Eur. J. Pharm. Sci.,* 10 (2000) 1-9.

Gombotz, W.R., Healy, H.S., Brown, R.L. Process for producing small particles of biologically active molecules. Patent WO 90/13285, 1990.

Gombotz, W.R., Healy, H.S., Brown, R.L. Very low temperature casting of controlled release microspheres. Patent U.S. 5,019,400, 1991.

Gonzalez, A.V., Tufeu, R., Subra, P. High-pressure vapor-liquid equilibrium for the binary sysytems carbon dioxide + dimethyl sulfoxide and carbon dioxide + dichloromethane. *J. Chem. Eng. Data,* 47 (2002) 492-495.

Gosselin, P.M., Thibert, R., Preda, M., McMullen, J.N. Polymorphic properties of micronized carbamazepine produced by RESS. *Int. J. Pharm.,* 252 (2003) 225-233.

Grange, Y. Etude d edissolution de cristaux associés LM4156/Excipient par cristallisation supercritique. Merck Santé – Centre de R & D de Lyon Lacassagne, Nº 627, 2004.

Hamaguchi, T., Shinkuma, D., Yamanaka, Y., Miyake, M., Tamura, S., Mizuno, N. Factors affecting dissolution rate of sulpiride from tablets coated with polyvinylacetal diethylaminoacetate, a gastric fluid-soluble polymer I. Effect of ionic strength of gastrointestinal fluids. *Chem. Pharm. Bull.,* 43 (1995a) 1204-1211.

Hamaguchi, T., Shinkuma, D., Yamanaka, Y., Miyake, M., Tamura, S., Mizuno, N. Factors affecting dissolution rate of sulpiride from tablets coated with polyvinylacetal diethylaminoacetate, a gastric fluid-soluble polymer II. Effect of mechanical destructive force and film coating strength in the gastrointestinal tract. *Chem. Pharm. Bull.,* 43 (1995b) 2205-2210.

Hancock, B.C., Zografi, G. The relationship between the glass transition temperature and the water content of amorphous pharmaceutical solids. *Pharm. Res.,* 11 (1994) 471-477.

Hanna, M., York, P., Method and apparatus for the formation of particles. Patent WO 95/01221, 1995

Hanna, M., York, P., Method and apparatus for the formation of particles. Patent WO 96/00610, 1996

Hanna, M., Humphreys, G.O., Storey, R., Shekunov, B. Method of particle formation. Patent WO 99/44733, 1999a.

Hanna, M., York, P. Method and apparatus for particle formation. Patent WO 99/59710, 1999b.

Hao, J., Whitaker, M.J., Wong, B., Serhatkulu, G., Shakesheff, K.M., Howdle, S.M. Plasticization and spraying of poly(D,L-lactic acid) using supercritical carbon dioxide: control of particle size. *J. Pharm. Sci.* 93 (2004) 1083-1090.

Hebert, P.F., Healy, M.S. Production scale method of forming microparticles. Patent US 5,922,253, 1999.

Henriksen, I.B., Mishra, A.K., Pace, G.W., Johnston, K.P., Mawson, S. Insoluble drug delivery. Patent WO 97/14407, 1997.

Higashi, H., Iwai, Y.,Arai, Y. Solubilities and diffusion coeffcients of high boiling compounds in supercritical carbon dioxide. *Chem. Eng. Sci.,* 56 (2001) 3027-3044.

Higuchi, W.I. Diffusional models useful in biopharmaceutics. *J. Pharm. Sci.*, 56 (1967) 315-324.

Higuchi, W.I., Mir, N.A. Desai S.J. Dissolution rates of polyphase mixtures. *J. Pharm. Sci.*, 54 (1965) 1405-1410.

Holderbaum, T. Die Forausberechnung von Dampf-Flüssig-Gleichgewichten mit einer Gruppenbeitragszustandsgleichung, Doctoral Thesis, Fortschritt-Berichte VDI, 3, 243, 1991.

Howdle, S.M., Watson, M.S., Whitaker, M.J., Popov, V.K., Davies, M.C., Mandel, F.S., Wang, J.D., Shakesheff, K.M. Supercritical fluid mixing: preparation of thermally sensitive polymer composites containing bioactive materials. *Chem. Commun.,* 01 (2001) 109-110.

Howdle, S.M., Shakesheff, K.M., Whitaker, M.J., Watson, M.S. Polymer composite with internally distributed deposition matter. Patent WO 03/078508, 2003.

Hu, J., Johnston, K.P., Williams, III O.R. Spray freezing into liquid (SFL) particle engineering technology to enhance dissolution of poorly water soluble drugs: organic solvent versus organic/aqueous co-solvent systems. *Eur. J. Pharma. Sci.,* 20 (2003) 295-303.

Hu, J., Johnston, K.P., Williams, III O.R. Rapid dissolving high potency danazol powders produced by spray freezing into liquid process. *Int. J. Pharma.,* 271 (2004) 145-154.

Huang, F.H., Li, M.H., Lee, L.L., Starling, K.E., Chung, F.T.H. An accurate equation of state for carbon dioxide. *J. Chem. Eng. Japan,* 18 (1985) 490-496.

Jans Frontini, H., Mielck, J.B. Stability of drugs in solid dispersions: effect of glass transition on degradation kinetics under stress in systems of reserpine and PVP. *Eur. J. Pharm. Biopharm.,* 42 (1996) 303-312.

Jung, J., Perrut, M. Particle design using supercritical fluids: Literature and patent survey. *J. Supercrit. Fluids,* 20 (2001) 179-219.

Jung, J., Clavier, J.Y., Perrut. M. Gram to kilogram scale-up of supercritical anti-solvent process. *Proceedings of the 6th International Symposium on Supercritical Fluids,* Versailles, 28–30 April, 2003.

Jung, J.-Y., Yoo, S. D., Lee, S.-H., Kim, K.-H., Yoon, D.-S., Lee, K.-H. Enhanced solubility and dissolution rate of itraconazole by a solid dispersion technique. *Int. J. Pharm.,* 187 (1999) 209-218.

Juppo, A.M., Boissier, C., Khoo C. Evaluation of solid dispersion particles prepared with SEDS. Int. J. Pharm. 250 (2003) 385-401.

Kearney, A.S., Gabriel, D.L., Mehta, S.C., Radebaugh, G.W. Effect of polyvinylpyrrolidone on the crystallinity and dissolution rate of solid dispersions of the antiinflammatory Ci-987. *Int. J. Pharm.,* 104 (1994) 169-174.

Kerc, J., Srcic, S., Knez, Z., Sencar-Bozic, P. Micronization of drugs using supercritical carbon dioxide. *Int. J. Pharm.,* 182 (1999) 33-39.

Kim, J., Paxton, T., Tomasko, D. Microencapsulation of naproxen using rapid expansion of supercritical solutions. *Biotech. Prog.,* 12 (1996) 650-661.

Klein, S., Rudolph, M.W., Dressman, J.B. Drug release characteristics of different mesalazine products using USP apparatus 3 to simulate passage through the GI tract. Dissolution Technologies, published online: http://www.dissolutiontech.com/

Khougaz, K., Clas, S.-D. Crystallization inhibition in solid dispersions of MK-0591 and poly(vinylpyrrolidone) polymers. *J. Pharm. Sci.,* 89 (2000) 1325-1334.

Kibbe, A.H. Handbook of Pharmaceutical Excipients, 3rd edition; American Pharmaceutical Association, Washington, D.C. and Pharmaceutical Press, London, UK, 2000.

Kikic, I., Alessi, P., Cortesi, A., Eva, F., Fogar, A., Moneghini, M., Perissutti, B., Voinovich, D. Supercritical antisolvent precipitation processes: different ways for improving the performance of drugs. *Proceedings of the 4th International Symposium on High Pressure Process Technology and Chemical Engineering,* Venice, 22-25 September, 2002.

Kordikowski, A., Shekunov, T., York, P. Polymorph control of sulfathiazole in supercritical CO_2. *Pharm. Res.,* 18 (2001) 682-688.

Krukonis, V.J., Gallagher, P.M., Coffey, M.P., Gas anti-solvent recrystallization process. Patent US 5,360,478, 1994.

Lazzaroni, M.J., Bush, D., Brown, J.S., Eckert, C.A. High-Pressure vapor-liquid equilibria of some carbon dioxide + organic binary systems. *J. Chem. Eng. Data*, 50 (2005) 60-65.

Leach, W.T., Simpson, D.T., Val, N.T., Anuta, E.C., Yu, Z., Williams, R.O. III, Johnston, K.P. Uniform encapsulation of stable protein nanoparticles produced by spray freezing for the reduction of burst release. *J. Pharm. Sci.*, 94 (2005) 56-69.

Leuner, C., Dressman, J. Improving drug solubility for oral delivery using solid dispersions. *Eur. J. Pharm.,* 50 (2000) 47-60.

Lin, C.W., Cham, T.M. Effect of particle size on the available surface area of nifedipine from nifedipine-polyethylene glycol 6000 solid dispersions. *Int. J. Pharm.,* 127 (1996) 261-272.

Lindenberg, M., Kopp, S., Dressman, J.B., Classification of orally administered drugs on the World Health Organization Model list of Essential Medicines according to the biopharmaceutics classification system. *Eur. J. Pharm. Biopharm.,* 58(2) (2004) 265-278.

Lochard, H., Rodier, E., Sauceau, M., Letourneau, J.J., Freiss, B., Joussot-Dubien, C., Fages, J. A three-step supercritical process to improve the dissolution rate of eflucimibe. *Proceedings of the 6th International Symposium on Supercritical Fluids,* Versailles, April 28 – 30, 2003, pp 1659-1664.

Lochard, H., Sauceau, M., Freiss, B. Method for the preparation of molecular complexes. Patent WO 04/096284, 2004.

Majerik, V., Horváth, G., Charbit, G., Badens, E., Szokonya, L., Bosc, N., Teillaud, E. Novel particle engineering techniques in drug delivery: review of formulations using supercritical fluids and liquefied gases. *Hun. J. Ind. Chem.*, 32 (2004) 41-56.

Magnan, C., Badens, E., Commenges, N., Charbit, G. Soy lecithin micronization by precipitaion with compressed fluid anisolvent- Influence of process parameters. *Proceedings of the 5th Conference on Supercritical Fluids and their Applications*, Garda, 1999, 479-484.

Manning, M.C., Randolph, T.W., Shefter, E., Falk, III R.F. Solubilization of pharmaceutical substances in an organic solvent and preparation of pharmaceutical powders using the same. Patent U.S. 5,770,559, 1998.

Martin, T.M., Bandi, N., Shultz, R, Roberts, C.B., Kompella, U.B. Preparation of budesonide and budesonide-PLA microparticles using supercritical fluid precipitation technology. *AAPS Pharm. Sci. Tech.,* 3(3) (2002) E18.

Martinez, M., Amidon, G., Clarke, L., Jones, W.W., Mitra, A., Riviere, J. Applying the biopharmaceutical classification system to veterinary pharmaceutical products. Part II. Physiological considerations. *Adv. Drug. Del. Rew.,* 54 (2002) 825-850.

Mason P. Drug-food interaction, Food and medicines I. *The Pharmaceutical Journal*, 269 (2002) 571-573.

Matsumoto, T., Zografi, G. Physical properties of solid molecular dispersions of indomethacin with poly(vinylpyrrolidone) and poly(vinylpyrrolidone-co-vinylacetate) in relation to indomethacin crystallization. *Pharm. Res.,* 16 (1999) 1722-1728.

Mawson, S., Kanakia, S., Johnston, K. Coaxial nozzle for controlled of particle morphology in precipitation with a compressed fluid antisolvent. *J. Appl. Polym. Sci.,* 64 11 (1997a) 2105-2118.

Mawson, S., Johnston, K.P., Betts, D.E., McClain, J.B., DeSimone, J.M. Stabilised polymer microparticles by precipitation with a compressed fluid antisolvent: 1. Poly(fluoro acrylates). *Macromolecules*, 30 (1997b) 71-77.

Meure, L.A., Warwick, B., Dehghani, F. Regtop, H.R., Foster, N.R. Increasing copper indomethacin solubility by coprecipitation with poly(vinylpyrrolidone) using the Aerosol Solvent Extraction System. *Ind. Eng. Chem. Res.,* 43(4) (2004) 1103-1112.

Miranda, S., Yaeger, S. Homing in on the best size reduction method. *Chem. Eng.,* 105 (1998) 102-110.

Mishima, K., Yamaguchi, S., Umemot H, Patent JP 8,104,830, 1996.

Mishima, K., Matsuyama, K., Uchiyama, H., Ide, M. Microcoating of flavone and 3-hydroxyflavone with polymer using supercritical carbon dioxide. *Proceedings of the 4th International Symposium on Supercritical Fluids,* 11–14 May, Sendai, 1997, 267–270.

Mishima, K., Matsuyama, K., Yamauchi S., Izumi H., Furudono D. Novel control of crystallinity and coating thickness of polymeric microcapsules of medicine by cosolvency of supercritical solution. *Proceedings of the 5th International Symposium on Supercritical Fluids,* 8–12 April, Atlanta, 2000a.

Mishima, K., Matsuyama, K., Tanabe, D., Yamauchi, S., Young, T.J., Johnston, K.P. Microencapsulation of proteins by rapid expansion of supercritical solution with a nonsolvent. *AIChE J.,* 46(4) (2000b) 857-865.

Moghimi, S.M., Hunter, A.C. Poloxamers and poloxamines in nanoparticle engineering and experimental medicine. *Trends in Biotech.,* 18 (2000) 412-420.

Moneghini, M., Kikic, I., Voinovich, D., Perissutti, B., Filipovic-Grcic, J. Processing of carbamazepine–PEG 4000 solid dispersions with supercritical carbon dioxide: preparation, characterisation, and in vitro dissolution, *Int. J. Pharm.,* 222 (2001) 129-138.

Mukhopadhyay, M. Phase equilibrium in solid-liquid-supercritical fluid systems. In: York P, Kompella UB, Shekunov BY. Supercritical fluid technology for drug product development, drugs and pharmaceutical sciences Vol 138, Marcel Dekker Inc., New York, 2004.

Mumenthaler, M., Leuenberger, H. Atmospheric spray-freeze drying: A suitable alternative in freeze-drying technology. *Int. J. Pharma.,* 72 (1991) 97-110

Nakate, T., Yoshida, H., Ohike, A., Tokunaga, Y., Ibuki, R., Kawashima, Y. Improvement of pulmonary absorption of cyclopeptide FK224 in rats by co-formulating with β-cyclodextrin. *Eur. J. Pharm. Biopharm.,* 55 (2003) 147-154.

Neuenfeld, S., Dospil, M. Investigation of polymorphic/pseudopolymorphic behaviour of LM4156; Report 600/00, 2000.

Noyes, A., Whitney, W., The rate of solution of solid substances in their own solutions. *J. Am. Chem. Soc.,* 19 (1897) 930-934.

Nuijen, B., Bouma, M., Henrar, R.E.C., Floriano, P., Jimeno, J.M., Talsma, H., Kettens-Van Den Bosch, J.J., Heck, A.J.R., Bult, A., Beijen, J.H. Pharmaceutical development of a parenteral lyophilized formulation of the novel antitumor agent aplidine. *PDA J. Pharm. Sci. Technol.,* 54 (2000) 193-208.

O'Hern, H.A., Martin, J.J. Diffusion in carbon dioxide at elevated pressure. *Ind. Eng. Chem. Res.,* 47 (1955) 2081.

Oyler, J.R. Liquid substances freeze-drying systems and methods. Patent US 5,208,998, 1993.

Pace, G.W., Vachon, G.M., Mishra, K.A., Henriksen, I.B., Krukonis, V., Godinas, A., Processes to generate submicron particles of water-insoluble compounds. Patent WO 99/65469, 1999.

Pallado, P., Benedetti, L., Callegaro, L. WO Pat. 96/29998, 1996.

Peng, D.-Yu, Robinson, D. B., A new two-constant equation of state. *Ind. Chem. Eng. Fund.,* 15 (1976) 59-64.

Perrut, M., Jung, J., Leboeuf, F., Fabing, I. Method for making very fine particles consisting of a principle inserted in a host molecule. Patent WO 02/32462, 2002a.

Perrut, M., Jung, J., Leboeuf, F., Fabing, I. Method for making host-client complexes. Patent WO 02/089851, 2002b.

Perry, R.H., Green, D.W. Perry's Chemical Engineers' Handbook, 50th editions, McGraw-Hill Book Co, Singapore, 1984.

Raffin Pohlmann, A., Weiss, V., Mertins, O., da Silveira, N.P., Stanisçuaski Guterres, S., Spray-dried indomethacin-loaded polyester nanocapsules and nanospheres: development, stability evaluation and nanostructure models. *Eur. J. Pharm. Sci.,* 16 (2002) 305-312.

Rajasingam, R., Lioe, L., Pham, Q.T. Lucien, F.P. Solubility of carbon dioxide in dimethylsulfoxide and N-methyl-2-pyrrolidone at elevated pressure. *J. Supercrit. Fluids,* 31, 2004, 227-234.

Randolph, T.W., Randolph, A.D., Mebes, M., Yeung, S. Sub-micrometer-sized biodegradable particles of poly(L-lactic acid) via the gas antisolvent spray precipitation process. *Biotechnol. Progress,* 9 (1993) 429.

Rantakylä, M., Jäntti, M., Aaltonen, O., Hurme, M. The effect of initial drop size on particle size in the supercritical antisolvent precipitation (SAS) technique *J. Supercrit. Fluids,* 24 (2002) 251-263.

Rantakylä, M. Particle production by supercritical antisolvent technique. Doctoral Thesis, Helsinki University of Technology, 2004.

Rasenack, N., Müller, B.W. Dissolution rate enhancement by in-situ-micronization of poorly water-soluble drugs using a controlled crystallization process. *Pharm. Res.* 19 (2002) 1896-1902.

Rasenack, N., Müller, B.W. Method for the production and the use of microparticles and nanoparticles by constructive micronisation. WO Patent 03/080034 2003a.

Rasenack, N., Hartenhauer, H., Müller, B.W. Microcrystals for dissolution rate enhancement of poorly water-soluble drugs. *Int. J. Pharm.,* 254 (2003b) 137-145.

Rasenack, N., Steckel, H., Müller, B.W. Preparation of microcrystals by in situ micronization. *Powder Tech.,* 143-144 (2004) 291-296.

Redlich, O., Kwong, J.N.S., On The thermodynamics of solutions. *Chem. Rev.,* 44 (1949) 233-244.

Rehman, M., Shekunov, B.Y., York, P., Lechuga-Ballesteros, D., Miller, D.P., Tan, T., Colthorpe, P. Optimisation of powders for pulmonary delivery using supercritical fluid technology. *Eur. J. Pharma. Sci.,* 22 (2004) 1-17.

Reverchon, E. Supercritical antisolvent precipitation of micro- and nano-particles. *J. Supercrit. Fluids,* 15 (1999a) 1-21.

Reverchon, E., Della Porta, G., Sannino, D., Ciambelli, P. Supercritical antisolvent precipitation of nanoparticles of a zinc oxide precursor. *Powder Tech.,* 102 (1999b) 127-134.

Reverchon, E., Della Porta, G. Production of antibiotic micro- and nano-particles by supercritical antisolvent precipitation. *Powder Tech.,* 106 (1999c) 23-29.

Reverchon, E., Della Porta, G., De Rosa, I., Subra, P., Letourneur, D. Supercritical antisolvent micronization of some biopolymers. *J. Supercrit. Fluids,* 18 (2000) 239-245.

Reverchon, E., Della Porta, G., Pallado, P. Supercritical antisolvent precipitation of Salbutamol microparticles, *Powder Tech.,* 114 (2001) 17-22.

Reverchon, E., Della Porta G., De Marco I., Rifampicin microparticles production by Supercritical antisolvent precipitation. *Int. J. Pharma.,* 243 (2002) 83-91.

Rodier, E., Lochard, H., Sauceau, M., Letourneau, J.-J., Freiss, B., Fages, J. A three step supercritical process to improve the dissolution rate of Eflucimibe, *Eur. J. Pharma. Sci.,* 26 (2005) 184-193.

Rogers, T.L., Johnston, K.P., Williams, III R.O. Solution-based particle formation of pharmaceutical powders by supercritical or compressed fluid CO_2 and cryogenic spray-freezing technologies. *Drug Dev. Ind. Pharm.*, 27(10) (2001) 1003-1015.

Rogers, T.L., Nelsen, A.C., Hu, J., Brown, J.N., Sarkari, M., Young, T.J., Johnston, K.P. Williams, III R.O. A novel particle engineering technology to enhance dissolution of poorly water soluble drugs: spray-freezing into liquid. *Eur. J. Pharma. Biopharma.,* 54 (2002a) 271-280.

Rogers, T.L., Hu, J., Yu, Z., Johnston, K.P., Williams, III R.O. A novel particle engineering technology: spray-freezing into liquid. *Int. J. Pharma.,* 242 (2002b) 93-100.

Rogers, T.L., Overhoff, K.A., Shah, P., Santiago, P., Yacaman, M.J., Johnston, K.P. Williams, III R.O. Micronized powders of a poorly water soluble drug produced by a spray-freezing into liquid-emulsion process. *Eur. J. Pharma. Biopharm.,* 55 (2003) 161-172.

Ruchatz, F., Müller, B.W. Peptide loaded microparticles produced by the ASES process. *Eur. J. Pharm. Sci.,* 4(1) (1996) S134.

Ruchatz, F., Kleinebudde, P., Müller, B.W. Residual solvents in biodegradable microparticles. Influence of process parameters on the residual solvent in microparticles produced by the Aerosol Solvent Extraction System (ASES) process. *Int. J. Pharm. Sci.*, 86 (1997) 101-105.

Russell, T.L., Berardi, R.R., Bamett, J.L. Upper gastrointestinal pH in seventy-nine healthy, elderly, North American men and women. *Pharm. Res.,* 10 (1993) 187–196.

Sarkari, M., Brown, J., Chen, X.X. Swinnea, S., Williams, III R.O. Enhanced drug dissolution using evaporative precipitation into aqueous solution. *Int. J. Pharm.,* 243 (2002) 17-31.

Sauer, H.A. Method and apparatus for freeze-freeze drying. Patent US 3,484,946, 1969.

Schmitt, W.J., Salada, M.C., Shook, G.G., Speaker, S.M. III, Finely-divided powders by carrier solution injection into a near or supercritical fluid. *AIChE J.* 41 (1995) 2476.

Schmolka, I.R. A review of block polymer surfactants. *J. Am. Oil Chem. Soc.*, 54 (1977) 3-27.

Scurto, A.M., Lubbers, C.M., Xu, G., Brennecke, J.F. Experimental measurement and modeling of the vapor–liquid equilibrium of carbon dioxide + chloroform. *Fluid Phase Equilibria*, 190 (2001) 135-147.

Sekikawa, H., Nakano, M., Arita, T. Inhibitory effect of polyvinylphyrrolidone on the crystallisation of drugs. *Chem. Pharm. Bull.,* 26 (1978) 118-126.

Sekikawa, H., Nakano, M., Arita, T. Dissolution mechanisms of drug–polyvinylpyrrolidone coprecipitates in aqueous solution. *Chem. Pharm. Bull.,* 27 (1979) 1223-1230.

Sekizaki, H., Danjo, K., Eguchi, H., Yonezawa, Y., Sunada, H., Otsuka, A. Solid-state interaction of ibuprofen with polyvinylpyrrolidone. *Chem. Pharm. Bull.,* 43 (1995) 988-993.

Sencar-Bozic, P., Srcic, S., Knez, Z., Kerc, J. Improvement of nifedipine dissolution characteristics using supercritical CO_2. *Int. J. Pharm.,* 148 (1997) 123-130.

Serajuddin, A.T.M. Solid dispersion of poorly water-soluble drugs: early promises, subsequent problems and recent breakthroughs. *J. Pharm. Sci.,* 88 (1999) 1058-1066.

Sethia, S., Squillante, E. Physicochemical characterization of solid dispersions of carbamazepine formulated by supercritical carbon dioxide and conventional solvent evaporation method. *J. of Pharm. Sci.,* 91 (2002) 1948-1957.

Sethia, S., Squillante, E. Solid dispersions of carbamazepine in PVP K30 by conventional solvent evaporation and supercritical methods. *Int. J. Pharm.,* 272 (2004) 1-10.

Shekunov, B.Y., Hanna, M., York, P. Crystallization process in turbulent supercritical flows. *J. Crystal Growth,* 198/199 (1999) 1345-1351.

Shekunov, B.Y., Feeley, J.C., Chow A.H.L., Tong, H.H.Y., York, P. Physical properties of supercritically-processed and micronised powders for respiratory drug delivery. KONA, 20 (2002) 178-187.

Shieh, Y.-T., Su, J.-H., Manivannan, G., Lee, P.H.C., Sawan, S.P.S., Spall, W.D. Interaction of supercritical carbon dioxide with polymers. II. Amorphous polymers. *J. Appl. Polym. Sci.*, 59 (1996) 707-717.

Shine, A., Gelb, J. Microencapsulation process using supercritical fluids. WO Pat. 98/15348, 1998.

Simonelli, A., Mehta, S.C., Higuchi, W.I. Inhibition of sulfathiazole crystal growth by polyvinylpyrrolidone. *J. Pharm. Sci.,* 59 (1970) 633-637.

Sjökvist-Saers, E., Craig, D.Q.M. An investigation into the mechanisms of dissolution of alkyl p-aminobenzoates from polyethylene glycol solid dispersions. *Int. J. Pharm.*, 83 (1992) 211–219.

Soave, G. Equilibrium constants from a modified Redlich-Kwong equation of state. *Chem. Eng. Sci.,* 27 (1972) 1197.

Song, H., Guo, T., Zhang, R., Zheng, C., Ma, Y., Li, X., Bi, K., Tang, X. Preparation of the traditional Chinese medicine compound recipe heart-protecting musk pH-dependent gradientrelease pellets. *Drug Dev. Ind. Pharm.,* 28 (2002) 1261–1273.

Squillante, E. III., Mehta, K.A. Extended-release chlorpheniramine maleate from polymethacrylate solid dispersions by supercritical fluid processing. *Drug Del. Tech.*, 2(5) 2004 [http://drugdeliverytech.com/]

Steckel, H., Thies, J., Müller, B.W. Micronizing of steroids for pulmonary delivery by supercritical carbon dioxide. *Int. J. Pharma.,* 152 (1997) 99-110.

Steckel, H., Rasenack, N., Müller, B.W. In-situ-micronization of disodium cromoglycate for pulmonary delivery. *Eur. J. Pharm. Biopharm.,* 55 (2003a) 173-180.

Steckel, H., Rasenack, N., Villax, P., Müller, B.W. In vitro characterization of jet-milled and in-situ-micronized fluticasone-17-propionate. *Int. J. Pharm.,* 258 (2003b) 65-75.

Stephan, K., Lucas, K. Viscosity of dense fluids. (1979) New York, Plenum Press

Subramaniam, B., Rajewski R.A., Snavely K. Pharmaceutical Processing with Supercritical Carbon Dioxide. *J. Pharm. Sci.,* 86 (1997) 885-890.

Susuki, H., Miyamoto, N., Masada, T., Haykwa, E., Ito, K. Solid dispersions of benedipine hydrochloride I. Preparations using different solvent systems and dissolution properties. *Chem. Pharm. Bull.,* 44 (1996) 364-371.

Sze Tu, L., Dehghani, F., Dillow, A.K., Foster, N.R. Application of dense gases in pharmaceutical processing; *Proceedings of The 5th Meeting on Supercritical Fluids,* INPL, Vandeuvre, 1998, 1, 263.

Sze Tu, L., Dehghani, F., Foster, N.R. Micronisation and microencapsulation of pharmaceuticals using a carbon dioxide antisolvent. *Powder Tech.,* 126 (2002) 134-149.

Szente, L., Szejtli, J. Highly soluble cyclodextrin derivatives: chemistry, properties, and trends in development. *Adv. Drug Delivery Rev.,* 36 (1999) 17-28.

Tachibana, T., Nakamura, A. A method for preparing an aqueous colloidal dispersion of organic materials by using water-soluble polymers: dispersion of beta-carotene by polyvinylpyrrolidone. *Kolloid-Z. Polym.,* 203 (1965) 130-133.

Taki, S., Badens, E., Charbit, G., Controlled release system formed by supercritical anti-solvent coprecipitation of a herbicide and a biodegradable polymer. *J. Supercrit. Fluids,* 21 (2001) 61-70.

Tantishaiyakul, V., Kaewnopparat, N., Ingkatawornwong, S. Properties of solid dispersions of piroxicam in polyvinylpyrrolidone K-30. *Int. J. Pharm.,* 143 (1996) 59-66.

Tantishaiyakul, V., Kaewnopparat, N., Ingkatawornwong, S. Properties of solid dispersions of piroxicam in polyvinylpyrrolidone *Int. J. Pharm.,* 181 (1999) 143-151.

Taylor, L.S., Zografi, G. Spectroscopic characterization of interactions between PVP and indomethacin in amorphous molecular dispersions. *Pharm. Res.,* 14 (1997) 1691-1698.

Teagarden, D.L., Petre, W.J., Gold, P.M. Stabilized Prostaglandin E_1. Patent US 5,741,523, 1998.

Teagarden, D.L., Baker, D.S. Practical aspects of lyophilization using non-aqueous co-solvent systems. *Eur. J. Pharm. Sci.* 15 (2002) 115-133.

Thies, J., Müller, B.W. Size controlled production of biodegradable microparticles with supercritical gases. *Eur. J. Pharm. Biopharm.,* 45 (1998) 67-74.

Tong, H.H.Y., Shekunov, B.Y., York, P., Chow A.H.L. Characterization of two polymorphs of salmeterol xinafoate crystallized from supercritical fluids. *Pharm. Res.,* 18 (2001) 852-858.

Torrado, S., Torrado, S., Torrado, J.J., Cadorniga, R. Preparation, dissolution and characterization of albendazole solid dispersions. *Int. J. Pharm.,* 140 (1996) 247-250.

Tservistas, M., Levy, M.S., Lo-Yim, M.Y.A., O'Kennedy, R.D., York, P., Humphrey, G.O., Hoare, M. The formation of plasmid DNA loaded pharmaceutical powders using supercritical fluid technology. *Biotech. Bioeng.*, 72 (2001) 12-18.

Tsivintzelis, I., Missopolinou, D., Kalogiannis, K., Panayiotou, C. Phase compositions and saturated densities for the binary systems of carbon dioxide with ethanol and dichloromethane. *Fluid Phase Equilibria*, 224 (2004) 89-96.

Uekama, K., Hirayama, F. Cyclodextrin-based controlled drug release system. *Adv. Drug Delivery Rev.,* 36 (1999) 125-141.

Van der Waals, J.D. Over de continuiteit van den gas- en vloeistoftoestand. Doctoral Thesis, Leiden, 1873.

Van Konynenburg, P., Scott, R. Critical Lines and Phase Equilibria in Binary van der Waals Mixtures, *Phil. Trans. Roy. Soc.,* A298, (1980) 495-540.

Vaughn, J.M., Gao, X., Yacaman, M.-J., Johnston, K.P., Williams, III R.O. Comparison of powder produced by evaporative precipitation into aqueous solution (EPAS) and spray freezing into liquid (SFL) technologies using novel Z-contrast STEM and complimentary techniques. *Eur. J. Pharma. Biopharma.,* 60 (2005) 81-89.

Velaga, S.P., Bergh, S., Carlfors, J. Stability and aerodynamic behaviour of glucocorticoid particles prepared by a supercritical fluids process. *Eur. J. Pharm. Sci.,* 21 (2004) 501-509

Vidgrén, M.T., Vidgrén, P.A., Paronen, T.P. Comparison of physical and inhalation properties of spray-dried and mechanically micronized disodium cromoglycate. *Int. J. Pharm.*, 35 (1987) 139–144.

Wang, Y., Dave, R. N., Pfeffer, R. Polymer coating/encapsulation of nanoparticles using a supercritical anti-solvent process. *J. Supercrit. Fluids,* 28 (2004) 85-99.

Watson, M.S., Whitaker, M.J., Howdle, S.M., Shakesheff, K.M. Incorporation of proteins into polymer materials by a novel supercritical fluid processing method. *Adv. Mater.,* 14 (2002) 1802-1804.

Won, D.-H., Kim, M.-S., Lee, S., Park, J.-S., Hwang, S.-J. Improved physicochemical characteristics of felodipine solid dispersion particles by supercritical anti-solvent precipitation process. *Int. J. Pharm.*, 301 (2005) 199-208.

Weidner, E., Knez, Z., Novak, Z., Process for the production of particles or powders. Patent WO 95/21688, 1995.

Werling, J.O., Debenedetti, P.G. Numerical modelling of mass transfer in the supercritical antisolvent process: miscible conditions. *J. Supercrit. Fluids*, 18 (2000) 11-24.

Whitaker, M.J., Hao, J., Davies, O.R., Serhatkulu, G., Stolnik-Trenkic, S., Howdle, S.M., Shakesheff, K.M. The production of protein-loaded microparticles by supercritical fluid enhanced mixing and spraying. *J. Cont. Rel.,* 101 (2005) 85-92.

WHO, World Health Organization, The 12th Model List of Essential Medicines, [www.who.int/medicines/] 2002.

Williams, R.O. III, Johnston, K.P., Young, T.J., Rogers, T.L., Barron, M.K., Yu, Z. Process for production of nanoparticles and microparticles by spray freezing into liquid. Patent WO 02/060411, 2002.

Witschi, C., Doelker, E. Influence of the microencapsulation method and peptide loading on poly(lactic acid) and poly(lactic-co-glycolic acid) degradation during in vitro testing. *J. Cont. Rel.,* 51 (1998a) 327-341.

Witschi, C., Doelker, E. Peptide degradation during preparation and in vitro release testing of poly(L-lactic acid) and poly(DL-lactic-co-glycolic acid) microparticles. *Int. J. Pharm.,* 171 (1998b) 1-18.

Wittaya-Areekus, S., Nail, S.L. Freeze-drying of tert-butyl alcohol / water cosolvent systems: effects of formulation and process variables on residual solvents. *J. Pharm. Sci.,* 87 (1998) 491-495.

Yang, X.B.B., Whitaker, M.J., Sebald, W., Clarke, N., Howdle, S.M., Shakesheff, K.M., Oreffo, R.O.C. Human osteoprogenitor bone formation using encapsulated bone morphogenetic protein 2 in porous polymer scaffolds. *Tissue Engineering,* 10 (2004) 1037-1045.

Ye, C. Enhanced dissolution of relatively insoluble drugs from small particles and solid dispersions formed from supercritical solution. Doctoral Thesis, Ohio State University, 2000.

Yeo, S.D., Ki, M.S., Lee, J.C. Recrystallisation of sulfathiazole and chlorpropamide using the supercritical fluid antisolvent process, *J. Supercrit. Fluids,* 25 (2003) 143-154.

York, P. Strategies for particle design using supercritical fluid technologies. *Pharma. Sci. Tech. Today*, 11 (1999) 430-440.

York, P., Wilkins, S.A., Storey, R.A., Walker, S.E., Harland, R.S. Cofomulation methods and their products. Patent WO 01/15664, 2001.

Young, T.J., Mawson, S., Johnston, P., Henriksen, I.B., Pace, G.W., Mishra, A.K. Rapid expansion from supercritical to aqueus solution to produce submicron suspensions of water-insoluble drugs. *Biotechnol. Prog.*, 16 (2000) 402-407.

Yu, Z., Rogers, T.L., Hu, J., Johnston, K.P., Williams, III R.O. Preparation and characterization of microparticles containing peptide produced by a novel process: spray freezing into liquid. *Eur. J. Pharma. Biopharma.,* 54 (2002) 221-228.

Yu, Z., Garcia, A.S., Johnston, K.P., Williams, III R.O. Spray freezing into liquid nitrogen for highly stable protein nanostructured microparticles. *Eur. J. Pharm. Biopharm.*, 58 (2004) 529-537.